Michael Perryman

SCI(79)10
December 1979

european space agency

esa

HIPPARCOS

SPACE ASTROMETRY

REPORT ON THE PHASE A STUDY

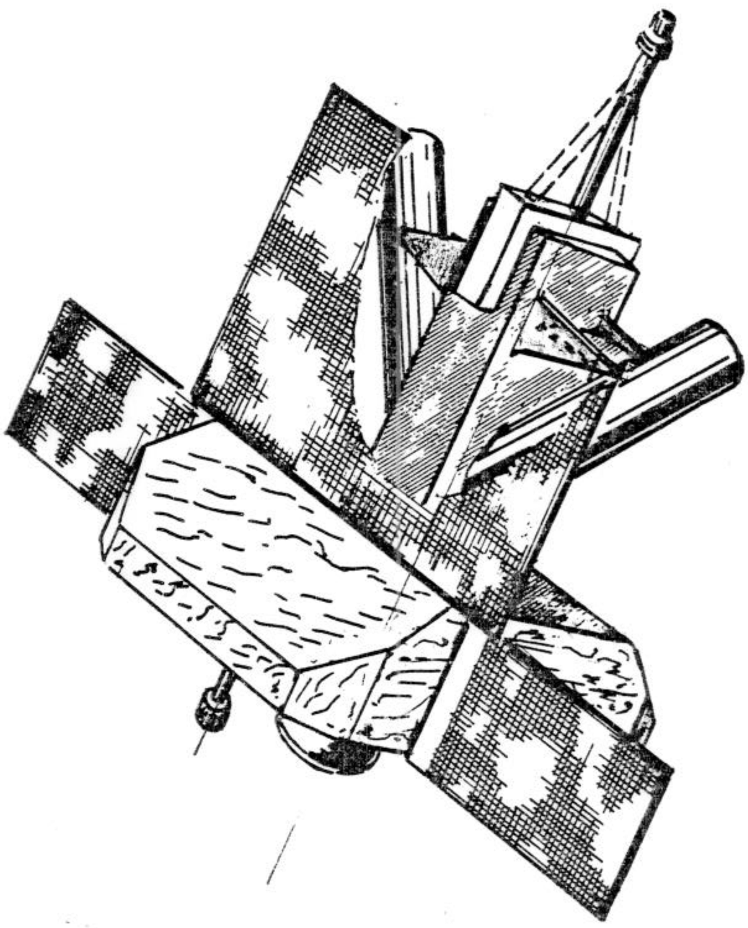

HIPPARCOS

Table of Contents

HIPPARCOS

The proposed name of the mission (HIPPARCOS) refers to the famous Greek astronomer (190-120 BC) who, by measuring the position of the Moon against the stars, determined the Moon's parallax and derived the correct distance of 30 times the diameter of the Earth.

Furthermore, he made the first accurate star map which led to an important discovery: comparing his observations with those of his predecessors, he found a uniform shift of the stellar positions from West to East. This effect could be accounted for by assuming that the North Celestial Pole rotates in the sky with a period of 25,700 years, giving rise to the "precession of the equinoxes".

HIPPARCOS is also an acronym for "HIgh Precision PARallax COllecting Satellite".

Abstract

The space astrometry mission HIPPARCOS aims at the accurate measurement of the trigonometric parallaxes, proper motions, and positions of about 100 000 selected stars, most of them brighter than magnitude 10. The expected average mean error is about 0".002 for the parallaxes and in each coordinate of the positions and proper motions per year.

Such an order-of-magnitude improvement in precision and number of data, as compared with the present and near future situation, can only be obtained with a dedicated astrometric instrument operating in space and taking advantage of zero gravity, full sky visibility, constant thermal environment, and absence of a refracting atmosphere.

Astrometric data are at the very base of most astrophysical theories and of our conception of the Universe, in terms of distances, masses, absolute luminosities and motions of the stars. The mission will yield the following direct results:

- a dense (2-3 stars per square degree) reference system, which can be related to an absolute frame of reference,
- at least five or six open clusters within the range of parallax determined distances,
- H-R diagram positions of many early type stars and red giants and the fine structure of the diagram for A-F-G stars,
- a catalogue of astrometric parameters for an enormous variety of kinematical, dynamical and astrophysical investigations,
- detection and measurement of a few thousand presently unknown binaries.

The mission will yield significant indirect benefits such as:

- the redefinition of the basis of the cosmic distance scale, leading to a detailed kinematic and dynamical description of a sizeable part of the Galaxy,
- together with photometric and spectroscopic data, the study of the chemical and dynamical evolution of the Galaxy (ages of clusters and families of stars),
- the testing of present cosmological theories.

The proposed satellite will be injected into transfer orbit by Ariane as a single passenger or in a dual configuration, i.e. together with another spacecraft, which can be a geostationary one. The final orbit of the astrometric satellite is circular, geosynchronous (period 24 hours), at an equatorial inclination of a few degrees. Thus, continuous telecommand and telemetry links will be maintained during the whole lifetime (nominally 2.5 years) using only one European ground station.

The principle applied for determining the astrometric parameters consists in measuring with high precision the angular distance between stars separated by a large angle, of the order of 70°. The measurements are obtained by a differential method, comparing in the focal surface of a single telescope the positions of stars imaged from two different fields of view, superimposed by means of a complex mirror with two reflecting surfaces. The attitude of the satellite is controlled in such a way that the telescope fields of view scan the whole celestial sphere in a smooth motion.

Already six months' observation with HIPPARCOS will provide a positional reference system with an accuracy of about 0".01 and comprising 100 000 stars distributed over the whole sky. After the nominal lifetime of 2.5years the following achievements are expected:

- accuracy (m_B < 10):
  - positions : 0.002 arcsec (present 0".04 at best)
  - proper motions : 0.002 arcsec/yr (comparable with best ground-based obtained after more than 50 years of observation)
  - parallaxes : 0.002 arcsec (present 0".010 for bright stars)
- absolute parallaxes instead of relative
- systematic errors < 0.001 arcsec, as compared to present errors of 0.005 arcsec for parallaxes and 0.04 arcsec for positions
- large number of stars : 100 000, compared to a few thousand contained in current fundamental catalogues
- faint stars : down to magnitude 12 (presently 7 for best positions and proper motions)
- homogeneous sky coverage: in particular a firm connection between the northern and southern celestial hemispheres.

Should this mission be fulfilled, such discoveries are likely to occur that will influence our basic understanding of stellar structure, galactic dynamics, stellar evolution, galactic evolution and cosmology. It is not too presumptive to state that many present concepts in these fields - and probably in others - will need to be revised as a result of the mission of the astrometric satellite.

1. SCIENTIFIC OBJECTIVES

1.1 Introduction

Optical astrometry provides the basic calibration for all cosmic distance measurements outside the solar system, an inertial reference frame for study of stellar and planetary motions and a positional reference frame for identification of celestial objects.

Ground-based astrometry can be divided into two broad categories: (a) global astrometry which seeks to measure large angles over the sky, for example with meridian instruments using the diurnal rotation of the Earth and accurately calibrated circles, and (b) local astrometry which is confined to small areas of sky which can be photographed with astrographs ($\sim 5^o \times 5^o$) or long focus telescopes ($\sim 1^o \times 1^o$). The primary reference frame of positions and proper motions is provided by (a) whereas extension to faint stars and also measurement of relative trigonometric parallaxes and proper motions are covered by (b). Although relative positions and displacements can be measured with very high precision with large telescopes, the accuracy of the absolute position of any target object is limited by the accuracy with which the primary reference frame is defined in the small area surrounding it.

The concept of the HIPPARCOS mission is essentially global, in that large angles are measured using the great circle scanning motion of the satellite with the two fields of the complex mirror defining a basic angle. In this way not only will relative positions and proper motions be measurable in a homogeneous fashion over the whole celestial sphere, but also absolute parallaxes will be obtained; this is possible because, in any one scan, which lasts for only a fraction of a day, the angular distance between stars with different angular separations from the Sun will be measured.

1.2 Stellar Reference Frame

The positional reference frame, and the inertial frame of proper motions are in principle defined by the positions, at some epoch, and the proper motions of a small sample of stars which are contained in a so-called fundamental catalogue. The angular coordinates are defined by the direction of the equinox and the plane of the equator at some standard epoch, that is by the orbital and rotational motions of the Earth. The absolute rotation of the proper motion system which includes any error in the adopted constant of precession of the Earth's axis, has so far only been determined directly, by analysis of catalogue proper motions using some model of galactic kinematics. Although in principle, observations of proper motion relative to extragalactic objects will provide data on stellar kinematics which are independent of any galactic model, results so far achieved appear to be significantly affected by systematic errors.

The currently adopted fundamental catalogue, which is known as FK4 (Fricke and Kopff 1963), contains data for only about one star per $5^o \times 5^o$ and is confined to stars brighter than $m_v \sim 7.5$. It represents the synthesis of observational data obtained with meridian instruments at a large number of observatories over more than a century. At the mean epoch ($\sim$ 1930) the average mean error of one coordinate was about $\pm$ 0.''04; but with a mean error of $\pm$ 0.''002 per year for a proper motion component, the accumulated error at 1980 amounts to about 0.''1 for a single coordinate. This represents the average mean error of the primary reference frame over the whole sky; accidental and systematic (i.e. locally correlated) errors are relatively larger in the southern hemisphere.

The absolute rotation of the FK4 proper motion system has been found by Fricke (1967) to be of the order of 0".005 per year with a mean error of about twenty per cent.

The FK4 cataloque will be superseded within about 5 years by a new catalogue, to be known as FK5, which is being compiled at A.R.I. Heidelberg. This catalogue will have a larger number of stars than FK4 (1 per ∿ $3^{\circ} \times 3^{\circ}$) and the uncertainty of the absolute rotation of the proper motion system of FK5 will be about 0".001 per year.

The system of FK4 has been extrapolated to fainter stars by special additional meridian observations of some 40,000 stars, organised on an international basis, which are used for calibration of photographic surveys made with wide angle astrographs. In the northern hemisphere, the AGK 3 catalogue (Dieckvoss et al. 1975) contains data for an average of 9 stars per square degree, whose positions at the current epoch, and proper motions, have mean errors of about ± 0".4 and ± 0".01 per year respectively. Plates for a similar photographic survey of the southern hemisphere have been taken at the Cape and are also being obtained at several other observatories.

The Smithsonian Astrophysical Observatory (SAO) catalogue contains positions and proper motions for some 259000 stars over the whole sky, compiled from heterogeneous sources. At the present time it is the only available standard for positions and proper motions of large numbers of stars in the southern hemisphere; individual positions have standard errors at the present epoch of between 0".5 and 1".0.

In summary, the main limitations of the ground based optical reference frame are:

(i) Large random errors in the realization of the reference frame in a local (∿ $1^{\circ} \times 1^{\circ}$) region.

(ii) Inhomogeneity of the system of positions and proper motions particularly between the northern and southern hemispheres.

The low accuracy of the local positional reference frame (∿ 0".1 to 0".2) compares unfavourably with the accuracies now being achieved for instance in VLBI measurements and positions of pulsars from timing observations which are between 0".01 and 0".1. When relative positions of faint optical objects can be measured with the Space Telescope, it will be essential to have a coherent whole-sky reference frame to match the high resolution of that instrument.

HIPPARCOS will provide just such a reference frame with a density of about 2.5 stars per square degree and standard error at epoch of observation of ± 0".002; even after ten years of accumulated proper motion error the error of a single star position will be only ± 0".02.

The lack of homogeneity of the proper motion system severely degrades analyses of kinematics of distant stars for which the proper motions are small anyway, for example in the study of galactic rotation which will be discussed below. Again, HIPPARCOS will give a homogeneous set of proper motions for about 50 times as many stars as are currently available with comparable accuracy.

The reference frame of the HIPPARCOS proper motions may be referred to an inertial frame through measurement of the apparent proper motions of extra-galactic objects. This can be achieved by using the astrometric facilities of the Space Telescope, or, with much lower precision, by conventional ground based astrometry with large telescopes.

Observations of solar system objects will provide a link between the improved astrometric frame and that defined dynamically by motion of the Moon and planets. Non-gravitational effects in the lunar motion and relativistic effects in the motions of all bodies will be measured with improved precision (cf. Kovalevsky, 1975).

1.3 Luminosities and Distances

At the present time, the direct calibration of absolute magnitudes by means of trigonometric parallaxes is confined generally to stars within about 20 parsecs of the Sun which are predominantly late main sequence stars with very few earlier than type F. Calibration of more luminous stars is obtained by analysis of average trigonometric parallaxes of distant stars and, kinematically, by comparing the statistics of proper motions with those of radial velocities. For intrinsically very bright stars such as supergiants and Cepheid variables, the calibration depends almost entirely on cluster main sequence fitting, which is based ultimately on the distance to the Hyades cluster. This is well determined kinematically with a formal error of less than five per cent; there is however some evidence that the Hyades F stars may be up to $0\overset{m}{.}15$ more luminous than corresponding stars in other clusters, and in the general vicinity of the Sun, which is not unexpected in view of a probable difference in abundance. This basic uncertainty in one of the primary calibrations of the extra galactic distance scale can only be resolved when trigonometric parallaxes of many more stars are available for detailed study of the dependence of luminosity on the various observable photometric parameters in, for example, the uvby β system .

The large increase in quantity and precision of parallax data which are required to solve this problem will be obtainable from HIPPARCOS. With a mean error of $\pm$ 0".002, which is some five times smaller than the typical error of a well determined ground-based trigonometric parallax in the General Catalogue of Trigonometric Parallaxes (Jenkins, 1952) and its supplement (1963), not only will the knowledge of luminosities of nearby stars be dramatically improved, but also the increase by a hundredfold in the volume which can be surveyed to the same relative precision as for currently available parallaxes, will bring many more stars including some late B type main sequence stars and many late type giants within reach of measurement.

1.3.1 Status of Ground-Based Parallax Measurements

Most of the data currently available on trigonometric parallaxes are contained in the General Catalogue and its supplement. These together contain data for 7000 stars based on some 10,000 independent determinations from 14 observatories. Many of these stars have very small parallaxes, and the average mean error is about $\pm$ 0".016 although this varies considerably between different observatories. Only a small number of stars have parallaxes with mean errors as small as $\pm$ 0".01 or less.

The original cooperative programme initiated by Schlesinger consisted of bright stars ($m_v \leq 5.5$) with spectral types later than B. Subsequently stars which were found to have large proper motions were preferentially selected for observation and in recent years special attention has been paid to later type (K-M) dwarfs discovered in objective prism surveys.

Table 1.1 Summary of parallax data published in the decade 1969-78: Source, total number of parallax determinations, typical standard deviation of a single determination, annual rate of accumulation of parallax information.

	N	σ (0″001)	wy^{-1}
USNO	488	4	305
VAN VLECK	213	8	33
ALLEGHENY	158	10	16
McCORMICK	121	15	5
LICK	109	8	17
SPROUL	101	(20)	(3)
YALE	64	15	3
YERKES	62	(11)	(5)
RGO	42	10	4
USSR	27	?	?

The level of current activity in this field is illustrated in Table 1.1 which summarises the parallax data published in the decade 1969-78; this has been compiled by R.B. Hanson. In the table, N is the total number of parallax determinations from each source and σ is the typical standard deviation of a single determination. For Sproul and Yerkes the data are rather heterogeneous and consequently not readily characterised by a single value of σ. In addition experimental parallax measurements on faint stars have been carried out on large telescopes (van Altena 1977; Murray 1974; Murray and Corben 1979) but it is entirely unrealistic to expect that a major contribution can be obtained from such sources in view of the heavy competition for observing time on such telescopes.

The last column of Table 1.1 gives the annual rate of accumulation of parallax information based on ± 0″01 as standard error of unit weight. The predominence of the US Naval Observatory 61-inch astrometric reflector which is dedicated to parallax work is evident. On the same weight scale the output of HIPPARCOS in a 2.5 year mission would be 10^6, and furthermore the resulting parallaxes would be absolute.

Nearby Stars

Although as we have seen, trigonometric parallaxes have been measured for upwards of 10^4 stars, the number of stars in the immediate solar neighbourhood for which the parallaxes have anything more than mere statistical value, is relatively small. Gliese has compiled a series of catalogues giving data for nearby stars; his first catalogue (1957) contains 915 systems with $\pi < 0''05$ and the first revision (1969) gives 1529 systems with $\pi < ''045$. A recent compilation (Gliese and Jahreiss 1979) brings the number of known systems within a radius of 22 parsecs to almost 2000.

A similar compilation which also contains data on galactic orbits was published by Woolley et al. (1970) and gives data for 1744 systems with $\pi > 0''.040$.

One of the aims of these catalogues is to provide a complete sample of the stellar population, to some absolute magnitude limit, within a well defined volume. This aim has not yet been achieved because the limiting radius has to be set by a value of observed parallax rather than true parallax and also because of selection effects in the choice of stars for which trigonometric parallaxes have been observed.

The most troublesome effect arises from the preferential selection of stars with large proper motion for parallax measurement, thus biassing the sample in favour of high velocity (halo) stars. This can only be eliminated by selection according to apparent magnitude, which of course means that the volume surveyed depends on absolute magnitude.

HIPPARCOS will provide an opportunity for observing a strictly unbiased sample. If for example the programme were to include all stars brighter than $m_V = 9$, then the sample would be complete to 20 parsecs for $M_V \leq 7.5$ which, on the main sequence corresponds to late K. Furthermore at this distance the relative parallax error would be only four percent, and so the boundary would be very well defined by the observed parallax. Main sequence stars intrinsically fainter than $M_V = 7.5$ can be readily identified in objective prism surveys, and hence do not suffer the same kinematic bias as do the brighter stars.

1.3.2 Luminosity Calibration

The main methods of luminosity calibration have already been described in the introduction to this section. Following Blaauw (1973) we show schematically in Fig.1. 1a the method which is used, with ground based data, appropriate to the various sequences in the H - R diagram. For all but late K and M dwarfs, the calibration generally involves either statistical assumptions about kinematic behaviour of stars, or in the case of main sequence fitting, assumptions about the relative luminosity of stars with the same spectral type in different clusters, which as we have already remarked may be significantly affected by chemical composition. It is clearly desirable that direct calibration by means of trigonometric parallaxes should be carried out for as much of the H - R diagram as possible.

The increase by a factor of about five in the precision with which absolute parallaxes will be measurable by HIPPARCOS extends the effective horizon for individually significant parallaxes to about 100 parsecs. In Fig. 1.2 we show the numbers of stars within this limit (distance modulus $m - M = 5$) at each apparent magnitude for various regions of the H - R diagram: (a) B stars, (b) A stars, (c) G, K, M giants (luminosity class III) and (d) G,K subgiants (class IV), based on data taken from Allen's Astrophysical Quantities (1955). For comparison the corresponding numbers within $m - M = 2$ ($\sim$ 25 parsecs) are also indicated. The dramatic increase in the number of stars which will be available for direct calibration is evident. A point to note is that in all cases illustrated, the numbers fall to zero at apparent magnitudes brighter than 10 and thus all these stars will be measurable with the best accuracy of which HIPPARCOS is capable. With many more stars available, particularly those on the lower main sequence, it will be practicable to divide the calibration according to age and chemical composition and thus make more secure the whole basis of main sequence fitting.

It will also be possible to measure directly the trigonometric parallax to several clusters and associations. Taking into account the reduction in statistical weight because of correlation between parallaxes of adjacent stars, the expected standard error ε_m of the mean distance modulus for five clusters is given in Table 1.2 where d is the approximate distance in parsecs as given by Allen (1973).

Table 1.2 Clusters and Associations for which trigonometric parallax could be measured with HIPPARCOS; name, distance in parsecs, expected standard error on the distance modulus, spectral type of the brightest member.

	d	ε_m	S_p
U Ma	30	$0^m.03$	A0 V
Hyades	40	$0^m.04$	A5 V; K 0 III
Coma	80	$0^m.09$	A4 V
Sco Cen	170	$0^m.06$	B2 V
α Per	180	$0^m.20$	F5 Ib

The final column gives the spectral type of the brightest member. For U Ma and Sco Cen the star density is very low and the value for ε_m is calculated assuming that all the parallaxes will be independent. For the remaining 3 clusters we have assumed $\pm$ ".0005 as the standard error of the mean absolute parallax. The importance of direct measurement of the Hyades parallax cannot be over-stressed. The best formal precision of the distance modulus of the cluster which has been obtained by kinematic methods is about $\pm$ $0^m.05$, but this does not include uncertainty in the proper motion systems (van Altena 1974). The standard error derived from the average trigonometric parallax of 30 Hyades members which are contained in the General Catalogue is $\pm$ $0^m.2$. In order to improve on this, van Altena (1973) proposed a list of about twenty faint members of the cluster which would be suitable for a special cooperative programme. So far, results have been obtained at three out of the seven participating observatories, and these indicate that the final mean error of the distance modulus, from ground-based trigonometric parallaxes, will be about $\pm$ $0^m.1$.

For two other clusters, Pleiades and Praesepe, the star density is so high that it is unlikely that the distance modulus derived from HIPPARCOS parallaxes will be more precise than about $\pm$ $0^m.3$.

In Fig.1.1b we show those parts of the H-R diagram which can be calibrated directly by means of absolute trigonometric parallaxes obtained from HIPPARCOS. In contrast to Fig.1.2a, we see that only for $M_V \lesssim 1$ will it be necessary still to appeal to other methods; and even for these intrinsically bright stars there will be statistical information from small parallaxes to supplement the indirect calibrations.

1.3.3 Stellar Structure and Evolution

The knowledge of the helium/hydrogen ratio in stars of different ages and in interstellar matter is of paramount importance for cosmology. Whereas it is possible to determine spectroscopically this ratio in hot young massive stars, it is only possible to infer it, from the location of the stars in the theoretical H-R diagram (log T_{eff}, M_{bol}) for stars later than A 0, i.e. stars older than 300 millions years. The immediate solar neighbourhood contains only stars significantly older than this limit, the rest having been depleted by evolution.

Theoretical computations of internal structure show that the locus of the theoretical zero age main sequence (ZAMS) depends upon the initial composition (X, Y, Z) of the homogeneous stellar model which defines the ZAMS. In other words, the position of the ZAMS in the (log T_{eff}, M_{bol}) plane is a computable function of the value of the helium-content Y and the metal content Z. There is some evidence that the observational width of the main sequence limited to disk-stars in the solar neighbourhood, having a heavy-element content [Fe/H] between -0.60 and + 0.50, and effective temperature smaller than 5500 K, is not well explained by a variation of the metal/hydrogen ratio alone. To account for the observations it seems necessary to assume the existence of a simultaneous variation of the helium content: roughly $\Delta Y \simeq 5\ \Delta Z$, which acts in the opposite way to the metal-content on the position of the observational ZAMS. On the other hand for the very metal-poor halo subdwarfs the evidence on which the current estimation of the primeval helium-content is based relies on only one good parallax.

The comparison between theoretical and observational HR diagrams is mainly limited by the inaccuracy of the trigonometric parallaxes of the stars. The apparent magnitudes of the stars in the solar neighbourhood are well determined but at the present time, absolute magnitudes are known to better than $0^m.1$ for less than fifty stars. An increase by an order of magnitude in the number of such stars, which will be obtained by HIPPARCOS, will give a quantitative solution to this problem.

1.3.4 Evolution of the Galaxy

Pagel (1979) has briefly reviewed the significance of enhanced trigonometric parallax data for the problem of galactic evolution.

The position of an evolved star in the H-R diagram depends on its mass, age and possibly also on its chemical composition. Therefore the observed distribution of giants and subgiants in the diagram contains information on the initial mass distribution of stars of about one solar mass and greater, and also past rates of star formation (e.g. Neckel 1975). In particular, the position of the lower envelope of the subgiant sequence, which from current data appears to be close to that of the old galactic cluster NGC 188, sets an upper limit to the age of the stars in the galactic disk (Wilson 1976).

There are too few evolved stars within 20 parsecs for any analysis of them to be significant, and in order to enlarge the sample volume it has been necessary to derive absolute magnitudes from calibration of spectroscopic criteria, particularly the $M_V(K)$ from the Wilson-Bappu effect. But the accidental error of an $M_V(K)$ is of the order $\pm\ 0^m.3$ and in addition, the basic calibration of the effect is still uncertain.

We have already seen, however, in Fig. 1.2 (c) and (d) above, that there are several hundred giants and thousands of subgiants within 100 parsecs for which parallaxes can be obtained from HIPPARCOS. From these data it will be possible to construct an H-R diagram for several hundred evolved stars within some well defined volume, with errors of less than $0^m.3$ in absolute magnitude, from which more refined estimates of the rate of star formation and the age of the disk can be made.

Similar observations in the Magellanic Clouds will be possible from the Space Telescope, thereby giving a comparison of age and evolutionary history between two different types of galaxy.

The age of the oldest known objects in the Galaxy, viz. globular clusters, depends directly on the brightness of the main-sequence turn-off point and hence on their distances. The best globular cluster distances will be obtained from the fitting of their main-sequences to subdwarfs of comparable chemical composition (cf. Sandage,A. 1970) , whose parallaxes will be measured by HIPPARCOS. The satellite will therefore make an important contribution to improve the minimum age of the Galaxy and hence of the universe.

1.3.5 Extragalactic Distances

For a few very nearby galaxies (Magellanic Clouds and several dwarf ellipticals) photometry is available of their RR Lyrae stars. The present uncertainty of the mean absolute magnitude of these stars is about $\pm$ $0^m.2$. This error shall be reduced through the many proper motions which shall yield an improved absolute magnitude of these variables from kinematical parallaxes, and through the improved distances of globular clusters as discussed above.

The fundamental extragalactic distance indicators are still Cepheids because of their high luminosity and the tightness of the period - luminosity - colour relation. The calibration of this relation depends essentially on those Cepheids which are members of galactic clusters, whose distances in turn are directly dependent on the distance of the Hyades cluster (cf. 1.3).

Spectroscopic data of individual stars in the Magellanic Clouds have increased considerably during recent years. Already the first spectral types of bright stars in other nearby galaxies become available. The Space Telescope will provide a vast amount of such data. It is therefore evident that an improvement of the luminosity calibration especially of the intrinsically bright stars will be beneficial for the extragalactic distance scale.

In general there can be no doubt that an improvement of the distances within the Galaxy shall have almost automatically an effect on the accuracy of the extragalactic distance scale and the value of the Hubble constant.

1.4 Stellar Masses

The traditional method of determining masses has been through the analysis of observations of visual binaries and appealing to Kepler's third law. According to this the sum of the masses, in solar units, is given by

$$M_1 + M_2 = \frac{a^3 \pi^{-3}}{P^2}$$

where P is the period in years and a is the semi major axis of the relative orbit in arc seconds. The ratio of the masses can be determined when the relative sizes of the orbits of each component about their centroid is known. We see that the relative error of the parallax, π, enters into the error of the mass determination with a factor of 3.

Although the latest catalogue of double star orbits (Finsen and Worley 1970) contains data for more than 700 systems, of which more than 50 percent are good or reasonably good, less than 50 pairs have parallaxes larger than $0''.04$ and only one of these, Capella (G0III + G5III) contains giants. Cester (1963) lists dynamical parallaxes for nearly 300 systems, most of which are within 100 parsecs. When good trigonometric parallaxes have been measured for these, as will be possible from HIPPARCOS, the number of mass determinations of visual binary components will increase by a factor of six, including many more giant stars.

A second, and very promising method, for deriving masses uses the angular diameters, θ , of single stars, obtained for example by interferometry (e.g. Hanbury Brown et al. 1974) or through measurement of the infrared flux (Blackwell and Shallis 1979). In this method (Oxford method), the mass is given by

$$M \propto g \, \theta^2 \, \pi^{-2}$$

where g, the surface gravity, must be determined by spectroscopic methods; in this case the relative parallax error only enters with a factor 2 into the mass error. Recently, Blackwell and Willis (1977) have developped a method for determining g for stars with spectral types in the range F5-K2, which is of particular importance for deriving the masses of single red giants. Masses for several hundred stars in the Yale Bright Star Catalogue (Hoffleit 1964) will be obtainable in principle by the Oxford method when angular diameters and parallaxes are available.

1.5 Stellar Kinematics and Dynamics

The component of velocity across the line of sight is given by

$$V_T = \frac{4.74\,\mu}{\pi} \text{ km s}^{-1}$$

where μ is the annual proper motion and π is the parallax, both measured in arc sec. Assuming that μ,π have the same error ε, the corresponding relative error in V_T is

$$\frac{\varepsilon_{V_T}}{V_T} = \frac{\varepsilon}{\pi} \left\{ 1 + \left(\frac{4.74}{V_T} \right)^2 \right\}^{\frac{1}{2}}$$

Beyond some critical value $\pi = \pi_o$ it is better to use a photometric parallax derived from the distance modulus. If this has a standard deviation ε_M, then

$$\frac{\varepsilon_{V_T}}{V_T} = \left\{ 0.212\, \varepsilon_M{}^2 + \left(\frac{4.74\, \varepsilon}{V_T\, \pi} \right)^2 \right\}^{\frac{1}{2}}$$

Assuming $\varepsilon_M = \pm 0^m.3$ and $\varepsilon = \pm 0''.01$, we find for ground based observations that $\pi_o = 0''.0725$, whereas for measurements from HIPPARCOS ($\varepsilon = \pm 0''.002$), $\pi_o = 0''.0145$. In the latter case transverse velocities with relative error not exceeding 15 per cent will be derived from purely astrometric data out to a distance of about 70 parsecs.

The proportional error in V_T for $V_T = 10$ km s^{-1} and $V_T = 50$ km s^{-1}, for various values of the parallax are given in Fig. 1.3. For ground based observations the curves are similar but the abscissa (π) for a given ordinate ε_{V_T} / V_T, must be multiplied by five.

With new data from HIPPARCOS, including revised photometric distances obtained by recalibration of absolute magnitudes, transverse velocities of low velocity objects within 200 parsecs will be determined to within 25 per cent. Investigation of the so called moving groups and the kinematics of Gould's Belt will then be possible in much greater detail than hitherto, For nearby young stars (age < 10^8 years) it will also be possible to trace the galactic orbits backwards to find the locations of star formation.

The calculation of orbits demands a model of the mass distribution in the Galaxy and also its size and angular momentum. Basic data for contructing such a model are Oort's constants A, B and the distance, R_O, from the Sun to the galactic centre. Measurement of proper motions of many distant young objects in the galactic plane, such as O, B stars, cepheids and open clusters, which do not suffer from the inhomogeneity of existing ground-based data will yield new determinations of A, B with perhaps errors of only ten percent. It will be recalled that B, reflecting a rigid rotation can only be measured directly by means of proper motions. Measurement of A by means of radial velocities involves an assumed scale of distances; therefore comparing this with the independent value from proper motions, and also using the revised photometric calibration, the galactic distance scale and in particular, R_O, should be determined with much greater confidence than is possible at present. Proper motions of distant young objects in the galactic centre and anticentre directions will provide new and independent data for determining the galactic rotation curve and hence evidence for or against the existence of a massive halo.

Analysis of stellar motions in the solar neighbourhood has hitherto in most cases been based on a steady state model of the galaxy with cylindrical symmetry. With the new data for many thousands of stars down to faint magnitudes which will be obtained with HIPPARCOS it will be possible to subdivide the data according to age, composition, and distance as well as galactic longitude and latitude in order to analyse systematic variations from the basic cylindrically symmetric steady-state model. In particular, tests for significant effects caused by spiral density waves or lack of dynamical symmetry in the motion perpendicular to the galactic plane could be performed. Study of these motions will also lead to improvement in our knowledge of the local mass density.

1.6 Solar System and Geodynamics.

At the present time, the measurement of the rotation of the earth and of polar motion are nominally referred to the system of the FK4 catalogue. However many of the observations, for instance those made for the International Latitude Service and those made with photographic zenith tubes use special catalogues which have been linked to the FK4 system by special meridian observations. The relative positions of the stars in these special catalogues are smoothed by the chain method in which time and latitude measurements made on the same night with respect to stars in different right ascensions are compared. Closing errors of the chain, of 0.2 arcsec or even greater, are commonly found at some stations. Uncertainty in the apportionment of such a closing error to the catalogue positions, as a function of right ascension sets a fundamental limit to the accuracy of the relative star positions, and to the determination of periodic variations in station coordinates and the nutational motion of the earth. Diurnal and annual periods are of course particularly vulnerable to this source of uncertainty. A re-examination of observations made over the past century, using the homogeneous stellar reference frame to be provided by HIPPARCOS will form the basis for a new determination of the geophysical parameters which describe the structure of the earth, and also new data on the local effects which give rise to the observed closing errors.

Inhomogeneity in the proper motion system of the FK4 causes spurious apparent rotation of the reference frame with respect to which the orbits of the earth and planets are referred. In particular, observations of the extreme outer planets Neptune and Pluto extend over less than one orbit and therefore regional errors in the stellar reference frame influence the accuracy of the determination of orbital elements and can also correlate with effects which arise from periodic perturbations. In the case of the earth's orbit, an apparent secular decrease in the obliquity of the ecliptic of 0.3 arcsec per century has been derived from planetary observations; this is far too large to be accounted for, by planetary theory, as a rotation of the earth's orbit. On the other hand, if it were a real rotation of the earth's equator, then the current estimate of the angular velocity of the galaxy in the solar neighbourhood would have to be approximately doubled. It is probable that this discrepancy arises because of errors in the proper motion system currently used.

A homogeneous stellar reference frame is also required for mapping the motions of the smaller bodies in the solar system, such as asteroids and satellites. Errors in the present reference frame limit the accuracy with which the motion of a moving object relative to the stars can be extrapolated, even over a period of a few weeks, to several tenths of an arc second; errors of this size are fatal, for example, in predicting occultations by these objects which are of considerable interest for physical studies. They also limit the precision with which the orbital elements of the satellites and physical properties of the parent planet can be measured.

The acceleration of the moon in its orbit, relative to atomic time, is obtained from analysis of lunar occultations. At the present time the star place error contributes about fifty per cent, statistically, to the error of a visual occultation observation (Morrison 1979) and proportionately more to a photo-electric one. Therefore the re-discussion, using the HIPPARCOS catalogue of occultations obtained since 1955, when atomic time was first introduced, will increase the weight of the observed acceleration by at least a factor of two. Now that the lunar tidal acceleration can be determined from modern observations of artificial satellites (Goad and Douglas 1978) comparison between this, and the acceleration determined from occultations, will provide a test of a possible secular change in the constant of gravitation (Van Flandern 1975).

1.7 Observational Programme

Considerable interest in the HIPPARCOS project has been shown by many individual astronomers, as the result of an informal survey conducted by E.Høg. This enquiry solicited suggestions for particular research programmes requiring data from HIPPARCOS; recipients were asked to give the approximate apparent magnitude limit (to the nearest whole magnitude) and total numbers and types of stars, as well as the data and accuracy required. Although it is not appropriate to give here details of the proposed programmes, it should be remarked that some 150 projects (not all independent) were proposed by 125 astronomers, mostly from ESA countries, this in itself shows the likely impact of HIPPARCOS on astronomical research.

Many of the suggested projects have been covered in general terms in the review of the capabilities of HIPPARCOS which has been given in previous sections; not all of them however are feasible within the set boundary conditions of accuracy or surface density.

Most projects would be feasible within a basic programme confined to stars brighter than $m_V = 9$, but a few require additional fainter stars. Feasible projects needing stars with $m_V > 9$ or $m_B > 10$ have therefore been examined and it is found that nearly all would be covered by the special selections listed in Table 1.3.

In Table 1.3, N is the required number of stars and m_V, m_B are magnitude limits given by the proposer. Clearly there may still be some duplication of stars in Table 1.3; in particular the requirements for the reference frame could partly be covered by stars in other categories.

The compilation of a definitive observing progamme for HIPPARCOS is clearly a non-trivial task. But nevertheless a good first approximation can be obtained by combining a general survey complete to $m_V \leq 9$ which would contain about 1.2×10^5 stars, together with the 2×10^4 stars in Table 1.3. The total of 1.4×10^5 is certainly an underestimate since the apparent magnitude cut off at $m_B = 10$ is on average fainter than $m_V = 9$. The numbers could readily be adjusted by adopting a slightly lower magnitude limit for the general survey. For example there are only about 7×10^4 stars with $m_V \leq 8.5$. The choice of the latter limit for the survey has the added advantage that it is approximately the completeness limit of the Henry Draper Catalogue of spectral types, for which modern two dimensional MK classifications are being published in the Michigan Spectral Catalogue (e.g. Houk 1979) . Apparent magnitudes and approximate coordinates (to the nearest $0^m.1$ in RA and 1' in Dec) are already available in HD.

Any selection of stars such as the one proposed above, based on purely astrophysical requirements would probably also satisfy the needs of a whole sky frame of reference, but this would have to be examined and, if necessary, stars added to the programme in any particularly sparse region.

Table 1.3 Example of a selection of stars to be included in the HIPPARCOS observing programme, as derived from an informal survey of astronomer's requirements.

	N	Limits m_V	m_B
Variable Stars			
RR Lyraes	200	12	
Cepheids	300	11	
Miras	1000		14
Others	100		14
Star Clusters			
Hyades members	80	12	
U Maj	200		11
Globulars (5 x 50)	250		12
Open (5 x 200)	1000	11	
Field Stars			
G-K III	2000	10	
K7-M2 V	1200	11	
G-K	5000		14
O-A	2000		14
Reference Frame			
Faint reference system	5000	12	
Radio star	50	13	
Quasar fields (5 x 400)	2000	12	

1.8 Related Ground-Based Astrophysical Observations

After the selection of the stars included in the programme, it is highly desirable to obtain more detailed and accurate astrophysical data for these stars. The basic astrophysical information required to make full use of the astrometric data obtained from space may be briefly summarized as follows:

1: accurate classification of the objects as to type (spectral class, population type, peculiarities);

2: distance modulus (if no trigonometric parallax);

3: effects of interstellar medium;

4: radial velocity.

Among existing observing techniques, it seems fairly clear that intermediate band photometry (points 1-3) and the Griffin photo-electric scanning method (point 4) would be the most efficient ways to obtain this information for large numbers of stars. The maximum effort involved can be estimated by considering, as a concrete example, a programme of 100 000 stars of average magnitude around 10^m.

A telescope size of 1.5 m seems a reasonable compromise between size and availability. Experience with existing multichannel photometers and radial velocity scanners indicates that integration times with a 1.5 m telescope would be of the order of 30-60 sec. 500 observations in an average night should thus be possible, assuming an efficient method of moving from star to star. If three observations of each type are required for the detection of most of the variable objects, one needs in each hemisphere about 600 clear nights, or some full two years on a first-rate site, to complete such a programme of astrophysical observations.

This obviously represents a major effort, but is not at all impossible if carried out over a decade or so, even if one contemplates to use existing telescopes. It does not follow however that it would remain a realistic proposition if its extent were doubled or tripled. It therefore seems imperative to select very judiciously the number and kinds of stars on the observing progamme in order to obtain the maximum useful information from the effort invested. The decision whether or not to follow up systematically all stars which are variable in light or velocity has a profound influence on the possible size of programme, since that alone implies about a doubling of the total number of observations estimated above.

Preparatory work for the supplementary astrophysical programme includes:

a: perfection of methods for rapidly setting and centering on a star ;

b: extension of photo-electric radial velocity methods to all spectral types;

c: development of optimum photometric systems with regard to both astrophysical information and efficiency in observing. In this connection, it should be recalled that the number of stars with good trigonometric parallaxes available for the basic calibration of such systems would be dramatically increased by the astrometric space programme.

It appears from above that a good deal of collaboration and coordination is required between on the one side space astrometry, and on the other side ground-based astrometry and astrophysically ground-based observations if full benefit and quick results are to be drawn from the satellite.

1.9 Summary and Conclusions

In the first six sections of this report, we have reviewed the potential significance of HIPPARCOS to many branches of astronomy, and in the seventh section a possible strategy for selecting stars for the programme has been outlined.

It is very likely that HIPPARCOS will lead to the discovery of physical processes inside the stars, which have escaped investigations until now. A new era of the theory of the internal structure of the stars will begin, with a large number of consequences for the problems concerning the structure and evolution of the galaxies and the structure of the Universe. The basic quantities, for which one needs an absolute determination are the total luminosity, i.e. the amount of energy radiated away per unit of time, the total mass and the radius which is defined by the surface which is opaque to continuum radiation at all wavelengths. To allow valuable tests of the theories, these quantities have to be known as precisely as possible.

Not all the problems discussed will be solved even when the new astrometric data become available; much complementary ground-based work particularly photometry and spectroscopy will be needed. Nevertheless, HIPPARCOS will provide astrometric data of very high quality, which will supersede nearly all the existing data for the brighter stars, particularly the trigonometric parallaxes, and ultimately lead to an order of magnitude refinement in our understanding of dynamics and structure of our Galaxy.

References (Section 1)

Allen C.W., 1955 Astrophysical Quantities 1st Edn. Athlone Press.
Allen C.W., 1973 Astrophysical Quantities 3rd Edn. Athlone Press.
Blaauw, A., 1973 IAU Symposium 54, 47. D. Reidel.
Blackwell, D.E. and Willis, R.B., 1977 Mon. Not. R. Astr. Soc. 180, 169.
Blackwell, D.E. and Shallis, M.J., 1977 Mon. Not. R. Astr. Soc. 180, 177.
Cester, B., 1963 Pubb. & Rist. Oss. Astron. Trieste. No. 319.
Dieckvoss, W., Kox, H., Gunther, A., and Brosterhus, E., 1975 AGK3, Hamburg Bergedorf.
Finsen, W.S., and Worley, C.E., 1970 Repub. Obs. Circ. 7, 203.
Fricke, W., 1967, Astron. J. 72, 1368.
Fricke, W., and Kopff, A., 1963, Fourth Fundamental Catalogue (FK4), Veroff. Astron. Rechen. Institut. Heidelberg, No. 10.
Gliese, W., 1957, Astron. Rechen-Institut, Heidelberg Mitt. Ser. A. No. 8.
Gliese, W., 1969, Veroff. Astron. Rechen Institut, Heidelberg, No. 22.
Gliese, W., and Jahreiss, H., 1979 (in press).
Goad, C.C. and Douglas, B.C., 1978, J. Geophys. Res. 83, 2306.
Hanbury Brown, R., Davis, J., and Allen. L.R., 1974, Mon. Not. R. Astr. Soc. 167, 121.
Hoffleit, D., 1964, Catalogue of Bright Stars, Yale University.
Houk, N., 1979 Ric. Astr. Specola Vaticana 9, 51.
Jenkins, L.F., 1952, General Catalogue of Trigonometric Stellar Parallaxes, Yale University.
Jenkins, L.F., 1963, ibid. Supplement.
Kovalevsky, J., 1975, Space Astrometry, ESRO Symposium Frascati 22-23 Oct. 1974, 67.
Morrison, L.V., 1979, Mon. Not. R. Astr. Soc. 187, 41.
Murray, C.A., 1974, IAU Symposium No. 61, 152, D. Reidel.
Murray, C.A. and Corben, P.M., 1979, Mon. Not. R. Astr. Soc. 187, 723.
Neckel, H., 1975, Astron. and Astrophys. 42, 379.
Pagel, B.E.J., 1979, European Satellite Astrometry, 211, U. of Padova.
Sandage, A., 1970, Astrophys. J. 162, 841.
Van Altena, W.F., 1973, IAU Symposium No. 54, 23, D. Reidel.
Van Altena, W.F., 1974, P.A.S.P. 86, 217.
Van Altena, W.F., 1977, Bull. A.A.S. 9, 278.
Van den Bergh, S., 1977, Astrophys. J. 215, L103.
Van Flandern, T.C., 1975, Mon. Not. R. Astr. Soc. 170, 333.
Wilson, O.C., 1976, Astrophys. J. 205, 823.
Woolley, R. v.d. R., Epps. E.A., Penston, M.J. and Pocock, S.B., 1970, R. Obs. Annals, No. 5.

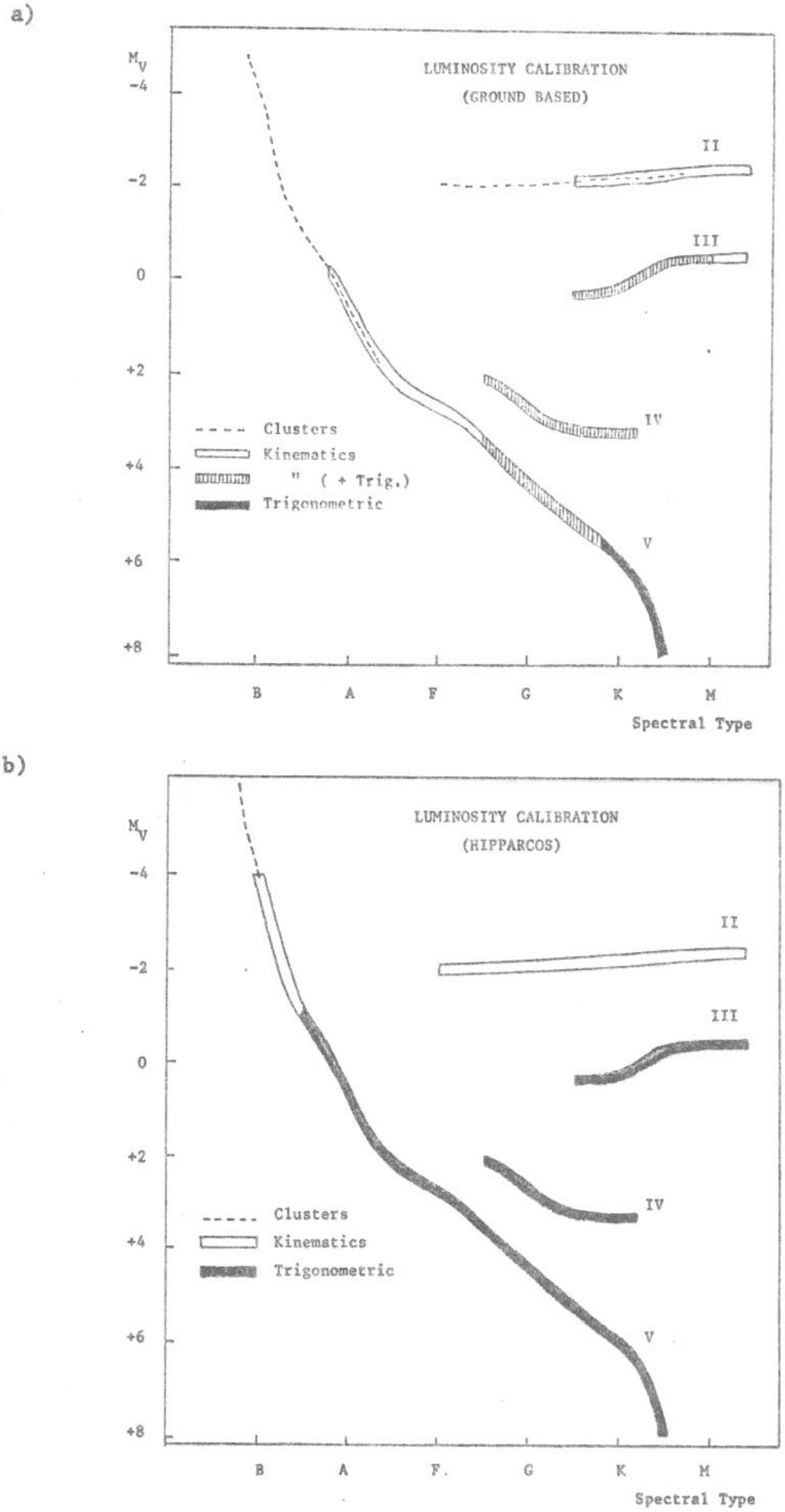
a)
LUMINOSITY CALIBRATION
(GROUND BASED)
M_V
-4
-2
0
+2
+4
+6
+8
II
III
IV
V
---- Clusters
Kinematics
" (+ Trig.)
Trigonometric
B
A
F
G
K
M
Spectral Type
b)
LUMINOSITY CALIBRATION
(HIPPARCOS)
M_V
-4
-2
0
+2
+4
+6
+8
II
III
IV
V
----- Clusters
Kinematics
Trigonometric
B
A
F.
G
K
M
Spectral Type

FIGURE 1.1

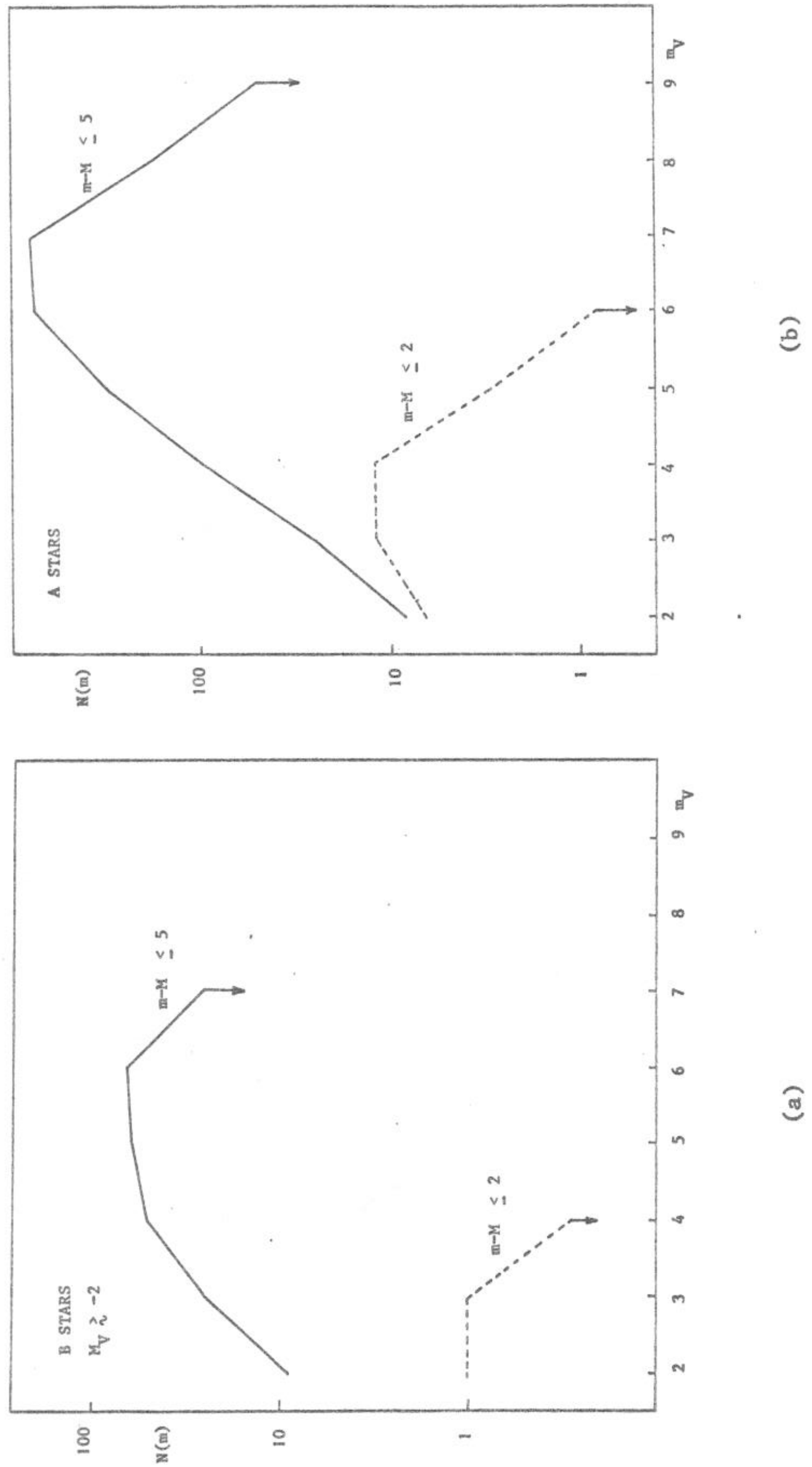
A STARS
m-M ≤ 5
m-M ≤ 2
N(m)
100
10
1
2
3
4
5
6
7
8
9
m_V
(b)
B STARS
$M_V \gtrsim -2$
m-M ≤ 5
m-M ≤ 2
100
N(m)
10
1
2
3
4
5
6
7
8
9
m_V
(a)

FIGURE 1.2

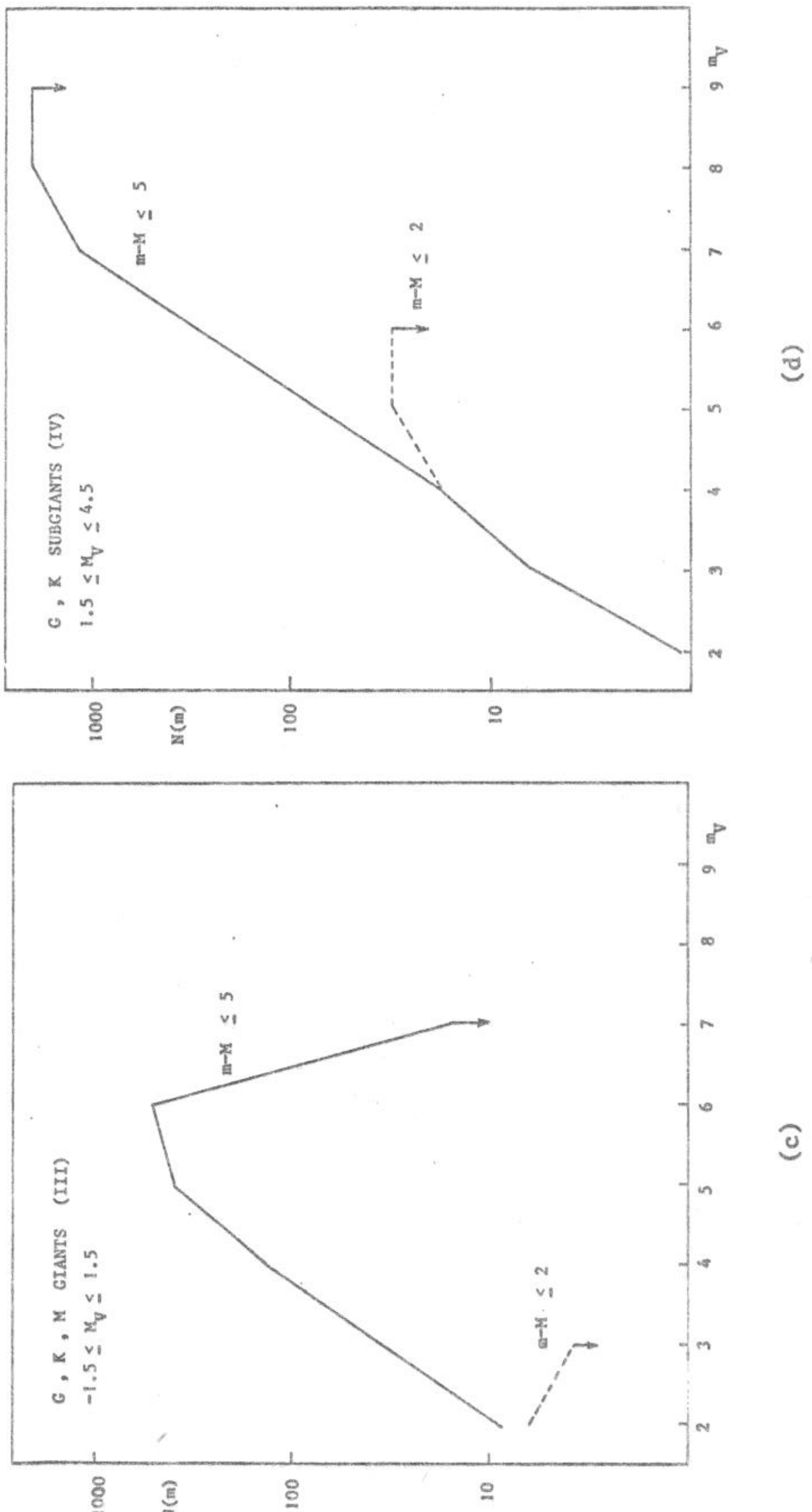

FIGURE 1.2 (cont.)

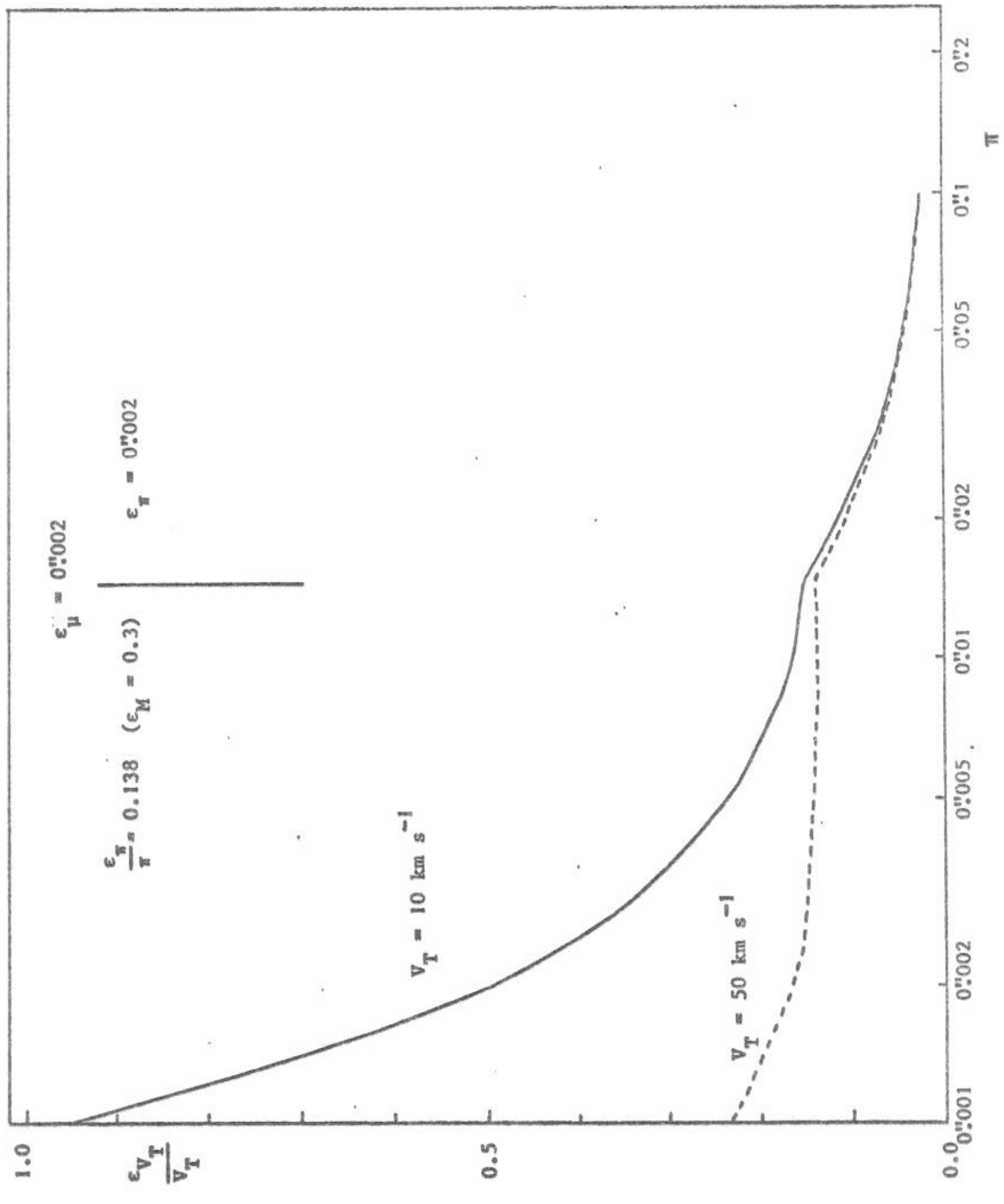
1.0
0.5
0.0
ε_VT / V_T
0".001
0".002
0".005
0".01
0".02
0".05
0".1
0".2
π
V_T = 10 km s^-1
V_T = 50 km s^-1
ε_π / π = 0.138 (ε_M = 0.3)
ε_μ = 0".002
ε_π = 0".002

FIGURE 1.3

2. OTHER MODERN ASTROMETRIC TECHNIQUES

2.1 Astrometric Use of the Space Telescope (ST)

It is intended to utilize the Fine Guidance System of the Space Telescope for relative astrometry. The system consists of three independent sensors, each capable of locating and guiding on a star in a separate annular segment of about 4' x 20'. While two sensors are used for guiding the telescope, the third is available for relative astrometric measurements within its field of view. A mean error of 0".002 is expected for a single observation and 0".0005 can be reached for a relative parallax after averaging and calibration. The magnitude range is approximately $m_V = 10 - 20$.

In addition, the Wide Field/Planetary Camera (2'.7 or 1'.1 field), and Faint Object Camera (11" or 22" field) can be used for determination of proper motions within very small fields, and occultations can be observed with the high speed photometer.

Thus, very accurate relative parallaxes and proper motions may be determined for selected faint stars in a number limited by the competition on observing time with the many other tasks of the ST. The HIPPARCOS project, on the other hand , aims at absolute astrometry of very many relatively bright stars. The two projects are therefore complementary and a certain coordination of observational programmes should be established in order to make the best use of this powerful combination of instruments. The contribution of the Space Telescope to the HIPPARCOS mission would include: (1) to determine a rotation-free proper motion system for the HIPPARCOS observations, and (2) to convert relative proper motions and parallaxes obtained by ST in other fields to absolute ones.

2.2 Ground-Based Photoelectric Techniques

The introduction of photoelectric detectors to replace the human eye or photographic plate has already permitted a significant improvement of efficiency, accuracy, and limiting magnitude in the areas of global astrometry (meridian circles) and very narrow-field astrometry (area scanners). For ground-based determination of relative parallaxes and proper motions, however, relative measurements over intermediate angles ($\leq 0.5^o$) are required. In this area photographic methods are still unsurpassed, although several experiments with photoelectric detectors have been made (mask detection system, area multiplexing) and still more refined techniques proposed.

The limiting factor is ultimately the turbulent atmosphere. For global astrometry, the practical limit set by the atmosphere (0".1 - 0".2) has already been reached, and expected improvements are rather in terms of efficiency and systematic accuracy. Automatic meridian circles currently under development are expected to produce, at the end of the 1980's, about 200.000 observations per year down to the 12th magnitude, with a mean error of 0".2 in positions. The existence of a highly accurate positional reference system provided by HIPPARCOS will by no means obviate the need of meridian observations; on the contrary, these will greatly benefit from the nearly complete elimination of instrumental and refractional systematic effects made possible by such a reference system. Future ground-based observing programmes will however necessarily concentrate more on fainter stars and solar-system objects than is presently the case.

The prospects of ground-based narrow-field astrometry, e.g. for determination of relative parallaxes, is a slightly controversial subject, owing to the lack of relevant observational and theoretical data on the relevant atmospheric effects. However, a recent theoretical study of the atmospheric limitations to narrow-field astrometry has shown that, with reasonable integration times, the practical limit of accuracy is around 0".001 (Lindegren, preprint 1979). A maximum of about 100 such parallaxes could be produced per year with an ideal instrument. The parallaxes would of course be relative only; the choice of background stars is a major problem and the derivation of their mean parallax may involve cumbersome spectroscopic and/or photometric investigations. On the other hand, in comparison with the astrometry satellite, ground-based narrow-field techniques, like the Space Telescope, has the advantage of a faint magnitude limit and a longer time base (the latter particularly important for astrometric detection of planetary systems), and is thus a necessary complement to HIPPARCOS.

2.3 Interferometry

2.3.1 Radio

Extragalactic objects, with no measurable proper motion, are ideal for defining an inertial system. Radio interferometry has already achieved the same accuracy as the best optical instruments and has the potential to decrease the error to 0".001 and less for the very long baselines (VLBI), if the overall system stability can be increased and calibration procedures refined. The interferometric measurements give the absolute declination and absolute right ascension differences free of regional, systematic errors. This allows the definition of a fundamental reference system, which, however, is restricted to optically faint objects of 15th to 19th magnitude so that the problem of the link to the reference stars remains. Furthermore, the large majority of the objects which can be observed radio interferometrically are resolved, both in the radio and in the optical domain (radio galaxies), so that one cannot truly rely on positional coïncidence at the level of the achievable accuracies.

For true point-source objects the linking problem might be solved by new optical interferometric techniques, provided that the astrometric mission includes several stars of magnitude 9-12 within a degree of the extragalactic reference point. There are also about 10-15 radio-stars that can and must be part of the programme of the astrometric satellite and that will contribute to this link.

2.3.2 Optical

Optical interferometry is an old technique that has just become operational for studying double stars. In the case of very narrow field astrometry (field diameter < 5") speckle and Michelson interferometry in visual and infrared light will permit an increase by two or three orders of magnitude on the precision of double star and diameter measurements. Reported results by speckle interferometry give for the separation of binaries a precision reaching 0".002 - 0".005. The best accuracy achieved in that field by Michelson interferometry is 0".0004. It is expected that from the ground and also if embarked upon a Spacelab, the direct interferometric techniques will permit the measurement of angular distances of stars with magnitude 17 or smaller to an accuracy of 0".001 or better, provided that they are within 1^{o} of separation. This technique, like the use of the Space Telescope, will complement the astrometric satellite mission by linking the reference frame to quasars.

It will also permit to increase the number of stars observed in open clusters whose distances will be determined by the mission. It will also be used to determine the orbits of close binaries whose distances will be measured by the astrometric satellite and therefore contribute to the determination of new precise stellar masses.

2.4 Ranging Techniques

The laser ranging technique, with an internal accuracy of a few cm, has been applied to the tracking of artificial satellites and the moon, where a number of corner reflectors have been placed. Reduction and interpretation of observations is considerably complicated by the large number of parameters occurring in the solution. Main implications are in the areas of geodesy and the dynamics of the earth-moon system.

The radar technique has been applied to the terrestrial planets, asteroids, Jupiter (satellites) and Saturn (rings). The achievable accuracy, of the order of a km, allows a very important improvement of the ephemerides of these objects. The method is however hampered by the errors due to the planetary topography.

Radio tracking of interplanetary probes and planetary orbiters and landers provide a small number of very precise fixes on planetary positions and determinations of masses and gravitational harmonics.

Ranging techniques employing laser, radar, and radio tracking of spacecraft thus allow to improve considerably the accuracy of the positions, motions, and masses of a limited number of solar-system objects and the definition of an absolute dynamical frame of reference. However, the connection of these observations to easily accessible reference stars, providing a sufficiently dense distribution over the whole celestial sphere, remains a major problem. HIPPARCOS can help to provide the necessary link by observing a small number of asteroids and satellites.

3. PAYLOAD

3.1 Principles

The methods used for the execution of the astrometric mission and the preliminary description of possible technical solutions were defined by the Mission Definition Group during their study in 1975/1976 and analyzed during the phase A study in 1977/1978 (Document DP/PS(78)13 of 26 April 1978).

The basic principle of observation is to scan continuously and systematically the entire sky with a telescope capable of accurately measuring the angles between stars separated by a large angle. By numerically combining several millions of such angle measurements collected over a time span of a few years, it is possible to derive the astrometric parameters (i.e. the parallax and the components of the position and proper motion) of each star.

The angles are measured by superimposing in the focal plane of a single telescope two fields of view, 68°.5 apart on the sky, each field containing one of the stars in a pair. The angle (γ) between the two fields of view is maintained by a complex mirror in front of the telescope, splitting its entrance pupil into two equal parts and directing the light from one star into one half of the entrance pupil and that from the other star into the other half. The value of the basic angle (γ) results from a compromise between scientific requirements and technical limitations. From a scientific point of view, a basic angle of the order of 1 or 2 radians is desirable in order to:

- improve the rigidity of the system of coordinates and proper motions by directly linking together widely separated parts of the sky, and

- to obtain absolute parallaxes by direct comparison of stars having very different parallax factors (the parallactic displacement of a star is the absolute parallax times the parallax factor, which is proportional to the sine of the angle between the sun and the star).

On the other hand, the value of the basic angle should not be a divisor of 360 and it is constrained by the length of the telescope (lower limit to the basic angle), and the Schmidt correcting surface at the level of the complex mirror (upper limit; cf. 3.2.1).

The attitude of the spacecraft about its centre of gravity is controlled in such a way as to scan the whole celestial sphere in a regular movement. As a result, the star images move across the focal surface of the telescope. A direct measurement of the relative positions of the stars in a pair on the focal surface could not be made with the required accuracy due to the non availability of a two-dimensional detector with a pixel size much smaller than 1 arcsec (about 12 microns), and with an adequate time resolution and positional stability. Instead, use is made of a system of grids situated at the focal surface, composed of alternatively opaque and transparent bands (cf. Fig. 3.4), normal to the apparent direction of motion of the stars, which modulate the incoming light. Behind these grids, an image dissector tube (IDT) whose instantaneous field of view (IFOV) follows the star path, converts the modulated light into a sequence of photon counts from which the phase of the entire pulse train corresponding to a star can be derived. The apparent angle between two stars in the combined field of view is obtained from the phase difference between the corresponding pulse trains.

With the image dissector tube it is no longer possible to obtain strictly simultaneous observations of several stars. Attitude irregularities will consequently introduce small errors into the angle measurements. These are however reduced to a negligible level by switching the IFOV rapidly between the different programme stars in the combined field of view in such a way that it periodically returns to a particular star several times per second. In order to direct the IFOV to the correct position and properly follow a star image across the field of view, the celestial coordinates of the star and the three-axes attitude of the instrument must be known in real time to within a few arcs. Star coordinates are up-linked from the ground, but the attitude determination for this purpose must be performed on board, using gyros and observations with a star mapper.

The basic principle of observation is one-dimensional, i.e. to measure instantaneous relative positions of stars along the scanning great circles. Only parameters producing measurable relative displacements along the scan are thus theoretically observable; in addition, since all five astrometric parameters of a particular star combine to produce a certain displacement at the instant of observation, that star has to be observed at least five times at which the parameters combine in distinctly different ways.

The photon counts are transmitted to the ground and processed to yield the times at which the star images crossed the different slits, and hence the relative positions of the stars in the combined field of view. The true angle between two stars belonging to different fields of view is obtained by adding the basic angle to the apparent angle in the combined field of view. The full data analysis will be discussed in detail in section 5.

The present study has shown that a satellite configuration comprising two sub-assemblies with minimum interfaces was to be preferred: these sub-assemblies are the payload and the spacecraft. The payload includes the optical sub-system (telescope, complex mirror), the modulation sub-system (grids and star mapper) and the detection sub-system (image dissector tube, photomultiplier); the spacecraft carries all the usual technical sub-systems, such as power supply, attitude control, telecommunications. Each sub-assembly can be separately developed and integrated in its specific structure and carries its own thermal control. All critical accuracy aspects are concentrated on the rigid payload sub-assembly, which is attached to the spacecraft with very moderate alignment specifications; the spacecraft is therefore composed of quite conventional equipment.

The description of the payload in the following sections 3.2 to 3.9 is a summary of a number of various studies, such as:

- the initial phase A study conducted by Aeritalia and MATRA,
- some sub-systems studies executed by ESTEC specialists (e.g. thermal control, data handling)
- the results of numerical computations using the software implemented by AML on the ESOC computers,
- theoretical analyses performed by members of the science consultancy group,
- and, finally, a short complementary study from MATRA, at the end of 1979, on some critical aspects.

3.2 Telescope

3.2.1 Optical Concept of the Telescope

As a result of the considerations contained in the report DP/PS (78)13 sections 2.2 and 2.3, the selected optical design is based on an all reflective Baker Schmidt system, in which the correction plate is obtained by deformation of the surfaces of the beam-splitting complex mirror located in front of the telescope.

The complex mirror consists of two mirrors, tilted in opposite direction, each occupying half of the entrance pupil. The entrance pupil has been made rectangular in order to improve in a significant way the theoretical optical transfer function (OTF). As a consequence, the secondary mirror is rectangular in shape

It is of interest to reduce as much as possible the angle between the normal to the beam-splitting mirrors and the telescope axis; however, the smaller the angle, the longer the minimum distance between the complex mirror and the primary mirror. As a trade-off, this last distance has been chosen as 1300 mm, which allows an inclination of about 17^{o}, leading to a basic angle of 68^{o}.5 (between the two fields of view).

Assuming for the deformed mirror profile a simple fourth order curve, a third order solution has been found and subsequently optimised by ray tracing. The main parameters are given in Table 3.1. Figure 3.1. represents the light path and Figure 3.2 is a drawing of the optical lay-out.

The unvignetted field of view is 94 arcminutes x 54 arcminutes, corresponding to linear dimensions of 67.2 mm x 38.6 mm at the focal surface, or 11.9 microns per arcsecond.

Table 3.1 Optics Main Parameters

Curvature radius of primary mirror	:	2.047	m
Curvature radius of secondary mirror	:	1.102	m
Distance primary - secondary	:	0.700	m
Distance primary - complex mirror (pupil)	:	1.300	m
Distance primary - focal surface	:	- 0.07473	m
Equivalent focal length	:	2.464	m
Field curvature radius	:	1.2	m
Inclination of complex mirror surfaces	:	± 17.125	deg
Rectangular pupil at the level of complex mirror	:		
Length	:	0.25	m
Width (per field)	:	0.10	m
Linear obscuration ratio	:	0.44	
Collecting aperture (per field)	:	0.020	m^2
Dimensions of the mirrors	:		
Primary mirror diameter	:	0.286	m
Secondary mirror	:	0.094 m x 0.110	m

Although the final optimisation of the telescope optical design may lead to some parameter changes in Table 3.1., it has been verified that the nominal instrument can be corrected beyond any practical significance. However, it is clear that the true instrument operating in orbit will differ from the nominal one, due to manufacturing tolerances and to the space environment, particularly thermal and radiative. Therefore, an important effort has been put in defining the required specifications and in verifying that they can technically be met.

The performance of the nominal instrument and its sensitivity to perturbations have been studied by means of extensive runs of the software package for the study of accuracy (see Section 5.1) implemented on the ESOC computers.

These computations have led to the following conclusions :

- absolute tolerances on misalignment: the most critical specification concerns the distance primary-secondary mirrors, which shall be fixed with a tolerance of a few micrometers. In order to correct possible permanent displacements due for instance to the launch environment, and also very slow variations due to ageing (e.g. radiations influences), it has been decided to incorporate in the payload an on-board refocussing device. This device, in fact, acts on the grid position. It will be operated from ground telecommand, and will permit the optimisation of the modulation signal. It is anticipated that refocussing will have to be checked at long intervals of time, perhaps every six months.

- tolerable variations over one full revolution (2.4 hours): the most critical specification again concerns the distance primary-secondary mirror, which shall not vary by more than about 0.5 micrometer; also, it is estimated that the angular position of the grid with respect to the complex mirror shall remain constant within 0.3 arc second. In addition, the basic angle between the two fields of view shall be stable within the expected accuracy, inc. about 1 milli-arcsecond.

All these stability requirements have been translated in terms of thermal control requirements and have been used to design the thermal control subsystem. It appears, subject to confirmation by a more detailed study, that the mechanical misalignment can be easily made negligible, and that the only critical aspect is the basic angle stability; the active control subsystem, however, can meet the corresponding requirements.

- mirrors surface deformations: the maximum acceptable surface deformations, due to manufacturing tolerance has been estimated to be of the order of $\lambda/50$ for each of the three mirrors. This point is further discussed in Section 3.2.2.

3.2.2 Manufacture of the mirrors

From the accuracy analysis carried out with the ESOC software developed by AML (section 5.1), it was determined that an overall wavefront error of about 0.04λ was acceptable. The following budget has then to be established :

- on-orbit misalignment	0.005 λ
- initial misalignment	0.0083 λ
- mirrors figure errors	0.0387 λ
combined rms error	0.04 λ

A reasonable allocation for each mirror takes into account their relative manufacturing conditions; a preliminary specification is:

- complex mirror	0.030 λ
- primary mirror	0.017 λ
- secondary mirror	0.017 λ

It has been verified, by consideration of the various elementary sources of error, that these tolerances can be realistically met for the primary and the secondary mirrors. For the complex mirror, the manufacturing process proposed by MATRA consists in evaporating under vacuum a source of silica which is deposited on a substrate under control of a rotating mask. This method yields an accuracy of about 0.5 to 1% of the maximum thickness of the deposit. To obtain the required accuracy, an optimisation of the shape of the mirror surface, aiming at decreasing the thickness at the edge, is necessary and is planned in the near future.

The proposed manufacture of the complex mirror follows the following steps:

- polishing of a prismatic circular blank to a plane, with a surface accuracy, controlled by interferometry, of 0.01 λ;
- cutting into two semicircular parts,
- polishing of the cut planes, and of the back sides,
- vacuum deposit on assembled parts to the required shape,
- assembling of the two parts by molecular adherence.

3.3 Grid System

The grid system comprises two sets of transparent slits manufactured on the curved surface of a supporting glass plate (Fig. 3.4):

- the star mapper grid, used for determining the approximate three-axis attitude of the telescope as a number of selected stars with approximately known positions enter the field of view: this grid is double, with two identical parts situated on both sides of the modulating grid;
- the modulating grid, which enables accurate determination of the one-dimensional coordinates, in the direction of scanning, of the programme stars as they move across the field of view.

The light originating from the modulating grids is reflected by a mirror on the top of the payload and directed, by means of a switching mirror towards one or the other of two redundant assemblies relay optics/IDT. The light originating from one or the other part of the star mapper is directed towards one of two redundant relay optics/photomultiplier assemblies.

It is to be noted that the association of the star mapper and modulating grid in close proximity on the same surface eliminates stringent alignment problems.

The star mapper grid, occupying an area of about 11 x 20 $arcmin^2$ near the edge of the field of view, consists of eight slits parallel to the z axis and eight slits inclined at 45°. The width of each slit is 0.6 arcsec. and the distance between centres of adjacent slits is 3 arcsec. The operation of the star mapper requires that the stars to be observed are selected on ground and their approximate positions periodically loaded in the spacecraft memory together with the scientific observing programme. When a star is expected to enter one of the slit systems the photomultiplier output is sampled and subsequently Fourier analysed by the on-board computer. Comparison of the observed phase of the star mapper signal with the predicted phase yields an error signal which is used to update the attitude and gyro drift rates. The accuracy analysis has shown that the telescope attitude can be continuously measured on board with an error less than 1 arcsec, using the gyro-readings to interpolate between star mapper observations.

Various shapes of the modulating grid have been considered, yielding information in one or two dimensions. The slit pattern finally selected is monodimensional and periodic, consisting of alternately transparent and opaque bands, nominally parallel to the z axis and covering the central 54 x 54 $arcmin^2$ of the field of view. A monodimensional grid gives minimum sensitivity to attitude errors around the x and y axes and is optimal from the point of view of photon statistics, by drawing information from the image only in the direction of maximum MTF of the telescope. It is also the simplest shape with regard to manufacturing, calibration, and data processing.

The selection of optimum parameters for the modulating grid (period and slit width) is a trade-off between several factors:

- consideration of the theoretical diffraction image and photon statistics shows that the expected mean error is minimised with a grid period $s = 2\lambda_{eff}/(1+\eta)D \simeq 0.5$ arcsec. and slit width $r \cong s/3 \cong 0.17$ arcsec, D and η being the length (along y) and linear obscuration ratio of the entrance pupil, respectively; however, a secondary minimum at $s \cong 1.0$ arcsec, $r \cong 0.25$ arcsec yields only 10 - 20 % bigger photon-statistical mean error. Both minima are quite shallow.

- The theoretical advantage of the smaller slit period may well be offset by a reduced light collection efficiency of the relay optics due to increased diffraction on the narrower slits, if the acceptance angle of the relay optics is technically constrained. The f/10 beam incident on the grid is in fact considerably widened after passing through slits much narrower than the full width of the stellar diffraction image (about 0.7 arcsec).

- Detectability of parasitic stars and components of double and multiple stars is much improved with a larger grid period, thanks to the higher harmonics present in the modulated signal.

- A study of residual chromatic aberrations of the nominal and misaligned telescope indicates, on the other hand, that the differential displacement of images of stars of different spectral types is minimised with a grid period of about 0.55 arcsec. A secondary minimum at twice this period is much less consistent, but is still acceptable.

The above considerations have led to the following specifications, which still may be subject to small modifications following the final definition of the operating wavelength band:

- length of slits	: 54'	=	38.6 mm
- width of slits	: 0".275	=	3.28 μm
- distance between slit centres (period)	: 1".1	=	13.11 μm
- total number of slits	: 2945		

3.4 Relay Optics

3.4.1 Requirements

The relay optics transfer the star image modulated by the grid system from the telescope focal surface onto the sensitive photocathode planes of the Image Dissector Tubes and photomultipliers.

The specifications for the relay optics behind the main grid towards the IDT take into account the light diffracted by the grid. During the course of the study, the following requirements have been agreed upon:

- a demagnification 3.0 in order to image the field of view within 30 arcmin from the optical axis on the IDT quality area (0.56 inch in diameter)
- an oversizing of the relay optics diameter is highly desirable in order to optimize the collecting and the modulation efficiencies.
- the blur circle diameter should not exceed 25 arcsecs (equivalent to 100 microns) in order to keep the chosen instantaneous field of view diameter of 30 arcseconds for the IDTs.
- a short wavelength cut-off of the transmittance at 350-380 nm is acceptable, with a long wavelength cut-off at 650-700 nm.

For the relay optics relative to the star mapper, the requirements on acceptance angle, transmittance and wavelength range (possible filter) are similar to those for the IDT relay optics; however, a much simpler design can be selected as the blur circle can be much larger.

3.4.2 Diffraction by the Grid. Relay Optics Diameter

As for most optical system containing a reimaging relay working over a relatively large linear field of view, it has been found necessary to have a field lens (diameter L) placed in the primary focal plane which forms an image of the telescope exit pupil (diameter Lo) onto a physical stop located in the relay lens assembly.

For HIPPARCOS, however, the main grid having a high spatial frequency acts as a transmission grating for the pupil imaging. Since the relay optics diameter is necessarily limited by physical and optical constraints (maximum f/number in the image space compatible with the required blur diameter) it is clear that some light is going to be lost.

The intensity of the light at the collecting aperture of the relay optics has been estimated in the case of an ideal telescope, with rectangular pupil and central obscuration. It is observed that, although the regions outside the geometrical image of the entrance pupil contain much light, the modulated light component fall off much faster with increasing distance from the pupil center.

The curves in Figure 3.5 show that with moderate or even no oversizing ($\beta = L/Lo = 1 - 1.5$) the astrometric weight of the collected light $(\sigma(\beta)/\sigma(\beta=\infty))^{-2}$, where σ is the photon statistical mean error of the timing of the Poisson process is already larger than for the "ideal" relay optics ($\beta = \infty$), in spite of the fact that only 60 - 75% of the energy is transmitted.

3.4.3 Relay Optics Characteristics

The main characteristics of a possible relay optics combination towards the IDT (cf. Fig. 3.1) which meets the above requirements, are the following:

- demagnification : 3
- oversizing: $\beta = 1.5$
- glasses FK 52 and KZFS6 (SCHOTT)
- 11 lenses (+ one filter if required)
- wavelength range: 380 to 800 nm (peak transmission around 550 nm; about 94%, including antireflective coatings)
- maximum blur circle at best focus plane: less than 100 microns (IDT plane) = 25 arcseconds at field edge (30 arcminutes radius) and better at field center.
- total length: 362 mm

3.5 Detection System

In order to decrease the influence of the sky-background and of interfering stars it appears mandatory to observe the programme stars with a small instantaneous field of view (IFOV) which tracks the star as it crosses the observing field. As there are about 4-5 program stars in the field at any time which must be observed essentially simultaneously, the ideal detection system would be built around a photon counting pictorial detector. This will allow to either set up a few IFOV's simultaneously or set the observing diaphragms a posteriori altogether.

An overview of the possible detectors should mention the solid state imaging detectors combined with intensification stages ICCD (Intensified Charge Coupled Device) and particularly ICID (Intensified Charge Injection Device) which has the great advantage of readout capability at random rather than sequentially as in the ICCD. Mention should also be made of the new family type most commonly called photicon with various position determination concepts such as crossed-wire systems, multilayer thin film circuit or target array of diffused planar diodes. (See D. di Serego A., T. Stapinsky, A. Rodgers, 1979, Asiago/Mt Stromlo Obs. Report).

Both ICID and photicon type tubes detect photon events with very high spatial and time resolution simultaneously while maintaining sensitivity over a larger area. Their use however has to be carefully weighted in view of their utilisation in a spacecraft as they still are very much state of the art and much research and development work is still expected before they can be space qualified. This might also have a sizeable cost-impact on the mission.

An alternative is to use only a simple IFOV, which in order to preserve the simultaneity must then be switchable at a rather high rate. The loss in effective integration time can then also, by spending a larger fraction of the observing time on the fainter available programme stars, be kept to significantly less than the factor 4-5 that would result from an even distribution. Data rate and data management are much simpler in this case.

This simple IFOV approach can be implemented by means of an Image Dissector Tube (IDT). This type of tube is actually currently available off the shelf and therefore is to be preferred in view of the recommended cost-effectiveness approach. It has the characteristics of a photomultiplier allowing photon counting over the range of magnitude to be observed. Repositioning of the sensitive spot to any other position can be achieved at a rate of at least 10 kHz (10 times faster than the sampling rate) allowing an essentially arbitrary observing strategy to be implemented.

The above considerations and the fact that proper implementation allows a performance not much more than a factor 2 below the optimum of an ideal detector as indicated above, while it, at the same time, streamlines the data handling, has caused the IDT to be preferred in the present phase A study.

The size of the IFOV is constrained by the following considerations:

- The adverse influence of sky-background, dark current and parasitic stars should preferably be negligible for the mission performance. Thus the background photon count should be less than 10% of the photon count of a star of blue magnitude 13, and less than 10% of the programme stars should appear accidentally accompanied by a second star of significant brightness. This calls for an IFOV of no more than about 30 arcseconds across.

- The size of the IFOV should be large as compared to the accuracy to which one can predict its required position in the observing field, and its setting accuracy. A combined positioning tolerance of 5 arcseconds has been shown to be feasible without significant difficulties. This indeed allows the choice of 30 arcseconds for the size of the IFOV without worries about intermodulation caused by loss of light outside the IFOV.

- The intermodulation that might be caused by sensitivity variations and blemishes on the photocathode have been shown to be negligible if the image of the star on the grid can be smeared over an area which is large with respect to the period of the modulating grid. An IFOV of 30 arcseconds across allows smearing of at least 20 arcseconds, which can be achieved either in the design of the relay optics or by defocussing its image of the modulating grid onto the photocathode.

The proposed tube is the model 4012 RP manufactured by ITT Electron Tube Division, which has been used on several space programmes and has a proven reliability; it is used in EXOSAT and a highly linearized version is being developed as a detector for the Spacelab Instrument Pointing System. It includes a S-20 photocathode as a baseline.

For the star mapper, an ordinary photomultiplier is planned. For reliability reasons, the IDT and the photomultiplier are duplicated; a switching mirror, controlled from the ground, allows selection of one or the other IDT operating tube. Mechanical shutters are provided as a protection against unforeseen exposure to the sun.

3.6 Baffles

The accuracy of star position measurement would be subject to degradation if a sizeable amount of straylight were reaching the detector. The tolerated amount of straylight should be kept below the sky irradiance outside the earth's atmosphere (about 300 photons/sec on the 30 arcseconds detector operating window). As the direct sunlight cannot penetrate the light shields (those are truncated accordingly by a canting angle in the xz plane, equal to the revolving angle as shown in early phase A study), the main contributor is the earth's light. Taking 5 W/m^2 for the earth irradiance at the baffle entrance plane in the useful spectral range, the baffle has to provide for about 10^6 attenuation.

The baffling system requirements have been revised for the present study, in order to be compatible with the modifications of other sub-systems or mission aspects. In particular:

- the baffles are rigidly linked on the main payload structure
- the compatibility with larger revolving angle (up to 45°, although 36° is the baseline angle) and
- diffraction effects due to the grid (oversizing of the physical stop in the relay optics) have to be taken into account
- the length is limited due to the antenna clearance (50°)
- the cross section is rectangular in shape.

The present study has shown that a two-stage baffle, with internal baffling rings (cf. Fig. 3.2) is to be preferred: the first (outer) stage is configured in such a way as to prevent direct illumination of the second one by earth radiation at earth vector-baffle axis angles larger then $\alpha = \alpha_L'$ (perpendicular to scanning direction) or $\beta = \beta_L'$ (in scanning plane), the values of which are defined by the baffle geometry. For lower earth angles, the system behaves more or less as a single-stage baffle.

However, the detector will receive not only straylight reaching it after a series of diffuse reflections (2 to 4) on the baffle walls and the entrance pupil. It happens also that some portion of the field is viewing directly the baffle walls through specular reflection on the complex mirror, increasing the straylight level at $\alpha < \alpha_L$. The only way to get rid of that would be to mount a baffle around the secondary mirror to prevent direct viewing of the complex mirror at any point in the measuring field of view. Hence, the central obscuration factor would be increased from 0.45 to 0.56, with a consequent MTF loss, if the measuring field is limited to 42 x 42 $(\text{arcmin})^2$, to get a manageable star signal (even for faint objects) at very low earth angle. The optimization of the system will make a compromise between the useful observing time and the obscuration factor. Without baffle around the secondary mirror, the updated baffle design gives a straylight level below the tolerated limit (300 photons/sec at the IDT) for earth angles larger than $\alpha_L = 30°$ and $\beta_L = 48°$, with a canting angle of 45°, and a baffle length ratio $L1/L2 = 0.9$. The dimensions of the rectangular section of the lower baffle are slightly larger than those of the entrance pupil and the total length of the baffling system is fixed by the maximum space available.

3.7 Mechanical Design and Thermal Control

3.7.1 Structure

The structure is composed of the following elements (see figures 3.2, 3.3 and 3.6):

i) the telescope structure, a parallelepipedic structure made of aluminium honeycomb panels of 9 mm thickness covered by quasi-isotropic sheets of 1 mm thickness in CFRP (carbon fiber reinforced plastics). The primary mirror, made of ULE, is circular in shape and fixed by a central cylindrical invar mount designed to minimise the bending thermal moment applied to the mirror. The secondary mirror, rectangular in shape, is held by an invar shell fixed on the primary mirror attachment; the spider arms are parallel to the y and z axes. The complex mirror is fixed on the lower baseplate, preferably by an isostatic mount.

ii) the detection compartment is located at the back of the focal surface, mounted on the end plate which holds the primary mirror mount. It is composed of a hood which closes the compartment and is used as fixation plate for the various items of the detection chain (tubes, splitting and switching mirrors, shutters, electronics boxes). It is made of aluminium and is thick enough (at least 4 mm) to provide radiation shielding. The hood and equipment fixed on it can be removed for tests purposes. When it is removed, the refocussing system remains on the telescope.

iii) the baffles which are attached to the payload structure, they are made of thin aluminium and can be removed for tests purposes;

iv) the structure for attachment to the spacecraft; in order to avoid coupling of thermal and mechanical deformations between the spacecraft and the payload, a statically determined (isostatic) mounting is preferred; this solution allows also the spacecraft design to proceed with limited knowledge of the payload, since the interface loads depend only upon the mass properties of the telescope (mass and center of mass position). In the proposed design, six rods transmitting only axial forces support the payload; they are attached on three hard points on the spacecraft structure. The rods are made of CFRP (thickness 4 mm, external diameter 65 mm) and are fixed on 6 points on the payload (2 at the bottom and 4 in the center of mass plane on a frame also in CFRP)

v) the boom system supporting the cardioid antenna on top of the payload.

A mathematical model using a finite element programme with 100 nodes has been developed. It has shown that the lowest dynamical frequency is about 65 Hertz, which satisfies all specifications.

3.7.2 Thermal Control (payload and spacecraft)

The spacecraft and the payload are decoupled from each other and are thermally controlled separately.

The thermal requirements of the spacecraft are quite conventional; they can be fulfilled by a passive thermal control. Heaters are however foreseen on the hydrazine lines to keep their temperature below 5°C and on the ABM forward dome.

On the contrary, the thermal requirements of the payload are very stringent, such as a variation with time of the temperature gradient across the complex mirror of 0.05°C during 3 hours. An active sub-system has to be implemented, at least in the optics compartment, which is well decoupled from the detectors compartment containing the electronic tubes. The telescope is controlled by means of electrical heaters, mounted on the components; every heater is controlled by one (two for redundancy) thermistor which automatically activates the heater when the temperature drops below 11.9°C and switches it off when it reaches 12°C. Axial temperature gradient in the telescope tube is controlled by eight heat pipes.

The thermal analysis carried out at ESTEC with a fairly complex mathematical model has shown that the specifications can be fully met, except for the primary mirror where the gradient (0.3°C) is slightly higher than required (0.2°C). Solutions for this problem are however thought to be available.

According to a recent study by MATRA, it would appear that further simplification of the payload thermal control could be obtained, and that use of heat pipes might not be necessary. Also, MATRA proposed to stabilise the temperature to about 20°C (and not at 12°C), at the expense of increased electrical power consumption, in order to ease the demanding optical calibrations and tests of the payload.

3.8 Data Handling

The on-board data handling aspects are discussed in Section 4.6.

3.9 Mass and Power Breakdowns

The mass and power breakdowns are given in Tables 3.1 and 3.2 respectively.

Table 3.1

Payload mass breakdown

Structure	Lateral panels and base		23 kg	
	Isostatic mount		16	
	Baffles		7	
		Subtotal		46 kg
Main optics	Telescope structure		5	
	Primary mirror (with support)		9.5	
	Secondary " " "		2.8	
	Complex " " "		18.5	
		Subtotal		35.8 kg
Detection compartment				20.2 kg
Miscellaneous				15.0 kg
		TOTAL		117.0 kg

Table 3.2

Power Supply

Detection electronics	10 W
IDT coils	6
Thermal control	27.5
Data handling	5.5
TOTAL	49.0 W.

In addition the mechanisms power consumption when operating is estimated as follows:

- refocalisation	10 W
- switching mirror	6 W
- Shutter	8 W

3.10 Alignment, Tests and Calibrations

3.10.1 Critical areas

Integration, testing and calibration of the HIPPARCOS payload will clearly involve a number of sophisticated technics and equipments which are normally not encountered in more classical projects. The critical activities are essentially related to optical tasks (alignments, optical tests and calibration). The measurements of the residual defects of the HIPPARCOS optics will in principle include an error of about 100%, if the contribution of the test equipment defects is as high as the defect to be measured (the optical quality for the payload is a factor 2 or 3 higher than it is for current astronomical experiment), and cannot be extracted by the data reduction.

The following tasks are considered as the most critical:

a) at unit level

- All mirrors: profile verification after manufacturing
- Complex mirror: verification of the basic angle stability
- Grid: measurement of local defects and large scale distorsion figure.

b) at telescope level

- Optical alignment of the telescope
- Verification of the residual wave front error after alignment

c) at payload level

- verification of the stray light level and baffling efficiency
- MTF measurements
- Overall geometrical distorsion calibration

Additional tests or calibrations are obviously required to verify the payload and/or collect the necessary instrumental parameters, but are not considered as critical. This is the case for all the photometric calibrations (at IDT or payload level) for which no difficulty is expected, because:

- the required accuracy is not severe
- the photometric calibration can be performed under laboratory conditions.

The calibration of the IDT geometrical properties is also regarded as not critical, because similar measurements have already been performed in different laboratories.

Another fundamental point of the verification philosophy concerns the thermal behaviour of the payload. As the computed distortions have been found to be well below the tolerances, it is possible to split the thermal tests and the optical tests. The thermal-vacuum-sun test will serve to verify the correct operation of the thermal control system and to validate the thermal modelisation. Assuming that the optical performances do not sensibly depend on the thermal environment, the optical test sequence can be performed at room temperature only.

The only point where a combined thermal/optical test is required is the verification of the basic angle stability of the complex mirror, because the requirementson the acceptable thermal gradients are so stringent that one cannot be fully confident in the thermo-mechanical modelisation of the complex mirror.

In the following sections, as few critical tests are presented as examples.

3.10.2 Mirror Profile Verification

The multiple waves interferometry (e.g. Fizeau interferometer) is certainly the most accurate method to verify a mirror profile; it is however applicable only to specific cases: plane, quasi-plane, or spherical elements (expected accuracy: 0.02λ overall profile and 0.01λ for local wave front errors (WFE) peak to peak for the complex mirror and the secondary mirror).

For the primary mirror (large concave, slightly aspheric mirror) and the verification of the whole telescope WFE, the point diffraction interferometer (PDI) which can be procured by Ealing is the most attractive device. Basically the PDI is a flat glass plate coated with nearly transparent coating on the front face; the coating has a small pinhole at the center of the plate. If this pinhole is placed at the image point of the system under test a fringe pattern results from the interference of two wave-fronts:

- the wave-front produced by the system under test, and transmitted through the coating,
- the spherical wave-front diffracted by the pinhole, considered as secondary point source.

For the primary mirror, the PDI can be used by autocollimation near the center of curvature. A practical accuracy of 0.05λ on the overall profile and 0.025λ on local WFE is expected (peak errors) if the interferograms are processed with a microdensitometer.

3.10.3 Verification of basic angle stability

The short term stability specification on the complex mirror angle is 10^{-3} arcsecond over 3 hours. The potential sources of angular drift are:

- thermal distorsion of each individual glass block,
- relative displacement of the two blocks (this likely does not occur if the two blocks are assembled by molecular adherence).

One of the steps for the verification of the angular stability is the direct angular measurement for different temperature cases. This test will be performed at unit level; the angular displacements are measured with a Fizeau interferometer. The interferences are produced between a plane reference mirror and the back sides of the two blocks of the complex mirror, which are polished and coplanar. With an interfringe distance of about 100 mm, and a detection of 1/30 interfringe, the final accuracy on the angular drift is about 5.10^{-3} arcsec (λ = 400 nm). The required accuracy of 10^{-3} arcsec can be artificially obtained if the temperature variations are amplified by a factor 10 (2°C thermal gradient).

3.10.4 MTF Measurements at Payload Level

The final performance of the instrument (tolerance and stability requirements) have been formulated in terms of the optical transfert function in the scanning direction at the grid frequency and its harmonics.

The method proposed to perform the MTF (modulus) measurement of the whole telescope and the grid is illustrated in Fig. 3.7. A Newton collimator (artificial star) able to provide a diffraction limited quality over a field of 1 arcminute (parabolic mirror polished at about 0.01 λ peak error) is moved across the field of the HIPPARCOS telescope with a constant speed (about 150 arcsec/sec), in order to explore the field. The fine translation (star motion) is achieved by displacement of a point source. The signal at the grid output is recorded by the IDT, as indicated on Fig. 3.7. In order to reduce as much as possible potential sources of errors, the tests should be performed in a primary vacuum (1 Torr), and the optical bench should be mounted on a seismic table.

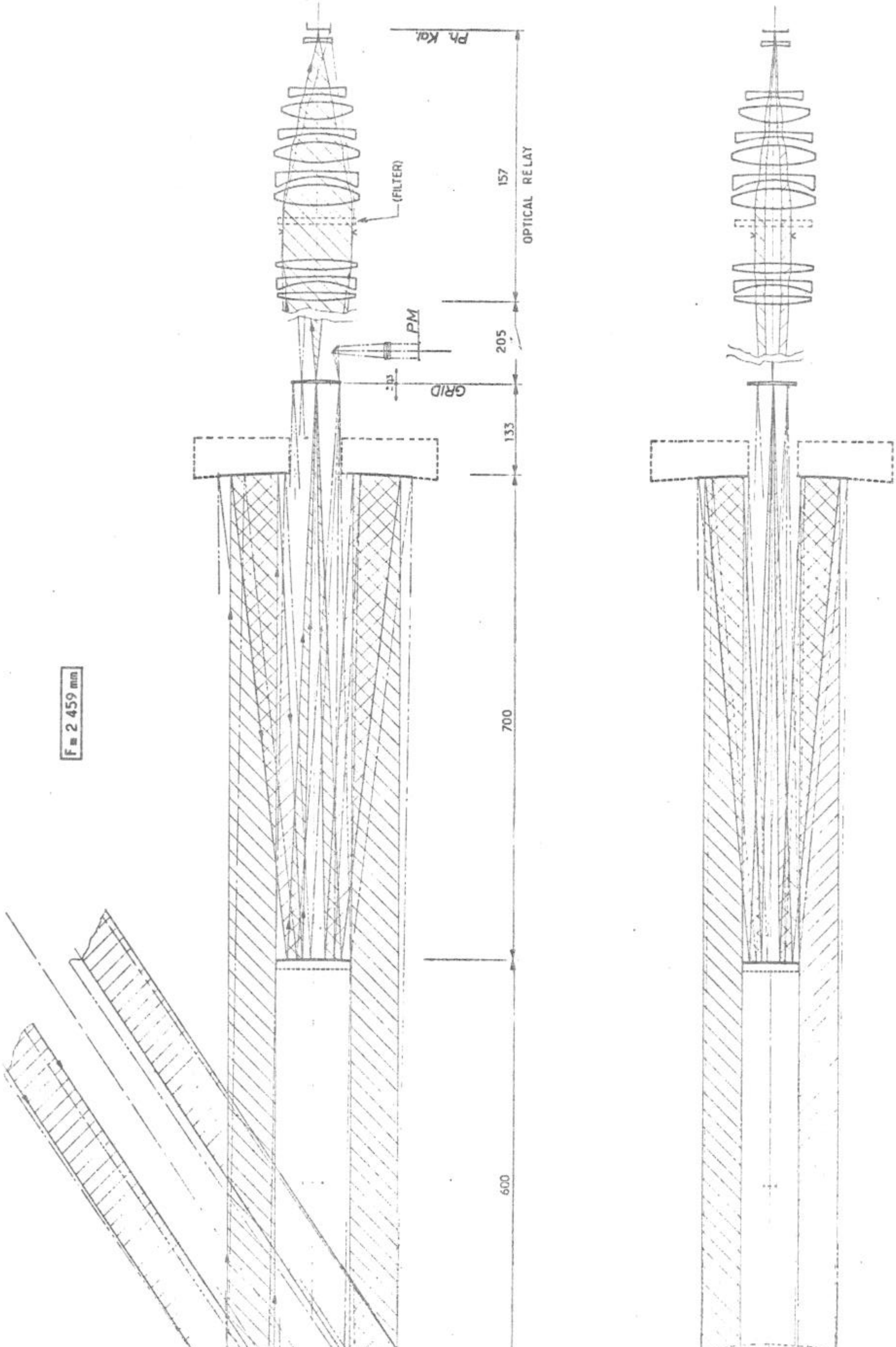

HIPPARCOS OPTICAL DIAGRAM

FIGURE 3.1

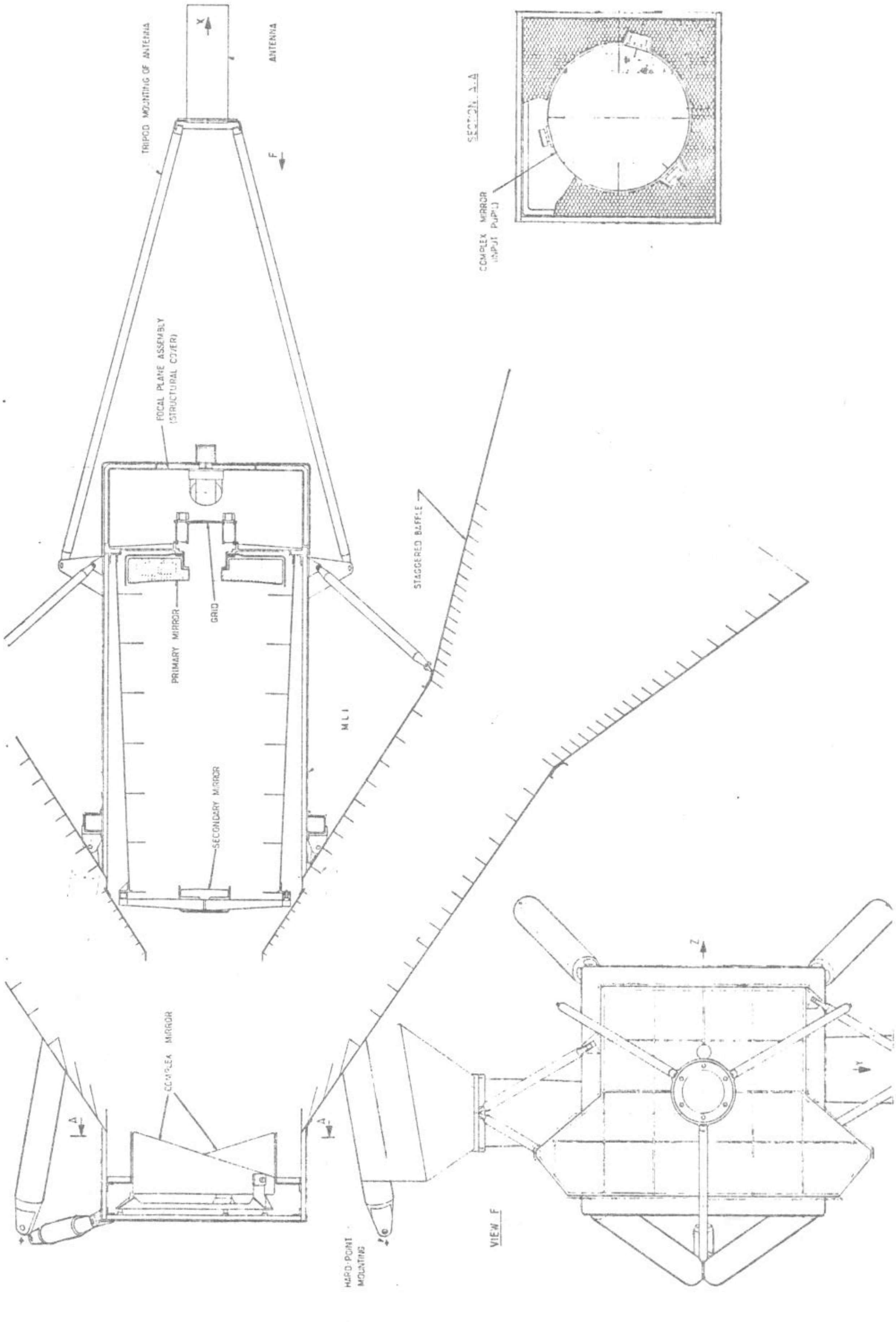

FIGURE 3.2

HIPPARCOS PAYLOAD LAY-OUT

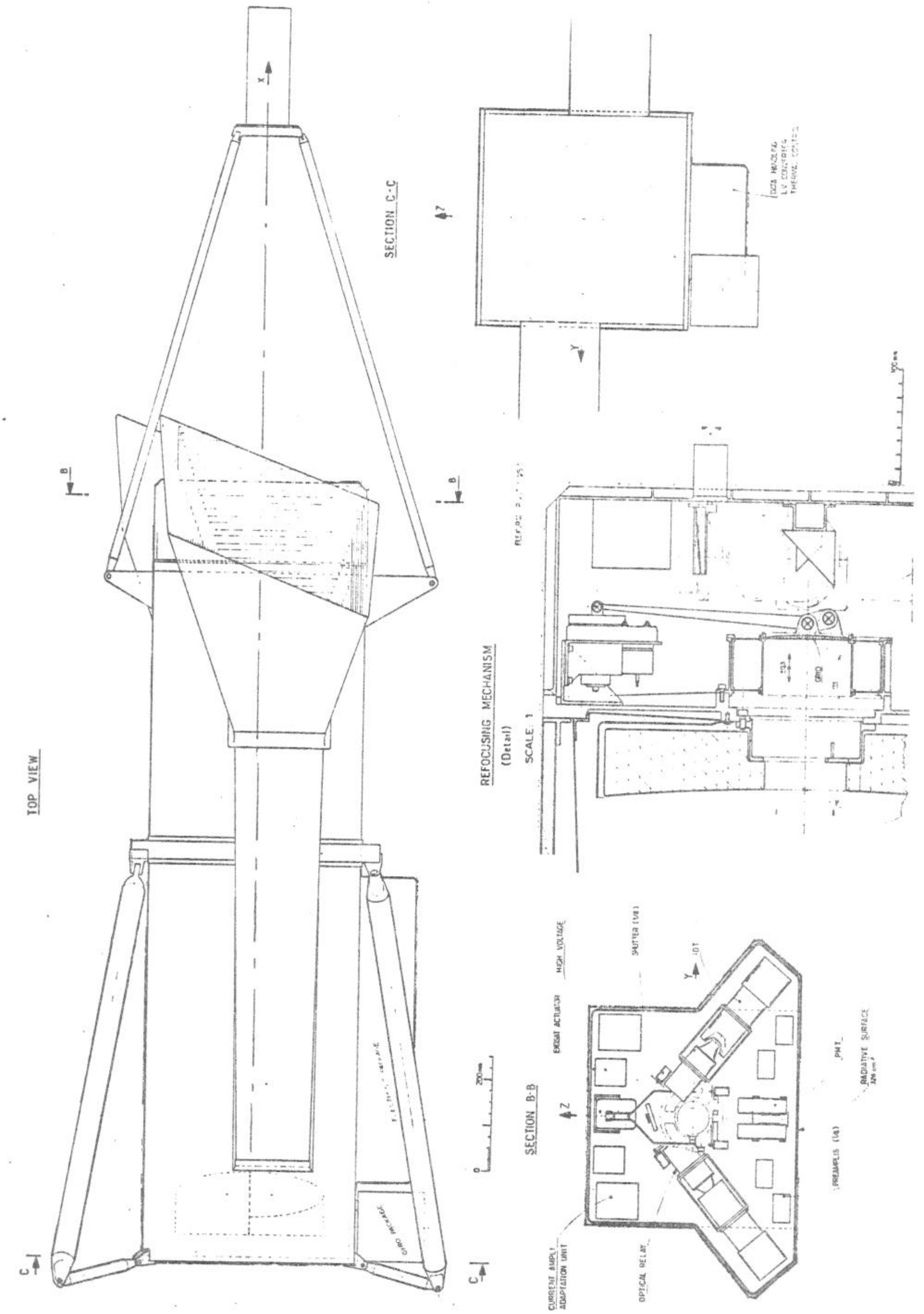
TOP VIEW
SECTION C-C
REFOCUSING MECHANISM
(Detail)
SCALE 1
SECTION B-B
HIGH VOLTAGE
CURRENT AMPLI
ADAPTATION UNIT
OPTICAL RELAY
PREAMPLIS (X4)
RADIATIVE SURFACE
GYRO PACKAGE
GRID

FIGURE 3.3

a)

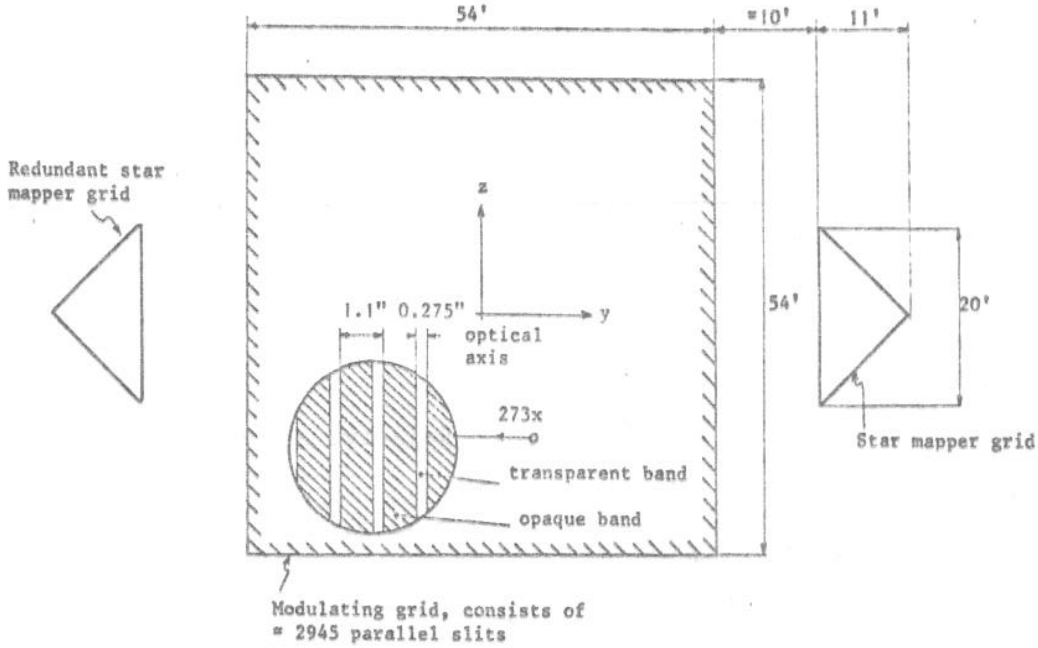

CONFIGURATION OF MODULATING GRID AND STAR MAPPER

b)

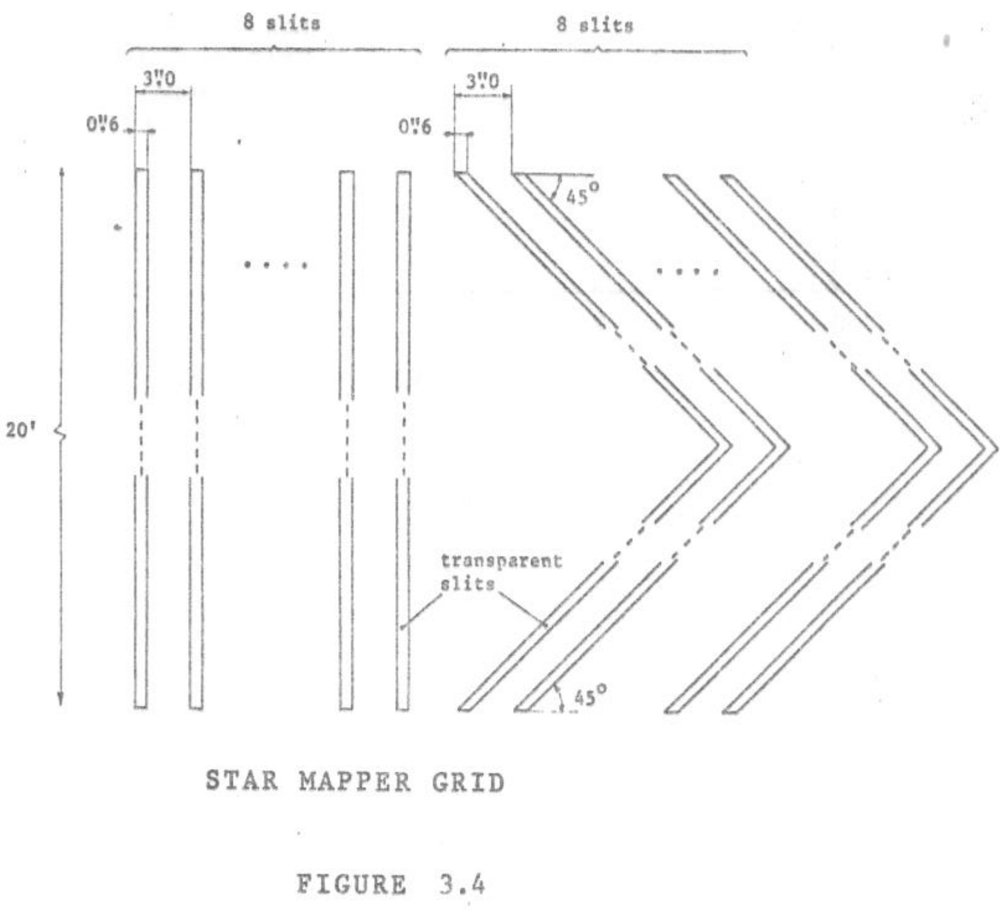

STAR MAPPER GRID

FIGURE 3.4

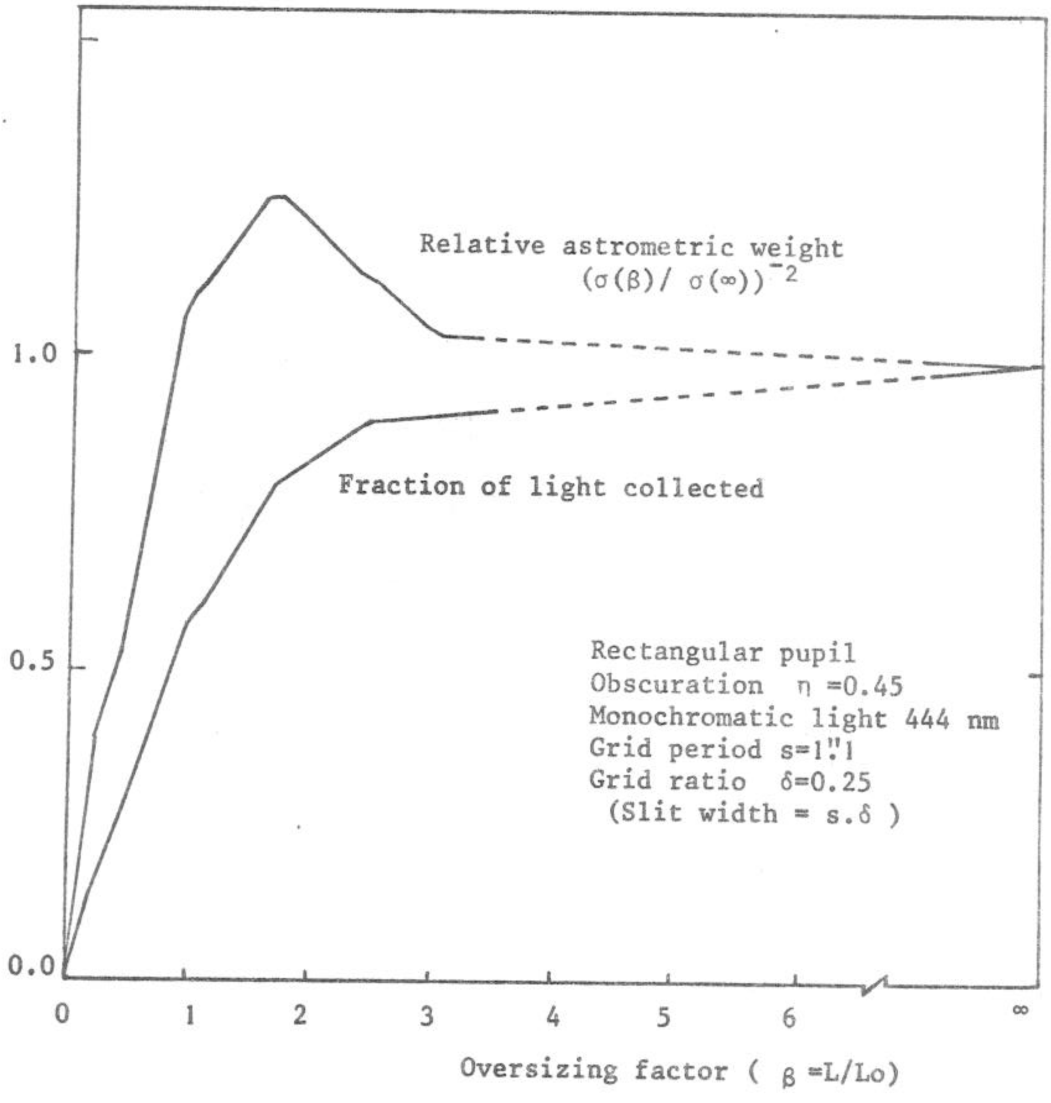

Relative astrometric weight
$(\sigma(\beta)/\sigma(\infty))^{-2}$
1.0
Fraction of light collected
0.5
Rectangular pupil
Obscuration η =0.45
Monochromatic light 444 nm
Grid period s=1".1
Grid ratio δ=0.25
(Slit width = s.δ)
0.0
0
1
2
3
4
5
6
∞
Oversizing factor (β =L/Lo)

FIGURE 3.5

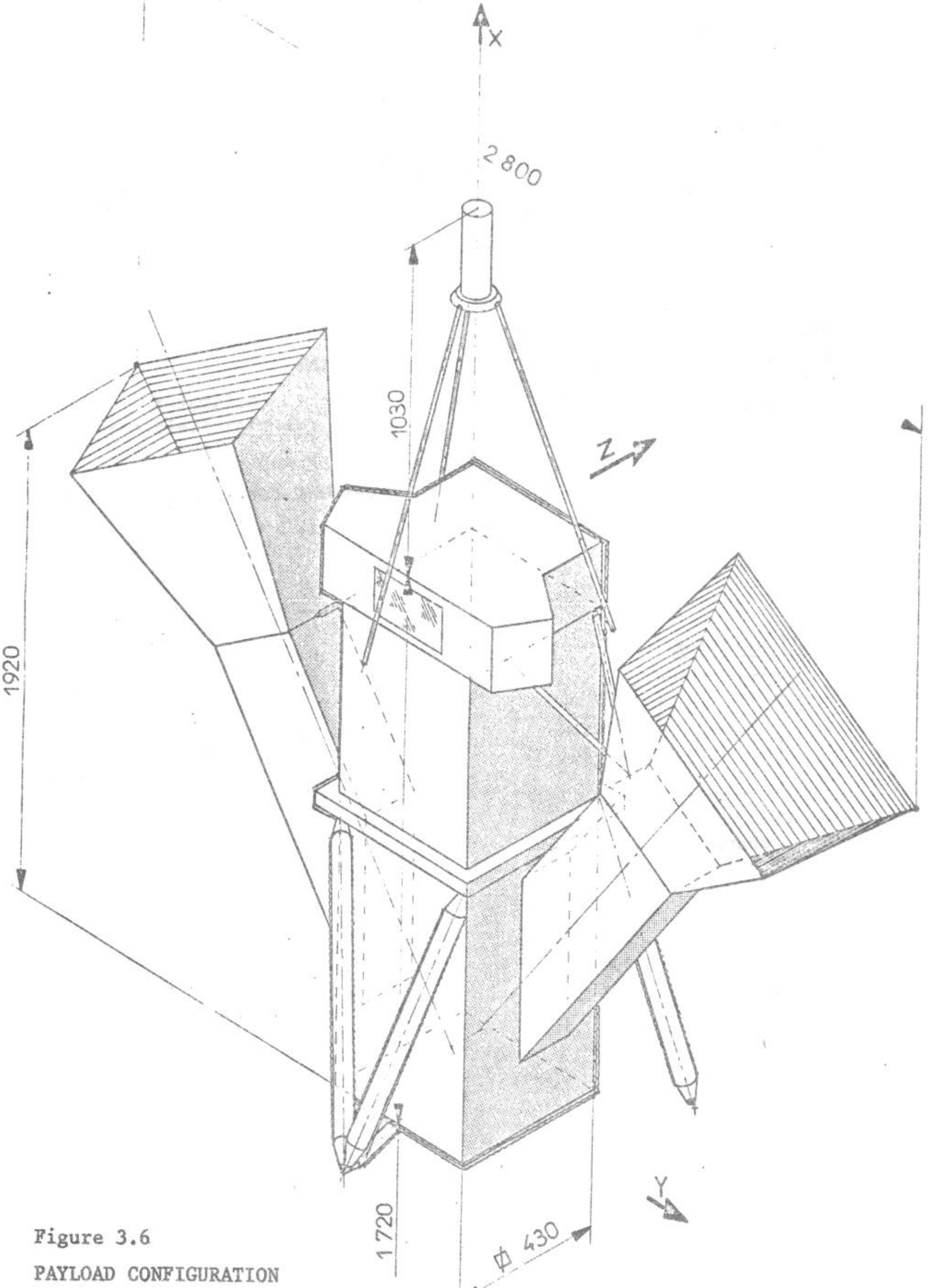

Figure 3.6
PAYLOAD CONFIGURATION

MTF MEASUREMENTS AT PAYLOAD LEVEL

Method:

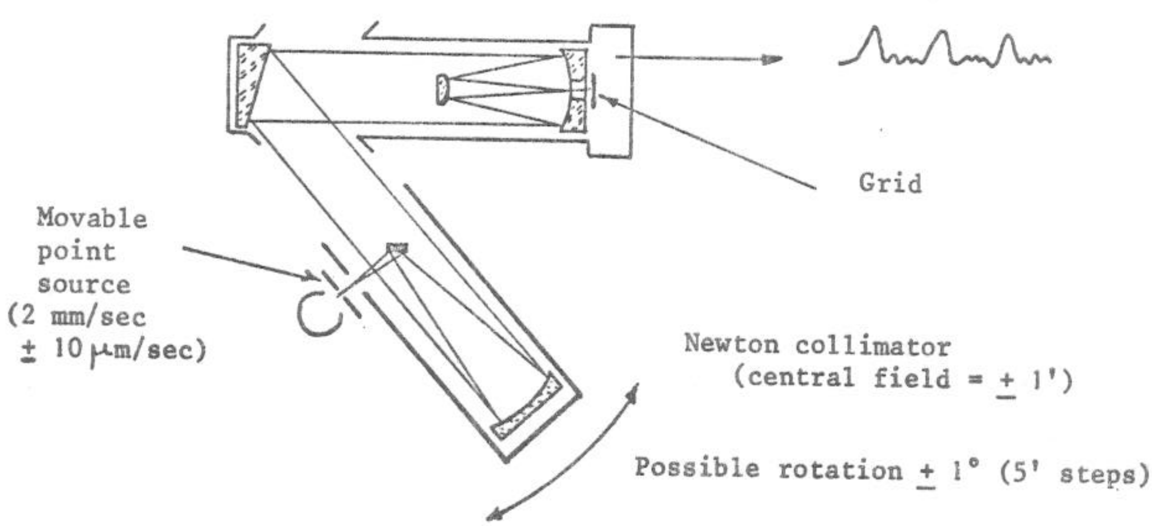

IDT piloting:

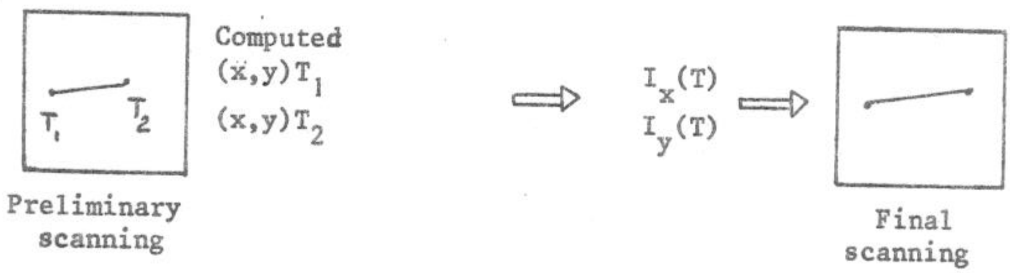

FIGURE 3.7

4. SPACECRAFT DESCRIPTION AND MISSION ANALYSIS

4.1 Launching and injection

The orbit finally selected for the HIPPARCOS satellite is almost geo-stationary, with an equatorial inclination lower than 3 degrees. Only East-West station-keeping is planned to maintain the satellite within boundaries of $\pm$ 0.5^{o} in longitude; no North-South station-keeping is foreseen.

This orbit presents the basic advantage of commonality of launch and orbit injection operations with other geostationary spacecraft potentially sharing the launch with HIPPARCOS. Eclipses will be relatively infrequent, occuring only within 23 days before and after equinoxes, with a maximum duration of 1.2 hours. In addition, all operations can be conducted by a single European ground station.

The satellite will be launched by an Ariane vehicle, either of nominal type Ariane 1 or an improved version Ariane 2 or 3. In all cases, HIPPARCOS is compatible with a double launch using the SYLDA (Système du Lancement Double Ariane), but must necessarily occupy the upper position. With Ariane 1, HIPPARCOS represents about 54% of the launcher capability, but only 48% or 40% for Ariane 2 or 3 respectively.

There is in principle no constraint on launch window imposed by the scientific mission: HIPPARCOS may be injected into orbit at any day of the year. This adds flexibility in case of dual launch.

The spacecraft carries a solid propellant apogee boost motor MAGE 1S (Motor d'Apogée Geostationnaire Européen) developed in Europe, which is fired near the apogee of one of the first transfer orbits. In the transfer orbit, the satellite is spinning at 60 revolutions per minute in the launching undeployed configuration; as this configuration is dynamically unstable, an active nutation damper is provided.

The nominal useful lifetime is 2.5 years; however, consumables are sized for a larger period of time, e.g. 4 years.

4.2 Configuration and structure (Figure 4.1)

The primary structure of the spacecraft consists of two platforms (upper and lower) and four vertical shear panels, all in aluminium honeycomb, and a thrust cone which interfaces with the Ariane adaptor and is the main load carrying structure for the apogee boost motor (ABM). The platforms and the cone are fitted with struts to increase stiffness and strength.

The payload is attached on three hard points on the upper platform with an isostatic mount (section 3.7.1). The ABM is mounted on the upper ring of the thrust cone.

The solar array subsystem consists of a large fixed array on top of the upper platform in front of the payload and two smaller deployable panels. The spacecraft equipment boxes are fixed on the lower platform and on the four vertical shear panels. Fixed antennae are located on the top and on the bottom of the satellite; the upper one is mounted with struts on the top of the payload housing.

The accommodation of the equipment is shown on Figure 4.2

4.3 Attitude and orbit control

The function of the attitude and orbit control subsystem is basically twofold; the subsystem shall control all manoeuvres after separation from the launcher third stage until start of the operational phase at the required geostationary position. It shall ensure the correct dynamic attitude control and determination during the full satellite lifetime.

The first function, although complex, is common to all geostationary spacecraft and a good deal of experience exists in Europe, on which the proposed solution is founded, using flight proven procedures and equipment. During the transfer orbit, the satellite is spinning; it contains an active nutation device (AND) similar to that of Meteosat. After firing of the apogee boost motor, the satellite is despun under gyros control, the solar panels are deployed and the sun and earth are sucessively acquired. In addition to the AND and gyros, various earth and sun sensors are used, controlling an hydrazine reaction subsystem. Then, by means of reaction wheels, the required scanning motion is acquired and the scientific mission starts.

The nominal attitude control law, called revolving scanning, is discussed in section 5.1.4. Let X be the telescope axis (bissector of the two fields of view) and Z the perpendicular to the plane containing the axes of these two fields of view. The Z axis is maintained at a constant angle to the Sun, the revolving angle ξ, fixed in the baseline design at 36°. The satellite scanning motion results from the composition of two rotations :

- a spinning motion around the Z axis, at a rate of R revolutions per day; in the baseline design R = 10, i.e. a great circle is scanned in 2.4 hours,

- a slow revolution of the Z axis around the satellite-sun line, at a rate of K revolutions per year; in the baseline design, K = 7.5.

The requirements for the absolute pointing accuracy are not critical, being of the order of 10 arc minutes or more.

Two basic concepts have been extensively investigated: a continuously acting control with reaction wheels and an intermittently acting control with cold gas jets. It is claimed by some scientists that the intermittent system may permit more easily to reconstruct the true attitude by parameters estimation between two successive actions of the jets with an accuracy of the order of one milliarc-second, thus allowing measurements of angular distances of stars observed during that period and therefore improving the astrometric accuracy. However, the short duration of the limit cycles, the lack of flexibility of the intermittent control and the inherent higher risks have led to select as baseline the continuous control. It must be emphasized that all results on the final expected accuracy on the astrometric parameters assume implementation of this continuous system.

Attitude information signals are provided in real time to the control system (reaction wheels and desaturating jets) by a set of four redundant gyros and the star mapper at the focal plane of the payload. The star mapper and gyros outputs are also used for piloting the instantaneous field of view of the image dissector tube.

4.4 Power Supply

The required power amounts to an average of about 230 watts during operation in geostationary orbit. As it is required that the satellite shall be fully operating in shadow, battery power is needed.

The primary source of electrical power is a solar array consisting of a fixed panel and two laterally deployable smaller panels. The fixed panel is of the same size as an IRAS panel, i.e. 1.3 x 1.9 m^2; each deployable panel is constituted by one half of such a panel.

Taking into account the various loss factors, such as micrometeroids, ultraviolet radiation, particle radiations during 3 years, and also the angle of 36° between the normal to the solar array and the sun direction, the power available at end of life in equinox will amount to 270 watts.

The power supply subsystem includes two redundant nickel-cadmium batteries of 15 Ah each; the power conditioning is decentralized and incorporates a switching shunt regulator, two battery chargers and two battery dischargers, two battery reconditioning units, a distribution box and four dedicated converters (attitude control, data handling, telecommunications and payload).

4.5 R.F. Subsystem

The R.F. subsystem shall be able to transmit to ground continuously by telemetry data at a rate of about 12.8 kilobits per second and to receive continuously telecommand data at a rate of about 750 bits per second. During the operational phase in geostationary orbit, a single dedicated European ground station in the S-band (2.0 - 2.3 GHz) will be used.

The scanning motion of the satellite is such that a full omnidirectional coverage is required for permanent telecommunications with the ground station. This is achieved by a set of two antennas with overlapping pattern. A cardioid standard antenna providing coverage from 0° to 140° is mounted on a boom on the top of the payload; a second antenna, extending towards the bottom of the spacecraft completes the coverage from 130° to 180°. Switching from one antenna to the other is required 5 to 8 times per day at predetermined instants. It has been shown experimentally that these switchings can be executed without any loss of scientific data.

Two standard redundant transponders are provided for telemetry transmission, telecommand reception and ranging. Each receiver is permanently connected to one of the redundant decoders, while each of the two transmitters can receive video telemetry from either of the two redundant parts of the CTU (Central Terminal Unit). During transfer orbit, to reduce power consumption, the transmitters will be able to operate in a low R.F. power mode delivering about 1 watt. In geostationary orbit, the R.F. power amounts to 5 watts.

The up link budget shows a large margin for a bit rate of 750 bits per second. The down link budget has been computed with the following main values:

- on-board antenna gain: = 5 dBi,
- distance to ground station = 40.000 km,
- frequency = 2.3 GHz,
- ground station G/T = 22 dB°K.

It shows that 10 kilobits per second can be transmitted with a margin of 4.9 dB in the nominal case.

4.6 Data Handling Subsystem of Spacecraft and Payload (Figure 4.3)

4.6.1 Purpose and functions

The data handling on-board consists essentially of two tasks, both of which will be implemented through the on-board computer.

- Data organisation for the communication with the ground

  This task includes aspects of coding, editing and inter-leaving scientific and housekeeping data for the downlink, and decoding and storing parameters provided by the uplink.

- Data acquisition

  In order to collect the scientific data the Image Dissector Tube (IDT) sensitive spot must be accurately positioned on the programme stars passing the observing field. Therefore an IDT piloting algorithm will be set up on-board to move the sensitive spot from star to star, tracking on each star temporarily. (Note that the average number of programme stars in the field at any time is about 4). This algorithm therefore will actually distribute the observing time in accord with the scientific programme. Also it will make observations of stars from the two fields almost simultaneously (interleaved) by switching rapidly between the stars.

The input to this programme consists of a small file which contains the coordinates and a priority parameter for those programme stars which may appear in the observing field in the next period of a few minutes. This file is regularly updated through the uplink. From an extrapolated prediction of the spacecraft attitude in time the algorithm will be able to find those programme stars which are available for observation at any given time. The real time attitude knowledge required for this derives from the Attitude Control Subsystem, which will therefore do a preliminary on-board reduction of the star mapper observations and the gyro-readings to a tolerance of about one arcsec. Knowing the programme stars in the field and their time-dependent positions the decision how to distribute the observing time is made on the basis of the priority-parameters of the stars. The piloting algorithm will then provide the proper parameters for the deflection coil currents with time, taking due account of the non-linearity of the deflection characteristics of the IDT.

4.6.2 Requirements

The on-board data handling subsystem shall meet the following requirements:

- acquire and format data generated from up to 350 telemetry channels; two formats are necessary (one in the preoperational phase at 1.6 K bits per second, one in the operational phase at 12.8 K bits per second,
- validate and distribute telecommand data, with up to 300 outputs,
- distribute synchronizing and control signals derived from the on-board clock,
- generate the star observing sequence, using the data corresponding to stars expected to appear in the telescope field of view over a period of a few minutes; this data is uplinked from the ground station,

- provide IDT piloting signal based on the computed star observing sequence; the piloting signal frequency is about 50 Hz, and this frequency shall be synchronous to the sampling signal; the piloting signals shall be corrected for possible non-linearities of the IDT control coils.
- be able to direct the instantaneous field of view at pre-defined grid areas for sensitivity calibration,
- acquire and process the data originating from the star mapper in the payload,
- compute in real time the satellite attitude,
- switch the antennas for continuous coverage.

4.6.3 Constitution

The proposed data handling subsystem is based on the standard OBDH (On-Board Data Handling) concept together with data processing capability. It consists of:

- a redundant CPDU (Command and Power Distribution Unit), for telecommand demodulation and execution and also control of power switching of all subsystem units,
- a modular CTU (Central Terminal Unit), for command handling, data acquisition and formatting for down-link telemetry, clock reference and timing, interfaces with dedicated processors,
- an OBC (On-Board Computer), similar to the computer of EXOSAT or FOC, with a memory of 8 K. An alternative option would consist of several independent processing modules operating sequentially (micro processors). Although the OBC solution is proposed as baseline, final selection would have to be made during phase B.
- remote terminal units (2 RTU and 4 mini RTU), to perform the data acquisition and distribution function at the user interface.

4.7 Mass Breakdown

4.7.1 Spacecraft mass breakdown

The "useful" spacecraft mass budget (i.e. without the apogee boost motor and the hydrazine used in the transfer orbit) is given in table 4.1 (without margin)

Table 4.1

Spacecraft Mass Breakdown

Structure (including balance mass)	56.0 kg
Thermal control	10.0
Attitude and orbit control (including hydrazine)	56.75
Power supply (including solar arrays)	83.5
Harness	22.0
Data handling	21.5
Telecommunications	9.45
TOTAL	259.2 kg

4.7.2 Launch Mass Budget

At launch, the HIPPARCOS mass budget is given in table 4.2.

Table 4.2

Hipparcos Mass at Launch

Useful spacecraft mass	259.2 kg
Payload	117
Satellite mass	376.2
Margin (20%)	75.2
Satellite mass (incl. margin)	451.4
MAGE IS empty mass	34
Total mass in geostationary orbit	485.4
Propellant mass	346.5
Hydrazine in transfer orbit	4
TOTAL MASS AT LAUNCH	835.9 kg

This mass has to be compared with Ariane capabilities, i.e. 1740 kg for the nominal Ariane 1, and respectively 1950 and 2300 kg for Ariane 2 and 3; however, in case of double launches, a support structure (SYLDA) weighing 180 kg for Ariane 1 and 200 kg for the advanced versions, has to be added to the total payload.

4.8 Operations

4.8.1 Ground stations

The operation plans are based on the following mission assumptions:

- launch by Ariane from Kourou, possibly in a SYLDA configuration with a companion whose final orbit is compatible with a geostationary transfer orbit,
- launch date: 1985-86,
- transfer orbit: 200 - 36.000 km, inclination: 10.5°,
- operational orbit: geostationary, circular at 36.000 km, in a longitudinal position such that full visibility from either Villafranca or Odenwald is assured,
- nominal operational lifetime: 30 months,
- communications: S-band up and down links,
- telemetry data rates: less than 1.7 k bits per second during the launch and early operation phase (LEOP) and in the range 10 to 15 kbits per second in operational phase.

During LEOP, the stations at Kourou, Réunion, Carnavon, all connected to the ESOC Operation Control Centre (OCC), plus the operational station will be used. The stations may have to be shared with the other passenger on dual launch. The injection into geostationary orbit can be delayed until after the fourth apogee in the transfer orbit.

For the operational phase, two options exist: Villafranca or Odenwald; the selected one would be required on a dedicated basis:

- option 1: Villafranca - All telemetry data will be transmitted to ESOC using 2 data links as proposed for EXOSAT. A third link would be used for back-up. Commanding would be controlled from ESOC via the data link.
- option 2: Odenwald - All telemetry data would be transmitted to the OCC using the existing wide band data link, which would also be used for transmitting commands to the ground station.

In both options, 15 m diameter antennae would be used for 24 hours per day.

4.8.2 Operational Software

4.8.2.1 Mission supporting software

The mission supporting software will be provided by the MSSS at ESOC. It will include the usual tasks, such as:

- mission planning,
- orbit determination and prediction, provision of auxiliary data to experimenters,
- attitude determination, monitoring of attitude control subsystem performances,
- attitude manoeuvre support, orbit corrections,
- quality control

4.8.2.2 Observing programme management

The observing programme is managed from the ground through the regular update of the small file of stars on-board from which the IDT piloting algorithm operates. In particular it is through the priority parameter assignment that one influences the progress of the observations.

Thus a programme is required which provides the regular update of the on-board observing file. In order to achieve this it must manage the complete file of programme stars, firstly to find all the stars which may enter the observing field shortly. Secondly it will assign the priority parameter for each of these stars.

This priority depends on:

- the priority as assigned to each star before the start of the mission;
- the mission's progress up to about two hours before real time (the last completed possible passage of the stars concerned through the observing field);
- input aimed at modifications of the mission's progress. This input may be expected from an evaluation of the telemetry and/or the "quick look", and marginally also from "second thoughts" of the contributors to the observing programme.

As the basic concept of the mission necessarily implies a rather rigid observing programme the required flexibility will affect mainly the optimal distribution of the observing time, which will be accomplished through the proper interplay of the on-board piloting algorithm and the observing programme management software. A proper optimisation in this programme can make a quite significant contribution to the statistical weight of the astrometric catalogue.

4.8.2.3 Quick-Look Facilities

As the true astrometric value of the data can only be exploited through the integral reduction of all data taken throughout the completed mission, any "quick-look" facility will mainly serve checking and trouble shooting purposes.

For this purpose it is necessary to provide the calibration of the basic angle of the complex mirror quite frequently. This requires a rather complete reduction of completed observations along one full scan, rather much the same as in Step 1 of the final data reduction (see section 5). A by-product of this great circle reduction will give essentially one dimensional but still quite useful astrometric data. These data shall be made available to the experimenters, who can then do some preliminary science while at the same time evaluating the mission's performance. Also this reduction shall identify "problem observations" (e.g. double stars) to provide a detailed insight in the mission's progress early into the mission.

The great circle reduction shall preferably run so close to real time, that it shall at the same time provide a back-up for the time-dependent attitude determination required for the uplink, and on-board for the IDT piloting. This appears to be the most stringent constraint on turn around time, as displaying the data for evaluation cannot be expected to provide for useful actions to be taken on timescales much less than one day. Note that actions affecting the observing programme will only take effect during the next appearance of the given programme star in the observation field, except for control parameters for the assignment of the priority paramaters to the stars in the uplink file.

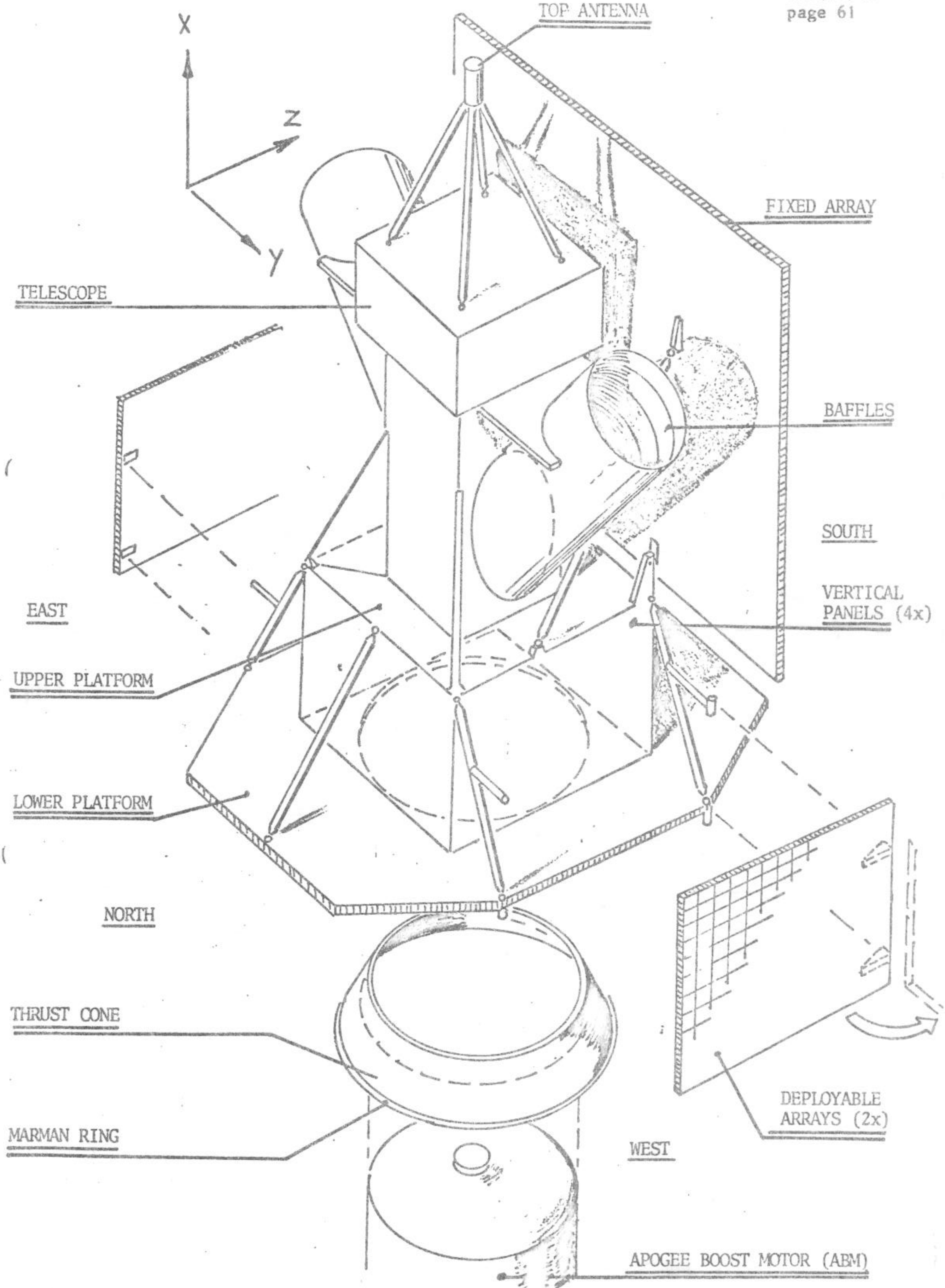

FIG. 4.1 STRUCTURAL CONFIGURATION

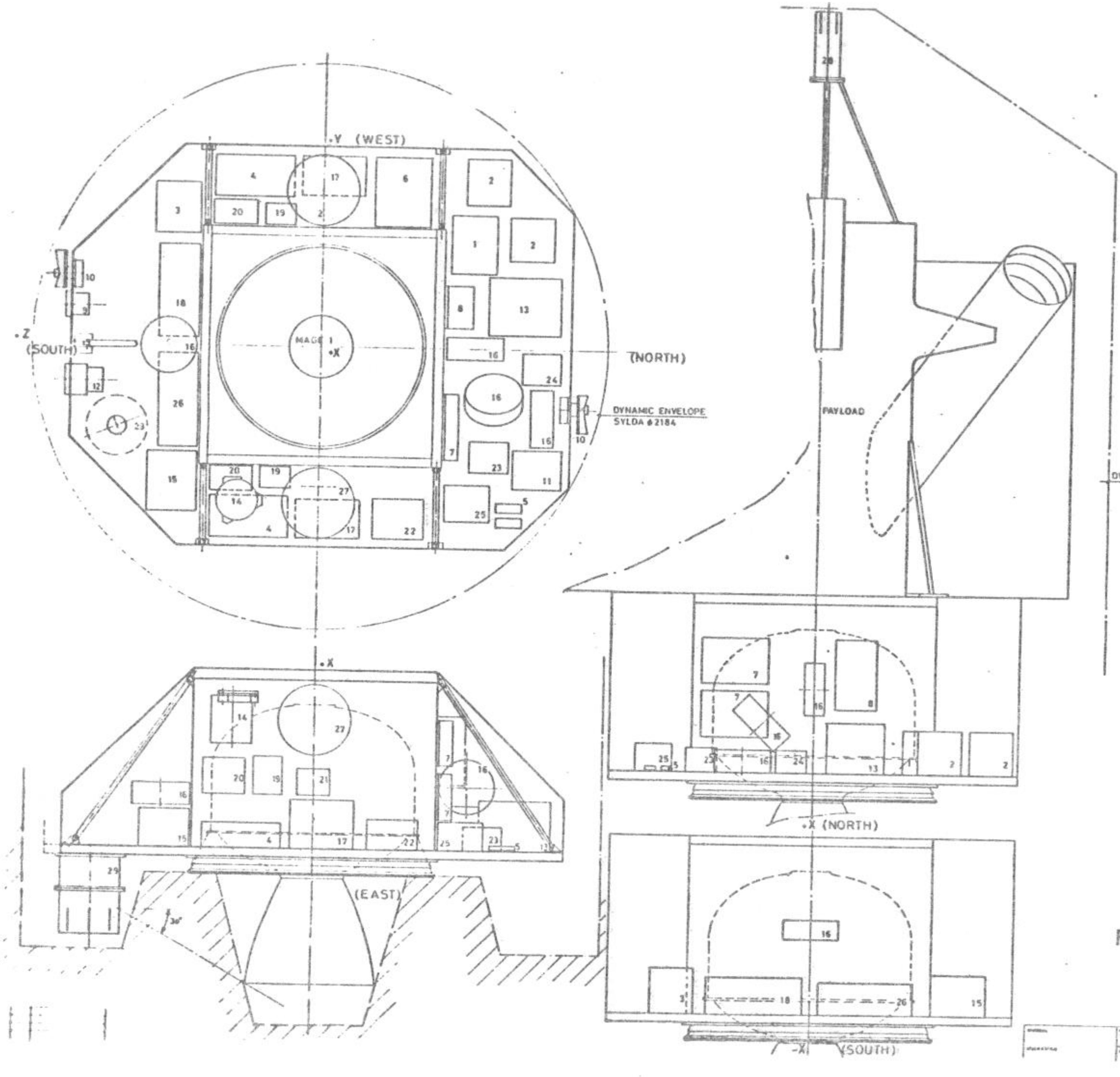

ITEM	MASS Kg	
1. Central Terminal Unit	5	
2. Remote Terminal Unit	1,2	2x
3. T.C. Decoder	3.5	
4. S-Band Transponder	4,1	2x
5. S-Band Switches	0,15	2x
6. OBC Main Unit	6,3	
7. OBC Memory	1,8	2x
9. ESS Sensor	1,3	
10. SAS	0,15	2x
11. IRES	2,6	
12. FSS	0,83	
13. Control Low Electr.	7.-	
14. Gyro Ferrant	3,6	
15. Gyro Electr.	4,9	
16. Reaction Wheel	3	4x
17. Battery	11,5	2x
18. Power Distr. Unit	4,5	
19. Recondition Unit	1,4	2x
20. BDR / RCR	2.-	2x
21. Pyrotechnic Unit	1,6	
22. AOCS Converter	3,4	
23. DH Converter	1,6	
24. Telecomm. Converter	1,6	
25. Payload Converter	2,5	
26. Shunt Regulator/PCU	3,5	
27. Hydrazine Tank	1,6	2x
28. Antenna (Cardioid) dual mode	0,738	
29. Antenna (Fill-in) " "	0,906	
RF Cables	1.-	
Structure + brackets	50.	
Thrusters + piping valves	6.- Kg	
Hydrazine	15.-	
Thermal Control	13.-	
PAYLOAD	117.3	
Harness	22.-	
Solar Panels	38.-	

Figure 4.2

HIPPARCHOS
EQUIPMENT ACCOMODATION
EUROPEAN SPACE TECHNOLOGY CENTRE
DRG

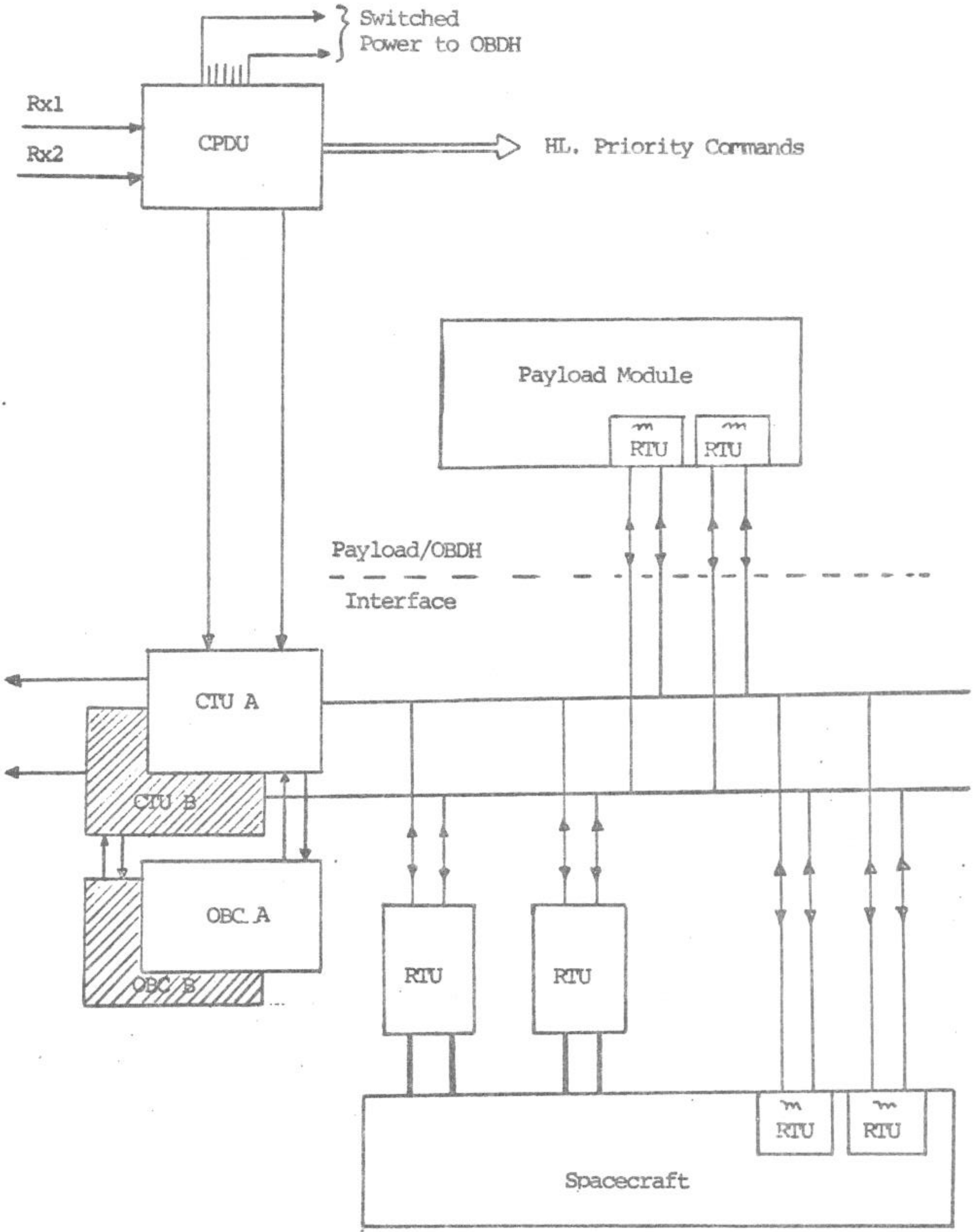

Figure 4.3 Data Handling Sub-System Block Diagram

5. ACCURACY ANALYSIS AND SCIENTIFIC DATA PROCESSING

5.1 Accuracy Analysis

5.1.1 Derivation of Mathematical Models

The accuracy evaluation and optimisation of the instrument and its operation depend on a detail modelisation of the different parts of the system. For this prupose a sophisticated modular system of mathematical models has been developed and exploited. The models can be used separately and together with optimisation algorithms for very detailed studies of specific problems, or to feed the filtering algorithm in a simulation of the functioning of the complete system.

Basically, the output signal obtained on board is modelised as a Poisson process, the intensity of which depends on a number of parameters related to each of the logical items in the breakdown, with some parameters (the residual attitude) even being stochastic processes themselves.

The star directions in the focal plane are obtained by a sequence of transformations from the astrometric parameters via a nominal scan frame to a frame bound to the spacecraft, taking into account the residual spacecraft attitude and misalignments of the complex mirror surfaces.

For the residual attitude angles, a very realistic model has been set up, closely following the hardware design and using stochastic differential equations. The model takes into account perturbing torques on each axis and the control angular momentum produced by the reaction wheels, with gyro noise and estimation errors introduced in the feedback loop.

The telescope, grid, and detector characteristics are largely represented by their Fourier transforms (FT). This allows a convenient formulation of the modulated signal, since this is basically a convolution of the point spread function and the grid, perturbed by the imperfections of the different items:

- the telescope is represented by its optical transfer function (OTF), which includes diffraction effects as well as all kinds of aberrations;

- the real modulating grid is represented by the FT of the characteristic transmittance function, which for a periodic grid is particularly simple;

- the image dissector cathode sensitivity is described by its FT;

- the instantaneous field of view (IFOV) is represented by the FT of the characteristic mask shape.

When considering the complete model it is seen that the astrometric parameters, together with a large number of auxiliary parameters for the attitude and instrument, enter the formal expressions for the observed signal strongly coupled to each other by approximately linear equations.

In the actual data processing the astrometric results will finally be obtained by iterative solution of the corresponding very large system of linearised equations, involving at least a few million unknowns. The decomposition of this system to a manageable format is essentially a numerical and data management problem which, although of utmost importance for the practical data processing, is relatively unimportant to the accuracy analysis, since it has been shown that the basic problem of reconstituting the celestial sphere is very well conditioned (rigid).

For the accuracy analysis it is thus sufficient to note that the basic one-dimensionality of observations, viz. along the scanning great circles, in essence produces measurements of star abscissae, i.e. angular positions of stars along the scanning great circles, reckoned (say) from the intersection of the great circle with the ecliptic. The five astrometric parameters of a particular star (its parallax and the components of its position and proper motion) are eventually obtained by solving an (almost) independent least-squares system of order five, in which the "observations" are the different abscissa determinations of the star.

Consequently, the rms error of an astrometric parameter may be estimated as the product of the average rms abscissa error (which depends mainly on the magnitude of the star and the fraction of the total observing time spent on the star) and a coefficient of improvement, which depends only on the dates and geometry of the different scans across the star, and hence on the scanning law, mission duration, and position on the sky.

Most of the effort to set up algorithmic tools was thus concentrated on the estimation of star abscissae: a rigorous data processing scheme was required to take into account the exact stochastic character of the output signal and the satellite attitude motion, as a reference for later simplifications. Only filtering methods are able to meet these requirements.

The software specifically developed for this study amounts to about 5000 statements of standard FORTRAN H, in addition to edition and plot utilities interfacing with the package UGP on the ESOC ICL 4/72 computer. Except for the solution of large systems of linear equations involved in the full reconstitution of the sphere, all models needed for optimisation and accuracy analysis have been implemented, including in particular:

- computation of the OTF of the telescope;
- observation simulation and filtering algorithm;
- evaluation of scanning laws (coefficients of improvement).

The main capabilities of the software packages and some numerical results are described in the next three sections.

5.1.2 OTF Computations

The software enables a complete study of any instrument of interest for the mission: design of the optimally corrected telescope, exact evaluation of OTF by raytracing, computation of derivatives if needed.

With this tool, effects of thermal and structural perturbations on the modulus and phase of the OTF, as well as chromatic aberrations, can be rigorously assessed.

The OTF has been computed for the all-catoptric Baker-Schmidt telescope, with circular and rectangular entrance pupil, symmetrically and asymmetrically split, and for various wavelengths and object directions. The optimally corrected instrument is close to perfection: over most of the field of view, the modulus of the OTF exceeds 90% of the theoretical (set by diffraction), and the non-linearity of the argument corresponds to image displacements by less than $2 \cdot 10^{-3}$ arcsec. Comparing the circular and rectangular pupils, the latter was found more efficient, for the same area, and having an even better phase linearity. A study of the symmetric pupil (complex mirror with three faces, the external faces nominally in one plane) showed that already a very small lack of parallelism between the external faces results in a catastrophic degradation of the OTF. For these reasons the rectangular asymmetric pupil (two-faces complex mirror) was selected as baseline for further studies.

In addition to the optimisation and performance evaluation of the nominal baseline instrument, the effects of all kinds of misalignments have been extensively studied with a view to define manufacturing tolerances and requirements on structural and thermal stability during operation.

By far the most critical item is the positioning and orientation of the secondary mirror with respect to the primary; already a displacement by 1.5 μm from the optimal position along the optical axis, or a rotation by 15-30 arcsec around the other axes, causes a significant (5%) deterioration of the modulus of the OTF, which will ultimately result in a similar increase of the rms errors of the astrometric data.

5.1.3 Filtering Algorithm

The observations consisting of a record of photoelectron counts are modelised as a Poisson process whose intensity is modulated as a function of time. The modulation depends on the constant but inaccurately known astrometric star parameters and instrument parameters, and also on the residual attitude which in turn is a stochastic function of time. The situation at a given time (and hence the intensity on the photocathode) is described by a state vector containing the constant parameters and the residual attitude angles and their time derivatives. The temporal evolution of the state vector is described by a stochastic differential equation.

The optimate estimate of the state vector, together with the covariance matrix measuring the incertainty of the estimate, is recursively obtained by a filtering algorithm as conditional expectations from the posterior probability of the state vector, given the record of counts. Since, for the accuracy analysis, we are only interested in the evolution of the covariance matrix, the filter reduces to the integration along the scan of a

Riccati matrix equation.

At first glance this would seem to be an insurmontable task, because of the large number of unknowns (up to 10^3 per great circle scan), the badly conditioned covariance matrix (strong correlations), the rapid intensity modulation (about 10^6 modulation period per scan), and the well known numerical problems with Riccati equations. However, efficient remedies have been found, resulting in an algorithm which is both stable and tractable:

- decomposition of the state vector: to reduce storage problems, the parameters corresponding to stars observed during the same period of time are grouped into batches;
- introduction of scaling factors: the condition of the covariance matrix is improved by automatic rescaling of variables in the course of computation;
- stabilization of integration: numerical integration of the decomposed equations proved to be extremely unstable. A slight modification of the integration scheme of the first order ensures however that the generated covariance matrix is positive even if truncation errors are large. The resulting algorithm is consistent and convergent, and thus stable;
- averaging: the covariance is nearly constant over one intensity modulation period (about 7 ms) and can be approximated by time averaging, This is advantageous since the average can be obtained in analytical form on a simplified model. This permits the use of an integration step long in comparison to the modulation period.

A number of experiments have been performed with the filtering algorithm in order to investigate the effects of various parameters and obtain a realistic estimate of the rms abscissa errors. Some typical results are shown in Figs. 5.1(a)-(c). The full capabilities of the filter have not yet been exploited; however, already restricted runs concerned with only a few stars and a small fraction of the complete great-circle scan confirm the results of a simplified error analysis and demonstrate in particular that the residual attitude errors (including a realistic amount of jitter caused by the reaction wheels) have a negligible effect on the measured star abscissae (cf. 5.1.5).

5.1.4 Evaluation of Scanning Laws

The software package for the study of different scanning laws allows determination of the total number of observations per star and the astrometric coefficients of improvement as functions of position on the sky, and estimation of observational dead time and frequency of interruptions by earth occultations. It is assumed that observation is impossible, due to physical occultation or too high a level of straylight, whenever the earth is within a certain angle from the centre of either field of view.

A complete and reasonably uniform sky coverage is obtained with a revolving scanning law (Fig. 5.2) defined by the three parameters ξ, K and R (cf. Section 4.3), provided that $K \geq 270^o/\xi$ and $R > 5$. These conditions being satisfied, there is little difference between different scanning laws as concerns accuracy, uniformity, and dead time, except that the global accuracy and uniformity generally improve with increasing revolving angle. As a baseline we may consider the following scanning law:

- sun/spin axis angle (revolving angle) : $\xi = 36^{\circ}$
- number of revolutions per year of the spin axis around the sun/spacecraft direction : K = 7.5
- number of revolutions per day of the spacecraft around the spin axis : R = 10

The revolving angle is in reality constrained by the design of the baffles ($\xi \leq 45^{\circ}$) and the electrical power requirements (variable in time). For the best overall accuracy the angle should then be adjusted several times per year to the maximum value compatible with the constraints. The value 36° is certainly conservative, since it will be possible to have $\xi = 45^{\circ}$ at least at the beginning of the mission and at winter solstices.

The dead time and frequency of interruptions due to intolerable straylight depend strongly on the efficiency of the baffling system, but are largely independent of other parameters, such as the scanning law and orbital inclination. Every third or second great-circle scan may be interrupted, but the fractional dead time is less than 20%.

Examples of the relative rms errors of the astrometric parameters (coefficients of improvement) versus ecliptical latitude, revolving angle, and mission duration are shown in Figs. 5.3 to 5.5.

5.1.5 Expected accuracy of Astrometric Data

The astrometry satellite is designed to obtain relative positions of stars with an accuracy essentially set by diffraction and photon statistics, but no longer hampered by atmospheric turbulence or refraction, instrumental flexure and other causes of errors present in all ground-based astrometric techniques.

A successful mission will yield astrometric data for about 100 000 stars down to the 13th photographic magnitude, each datum with an rms error of a few milliarcsec. Trigonometric parallaxes and the components of positions and yearly proper motions will be obtained with rms errors of 0.001 - 0.002 arcsec for stars brighter than 10th magnitude, increasing to 0.002 - 0.005 arcsec for the fainter stars.

The mean error of an astrometric parameter is obtained as the product of the corresponding geometrical improvement factor, due to the scanning law and mission duration, and the average abscissa mean error (per great-circle scan). Examples of improvement factors are given in Figs. 5.3 to 5.5 while a typical budget for the abscissa mean error is shown in Table 5.1.

Within the overall limitations set by the continuous scanning, which implies for instance that the total integration time per unit area of the sky should be roughly uniform, there is a certain freedom to distribute integration time between stars of different magnitudes and between individual

Table 5.1 Typical error budget for the abscissa of a 9th magnitude star (average count rate 2.5 kHz on star, <100 Hz on background; total integration time on the star is 8 sec per scan).

photon statistics	: $3.8\ 10^{-3}$ arcsec
uncalibrated grid irregularities	: 1.3 " "
attitude uncertainty (x and y axes)	: 0.5 " "
attitude jitter (z axis)	: 0.2 " "
basic angle uncertainty	: 0.4 " "
intermodulation errors (IFOV piloting errors, photocathode inhomogeneities, parasitic stars)	: 0.7 " "
margin (+ 40%)	: 4.0 " "
total abscissa mean error	: $5.8\ 10^{-3}$ arcsec

objects, thereby increasing the astrometric precision on some objects at the expense of the precision on others.

Consider as a realistic example the distribution of stars and integration time given in Table 5.2. This observing programme includes a complete survey of all 64 000 stars down to 9th magnitude and an additional 36 000 fainter stars selected on astrophysical grounds and/or as astrometric reference stars. Note that 54% of the total integration time is spent on the 36% fainter stars in this particular example.

Conservative estimates of resulting average rms errors are given to the right in Table 5.2. A mission length of 2.5 years is assumed and revolving scanning with sun/spin-axis angle $\xi = 36^{\circ}$.

The astrometric accuracy is in fact a function of position on the sky. There is a pronounced variation with ecliptical latitude (β) and smaller periodical variations with longitude (λ). The mean errors in Table 5.2 are sky averages; the relative variations with latitude are given in Table 5.3. These variations may be somewhat reduced by the use of a larger and variable revolving angle (ξ), and by redistribution of observing time between the two fields of view when they are not at the same latitude.

The mean parallax and proper motion of an open cluster of stars will be determined somewhat better than individual parallaxes and proper motions; however, because of the limited integration time available per unit area of the sky and a slight correlation between observations within an area comparable to the field of view, a significant improvement by averaging should be expected only for clusters and associations extending over many square degrees.

Table 5.2 Example of an observing programme: number of stars, distribution of observing time, and expected astrometric accuracy.

m_{pg}	Number of Stars	Com-plete-ness	Obs. time per star	% of total obs.time	Mean errors (sky averages) pos.	p.m.	par.
		(%)	(s)	(%)	(10^{-3} arcsec)		
< 6	3 000	100	270	1	1.0	1.4	1.4
6 - 7	5 400	100	310	3	1.0	1.4	1.4
7 - 8	14 800	100	390	9	1.1	1.5	1.5
8 - 9	40 800	100	530	33	1.2	1.6	1.7
9 - 10	16 000	15	730	18	1.3	1.9	1.9
10 - 11	12 000	4	990	18	1.7	2.3	2.4
11 - 12	6 000	0.8	1330	12	2.2	3.0	3.1
12 - 13	2 000	0.1	1780	6	3.0	4.3	4.3
Total	100 000		$6.5\ 10^7$ s	100%			
Average			650 s		1.3	1.8	1.9

Table 5.3 Relative mean errors of astrometric parameters as functions of ecliptical latitude.

β	$\Delta\lambda \cos \beta$	$\Delta\beta$	$\mu_\lambda \cos \beta$	μ_β	$\tilde{\omega}$
0°	1.8	0.9	1.8	0.9	1.2
$\pm 30^\circ$	1.3	0.8	1.3	0.8	1.1
$\pm 60^\circ$	0.6	0.7	0.6	0.7	0.8
$\pm 85^\circ$	0.3	0.8	0.3	0.8	0.4
Mean sky	1.2	0.8	1.2	0.8	1.0

Possible sources of systematic errors are by their very nature difficult to evaluate. Among identified potential sources, chromatism and variations of the basic angle are the most important ones. Both are expected to give effects well below the random errors, but may ultimately become important for statistical investigations. Residual chromatism due to uncorrected optical aberrations may give colour and position dependent errors on the astrometric results amounting to 0"001. Most of this effect can be eliminated by introducing one or a few colour dependent terms into the solution for the optical distorsions in the field. A periodic variation of the basic angle related to the continuously varying solar aspect angles may give rise to a parallax bias (zero-point error) which can only be eliminated by the use of exterior information (e.g. photometric distances of distant stars). However, the bias is expected to be less than 0"001 and independent of position and magnitude, the same for all stars, which justifies calling the parallaxes "absolute".

5.1.6 Double and Variable Stars; Photometric Data

The particular method of observation, using a modulating grid, does not permit resolved double or multiple stars to be represented by equivalent point sources. If such systems are not recognized and appropriately treated in the scientific data processing, the resulting astrometric data on them may be severely biassed and inconsistent. Moreover, due to the rigidity of the spherical reconstitution, such errors are likely to propagate to other stars as well. The potentially difficult systems are those having magnitude differences between the components of less than $\Delta m = 3.5$ and separations (ρ) between 0"3 and 15". Systems with $\rho <$ 0"3 are observed by their photocentres; if $\rho >$ 15" one component can be singled out by means of the IFOV. It is estimated that about 10% of the programme stars are double stars belonging to this category. Only half of them are presently listed in double stars catalogues.

Fortunately, practically all the potentially difficult cases are easily detected in the course of the data processing e.g. by application of a fairly simple likelihood-ratio test with negligible probability of false detection. It is also quite easy to exclude these stars from some of the preliminary solutions to avoid their contaminating the results for the remaining stars. In the final solution it will be possible to include all programme stars, irrespective of duplicity; the individual positions of double-star components and the common proper motions and parallaxes of the systems will be obtained with essentially the same accuracy as for the single stars or unresolved double stars. Thus, about 10,000 double stars, half of which are presently unknown, will be detected and accurately measured by the satellite.

Photometric data on all programme stars can be obtained with little additional effort (photometric mapping of the IDT photocathode and calibration against standard stars). The spectral sensitivity extends from 390 nm to about 700 nm (effective wavelength 480 to 550 nm, depending on spectral type). An accuracy of $0^{m}.03$ per great-circle scan is expected down to 11th magnitude. Since each star is observed in (on the average) 60 scans distributed over the length of the mission, a significant contribution to the detection of variable stars is expected.

5.2 Scientific Data Processing

5.2.1 Reconstitution of the Sphere

The principle of measurement is to observe the abscissae of stars projected on great circles by means of photoelectric scanning whith a system of narrow parallel slits, Fig. 3.4, oriented perpendicular to the direction of scanning. The detector is an IDT (Image Dissector Tube). The telescope, Fig. 3.1, images stars from two directions separated by a large angle on the slits and the two axes follow each other in a smooth rotation of one scan circle of 360° per 2.4 hours. The large basic angle $\gamma = 68\overset{\circ}{.}5$ and its high stability during a scan of 360° are crucial for the accurate measurement of the abscissae.

Any part of the sky must be covered by at least two circles intersecting at fairly large angles in order to obtain the two spherical coordinates. Furthermore, this must happen several times during the mission in order to separate position, proper motion and parallax from each other. The most satisfactory solution is revolving scanning, illustrated in Fig.5.2, in which the spin axis is pointed about 40° from the sun (revolving angle ξ) and moves slowly around the sun K times per year where $K = 270^{\circ}/\xi$.

The purpose and extent of the scientific data processing are defined by the input and output data specifications. Input data are listed here and will be further explained below:

- a catalogue of observed objects with identification, categorisation, and a priori astrometric and photometric data;
- the IDT count record, i.e. the sequence of photoelectron counts (or equivalent) for the entire mission;
- the star mapper count record, containing the photomultiplier counts (or equivalent), possibly in a compressed form;
- the gyro readings;
- the observation log, containing timing of samples and object identifications for IDT and star mapper observations;
- calibration data obtained in the laboratory and in orbit;
- the heliocentric ephemerides of satellite position and velocity.

The output consists of the catalogue with updated (a posteriori) astrometric and photometric data on the observed objects. In particular, the positions and proper motions are given in a consistent, but not necessarily absolute or inertial, celestial reference system. Trigonometric parallaxes are quasi-absolute, i.e. a global zero-point may in principle be present due to the systematics of sun aspect angle and parallax factor, but the thermal control is designed so that it is expected to be much smaller than a milliarcsec. Furthermore, it may be determined by means of observations of stars with very small parallaxes. Detectable double stars are characterised by additional parameters. The output catalogue should also provide information on the quality of data, e.g. estimated mean errors, number of observations, and rms residuals.

The observations shall lead to the determination of five astrometric parameters two spherical coordinates, two annual proper motion components and the trigonometric parallax for 100,000 stars. If this would be attempted by a rigorous least squares method normal equations with at least 500,000 unknowns would result and the computational task would widely exceed the capability of existing computing equipment because the matrix is quite full. This problem is overcome by breaking down the data analysis in a number of steps which have to be carried out consecutively and which use the output from the preceeding steps. Furthermore, most of the steps must be repeated several times using results from the last steps in the sequence in order to cope with non-linearities, with double stars, erroneous observations, blunders etc. A flow chart showing the essential features in the process is given as Fig. 5.6. It is due to L. Lindegren, who has proposed and developed the so-called three-step method. Recently K. Poder of the Danish Geodetic Institute has contributed to the development of the method. The following presentation of the data analysis will closely follow the method illustrated in the flow chart, but it should be noted that other methods are possible and should be studied. This has however not yet happened in similar detail as with the present method.

Reconstitution of the satellite attitude is one of the first tasks, see upper left of the flow chart. The photon record from a photomultiplier behind a star mapper (SM), Fig. 3.4, serves to determine the attitude when a programme star crosses the SM. Frequent readings of gyros provide interpolation of attitude between SM observations. The final accuracy will be ± 0".1 when the star positions have been sufficiently improved through iteration.

The IDT data consists of short stretches for each star of about 100 samples each giving the photoelectron counts during 0.8 ms (Fig. 5.7). They will be processed and give a series of elementary observations each belonging to a star and obtained within a short time interval of about 2 s. In each such frame the IDT will interleave on average 4 stars with each other, some of which will also occur in neighbouring frames, since every star will be observed in all frames during its passage of the whole field. An elementary observation gives the abscissa of the star on the grid referred to the time at the middle of the frame by means of the rate of attitude known from the gyros (Fig. 5.6, dashed line). Less accurately, the ordinate of the star is also given as derived from the attitude reconstitution. Calibrations obtained in laboratory and in orbit are applied to give the grid coordinates of the star suitable as input for the following Three-Step processing.

Step 1: Consecutive scan circles are tilted only 27' relative to each other, so that observations from one set of e.g. 5 circles may be reduced separately giving abscissae projected on a common reference great circle. Since the scan has a width of 0°.9 a set will contain about 1800 stars. This reduction will make use of the attitude parameters and give improved values for instrument parameters: basic angle γ, orientation and scale values, taking into account that they may be slowly varying.

Step 2: Each star will appear in at least six different sets per year, Fig. 5.2, in which the reference great circles intersect each other at fairly large angles, so that the two dimensions of the sphere may be well reconstituted from the abscissae. But the common zero-point for the abscissae belonging to one set must remain arbitrary in Step 1 where each set is considered separately. It is the purpose of Step 2 to derive these zero-points.

For this purpose a number of e.g. 1000 stars uniformly distributed on the sky are chosen as Primary Stars (PRS). Each set will contain about 20 PRSs, and during Step 1 they are treated as having all 5 astrometric unknowns in such a way that normal equations with the 5000 unknowns for all PRSs will be gradually formed from the 2000 sets of the whole mission. They can then be solved obtaining the astrometric parameters for the 1000 primary stars.

The properties of such rigorous reconstitutions for primary stars have been studied by Høyer et al. with up to 450 stars and 3 unknowns per star, namely positions and parallaxes, and the expected rigidity and accuracy was confirmed.

Step 3: Having the results from the two first steps the final abscissae and astrometric parameters for all 100 000 stars and the final instrumental parameters as functions of time can now be obtained by back-substitution into the normal equations of Step 1.

The many abscissae thus obtained for each star will not necessarily be consistent with one set of 5 astrometric parameters, since the approximation contained in the 3-step method is just to neglect the fact that any abscissa star observed in different scanning sets is one and the same star. This approximation gives an advantage, as a by-product, that some of the partly resolved double stars may be used in different sets. Another advantage is that inconsistency of the abscissae for a particular star may be used to detect duplicity in cases where it is not already known from a-priori knowledge of duplicity or from analysis of the photon records. All these three methods must be used in dealing with the double stars as pointed out by Lindegren.

With the ensuing improved catalogue of the stars all previous steps must be repeated as indicated in the block diagram in order to recognize and eliminate erroneous observations and similar. Perhaps five such iterations will be required.

The execution of Step 1 is probably the best method for monitoring the observations during the mission. Execution of the Steps 2 and 3 after the first half year of observation will already give a very accurate ($\pm$ 0".01) positional catalogue and simultaneously a most thorough check of the performance. Thus, these computations should be run on one computer and should be considered an integral part of the scientific payload.

It must, however, also be stressed that the computations leading to a final catalogue should be carried out by at least two independent scientific teams in order to control efficiently what influence may occur due to differences in choice of methods. Since it must be the goal to obtain just one final agreed catalogue a close contact between these teams must be instituted to a degree which does not hinder them in carrying their independent scientific responsibility.

5.2.2 Computing Requirements

The reconstitution of the sphere from satellite observations does not involve a large number of unknowns compared with the big problems met in geodesy, but the number of observations is an order of magnitude larger. Furthermore, the matrix of the normal equations of an Abscissa Set is quite compact although it contains only 5 percent non-zeros in a few narrow bands. The large basic angle γ gives at the same time a very rigid abscissa system and a major computational task. A preliminary estimate says that the solution of an abscissa matrix takes 40 percent of the time required for a full matrix.

The Primary Star matrix is nearly full due to the large revolving angle and therefore a very rigid two-dimensional coordinate system is obtained. The computational task is however not large for a set of 1000 stars since it must be performed only once per iteration of the three-step process.

The IDT count record consists of about 10^{11} samples of photoelectron counts, corresponding to 5000 magnetic tapes of 1600 bpi, but larger density tapes may of course be preferred. The preprocessing (upper right of the flow chart) of the raw IDT stretches shortly after observation takes advantage of the limited harmonic content of the signal and of the preliminary a posteriori attitude (based on inaccurate star positions) available within a day or so of the observation. Since about 20 signal parameters per elementary observation will be sufficient, there is a factor 5-10 reduction of storage compared with the raw data and only the ensuing 1000 tapes need to be distributed to the institutes for reconstitution of the sphere. This data compression may be done by a dedicated small computer and is estimated to be a small task compared with the other computations.

From the 1000 tapes with harmonics a subset of input data (abscissae in the field) can be contained on about 60 tapes and data from star mapper, gyros, etc. need a similar number of tapes so that about 100 tapes can contain the input for the three-step process.

The 1000 tapes will also be used for detection of double stars from the photoelectric record. This will be a considerable computational task but no realistic estimate of its size is presently available.

We assume that a medium size and medium speed computer will be used for the reconstitution and that it will take 6 microseconds for an operation consisting of a double-precision multiplication, addition and storage with 20 decimal digits. It must be equipped with 1 or 2 arithmetic processors, a work storage of 50-100 K numbers (one number being about 40-60 bits), 2-3 discs with total of 100-200 M numbers and 2-3 magnetic tape stations (if 1600 bpi). A share of a bigger computer may be used but will not necessarily be advantageous since the required 70 bit mantissa arithmetic may be too slow or have truncation instead of correct rounding, and since the handling of a large number of tapes for a single job often presents problems at a computing centre.

The computing times are then approximately:

Abscissa matrices $1800^3/6 \cdot 2000 \cdot 6\ \mu s \cdot 0.4$	1300 hours
Primary stars $5000^3/\ 6 \cdot 6\ \mu s$	35
Other	500
about	2000 hours

or 6 months with 10 hours per day, to be repeated 5 times, presumably.

This estimate is a pessimistic one since the dominating time for the abscissa stars assumes that the Cholesky method is used, although most probably a more efficient method can be found utilizing the sparceness off the dominant diagonal, and the cyclic banded structure of the matrix.

It is estimated that the programme for doing the three-step solution would have 10-20 000 statements in a high level language and require 3 to 5 man-years of programming, testing and documentation. It is noted that the programme would have an automatic restart mechanism so that intended or unintended machine stops will give no problems.

A data management programme will be needed for the preprocessing of the raw input data and for the administration of the structured files processed by the main programme. Its development will require a similar total effort of man-power.

The staff could have 4 scientific programmers, some of them data-logists, and 2 operators, and it would have to work for 6-10 years.

This estimate of man-power requirements places the computational task of the astrometry mission as a large one compared with other astrometry computations. Compared with the total man-power requirements of many ground based astrometry projects it is also large, but not among the largest. It is e.g. smaller than the recent Hamburg Meridian Circle Expedition to Perth.

Evolution of the uncertainty of the attitude angle (ψ) around the spin axis. The instantaneous field of view (IFOV) is switched at a frequency of 5 Hz between two stars of 9th magnitude, one of which is taken as coordinate reference.

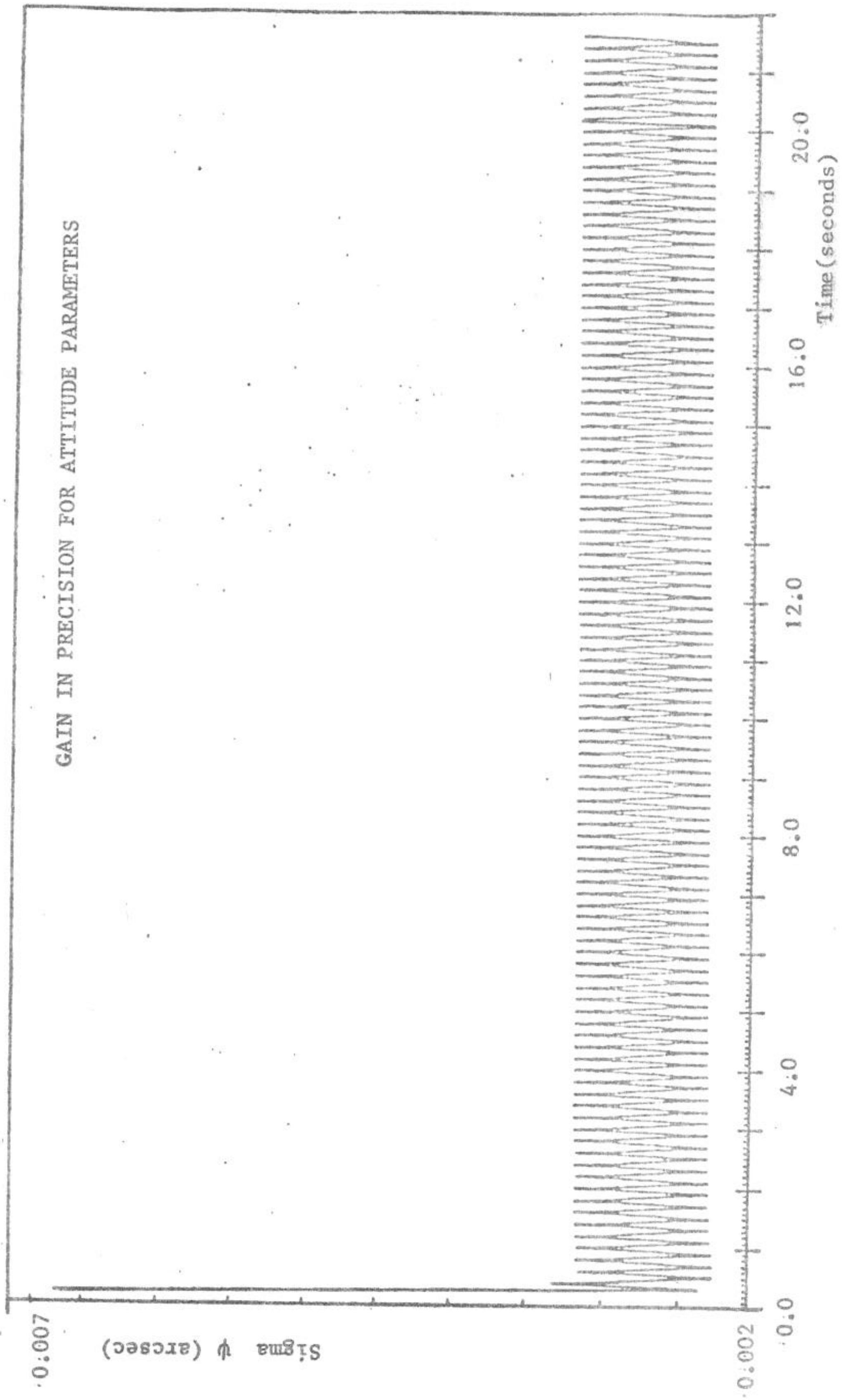

FIGURE 5.1(a)

Evolution of the uncertainty of the time derivative of the attitude angle ψ ($\dot{\psi}$ = spin rate). Same experiment as in Fig.5.1(a).

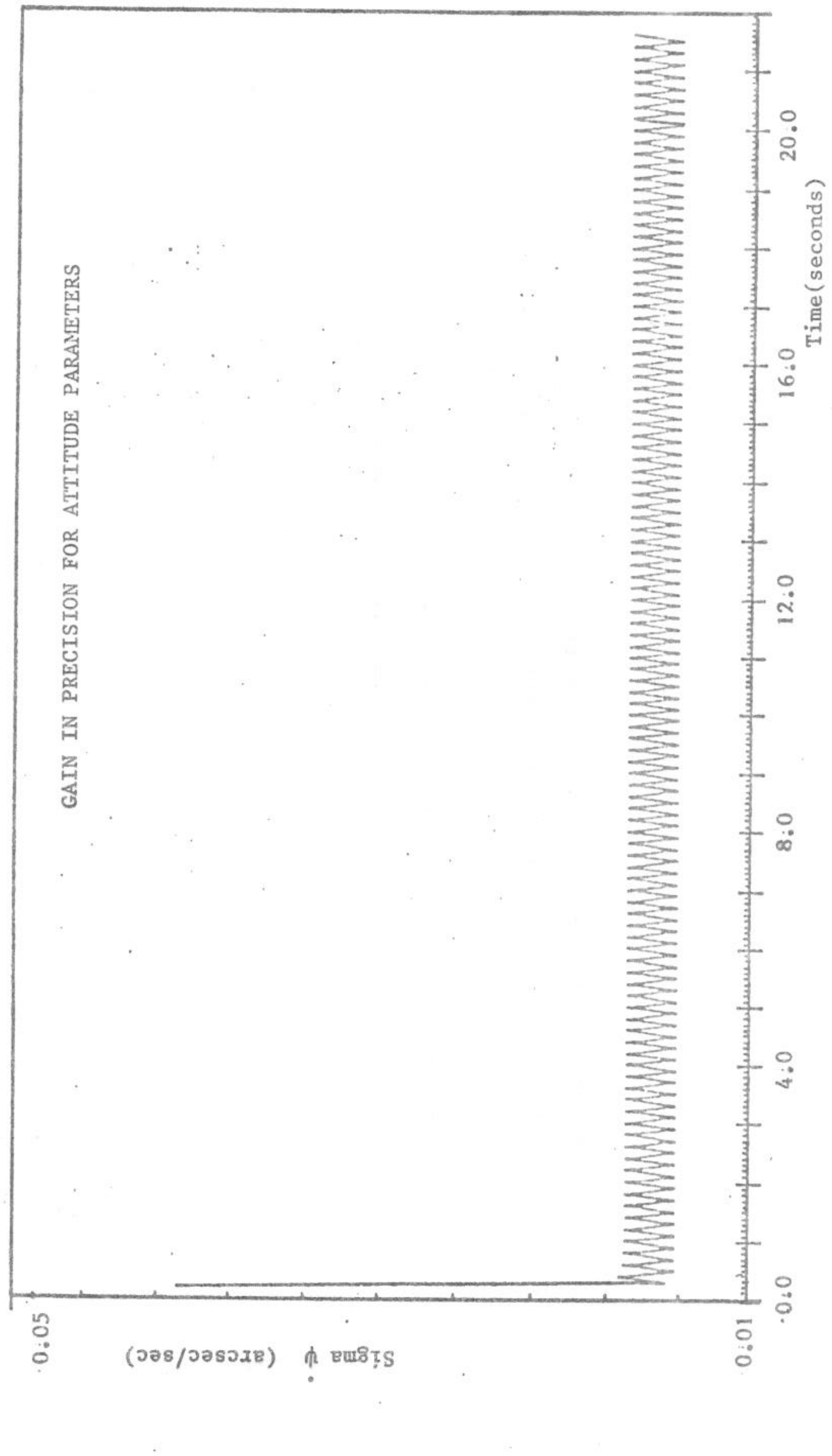

FIGURE 5.1(b)

Evolution of the uncertainty of the angle (abscissa difference) between the two stars. Same experiment as in Figs.5.1 (a) and (b).

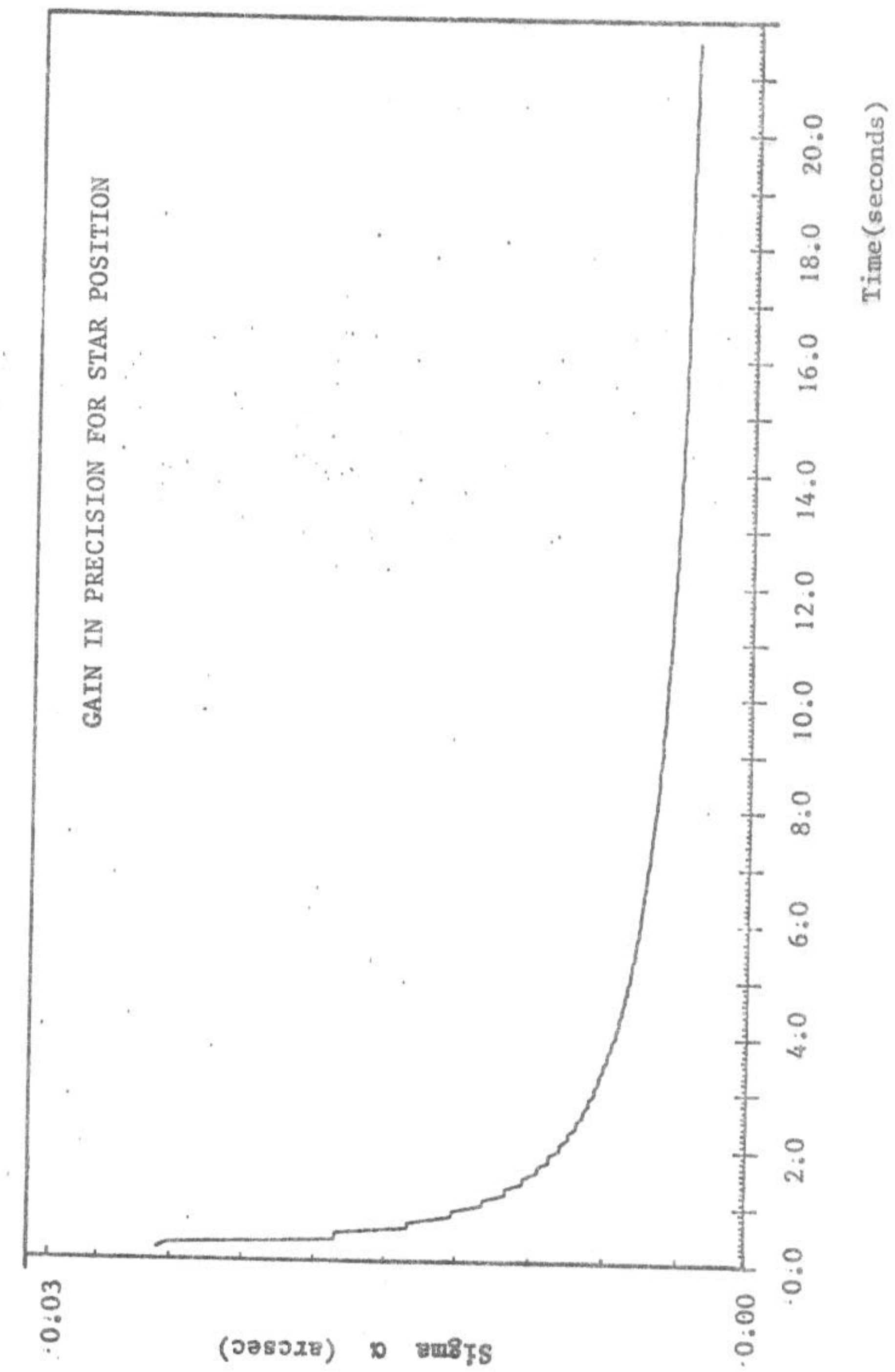

FIGURE 5.1(c)

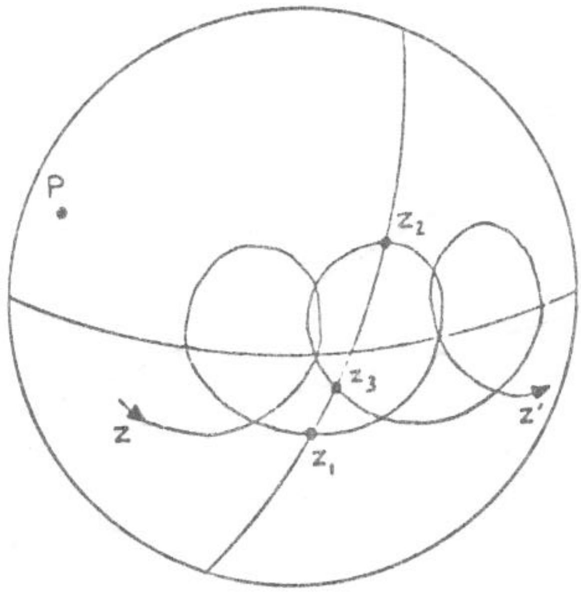

Path of z axis for revolving scanning with $K = 270^{\circ}/\xi$. Observation of a star at P is possible when the z axis is at z_1, z_2, or z_3.

FIGURE 5.2

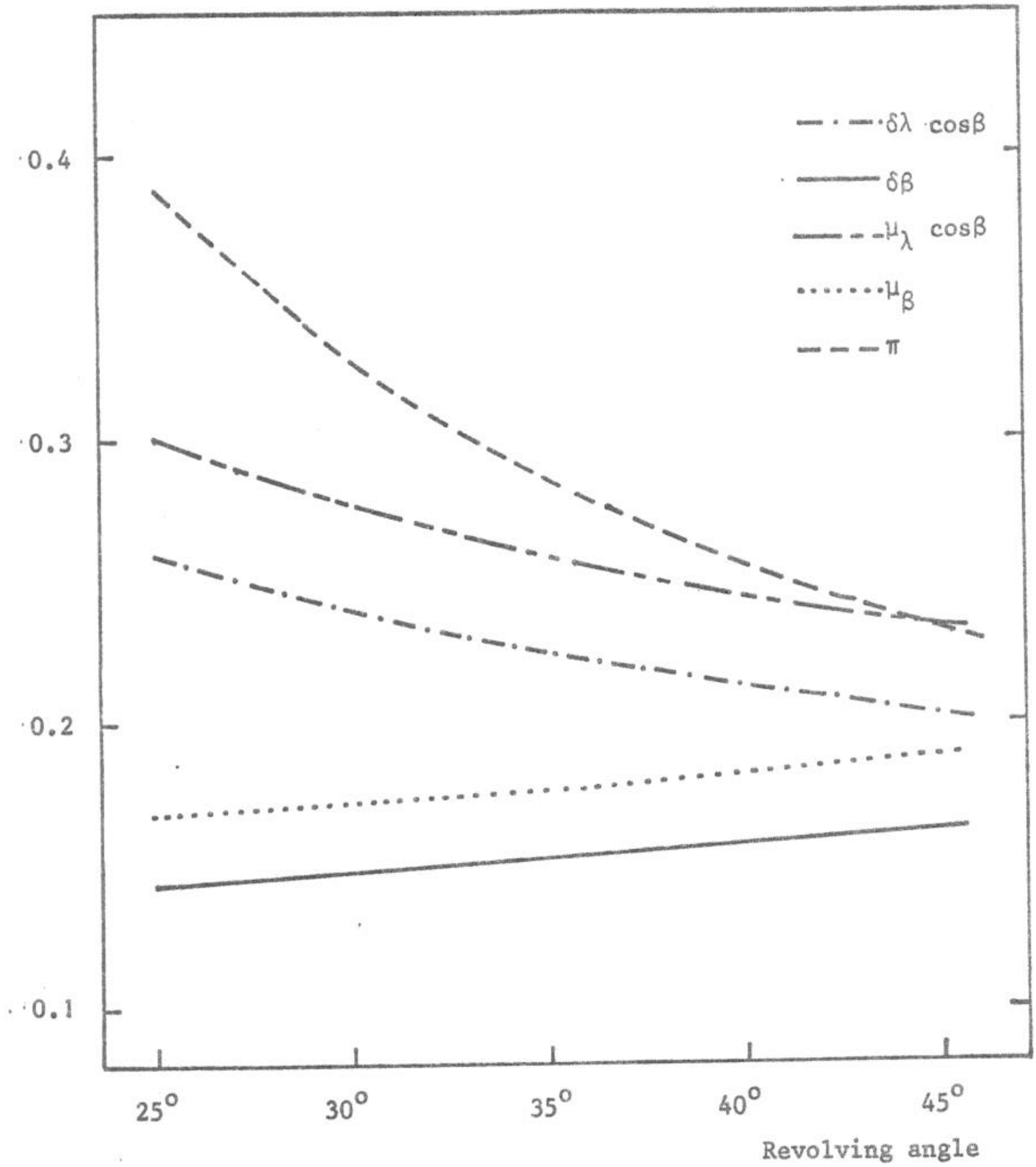

Improvement vs revolving angle; 3 years mission.

FIGURE 5.3

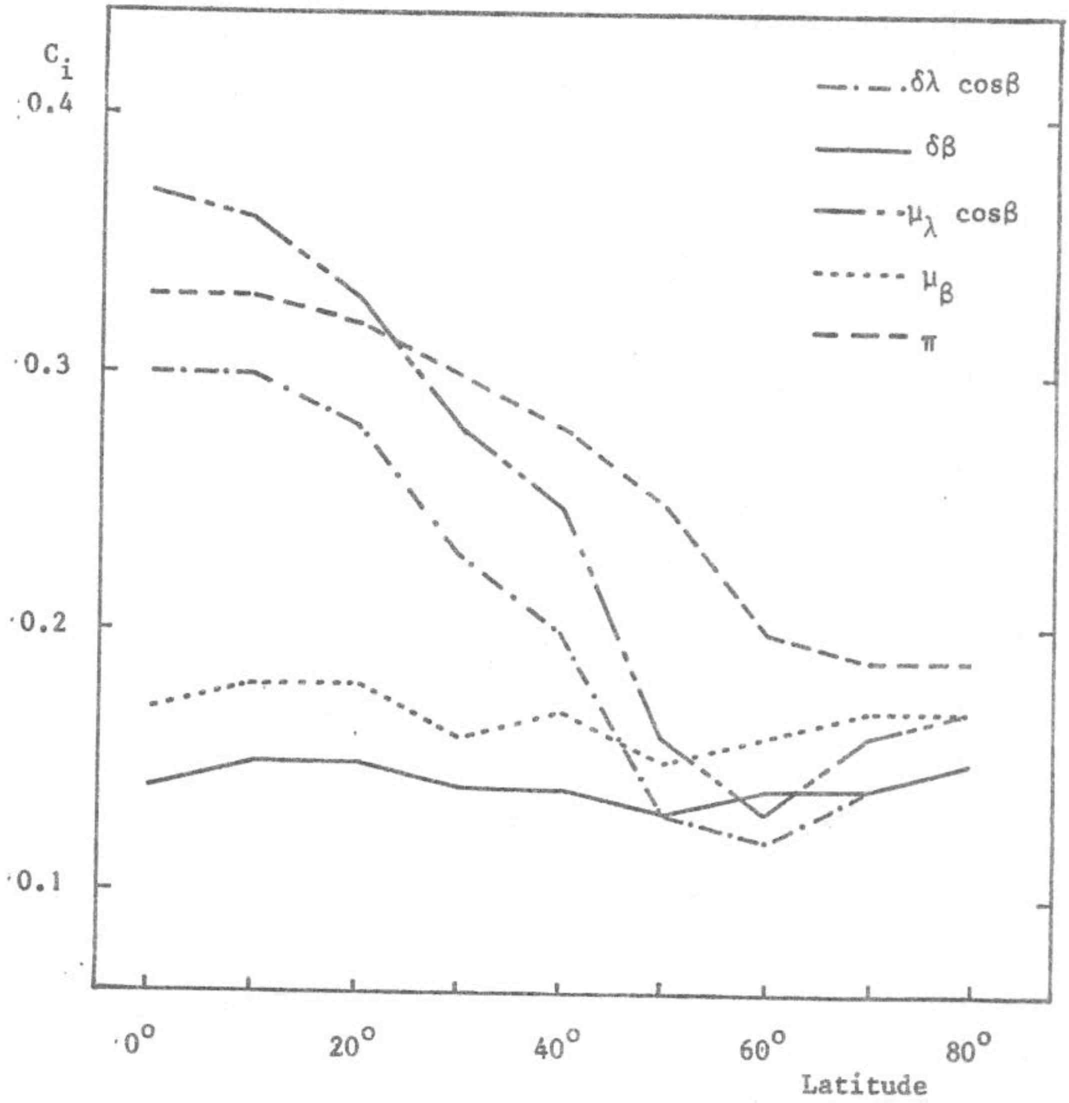

Improvement vs latitude; 3 years mission
Scanning law (K=7.5 , ξ=36°)

FIGURE 5.4

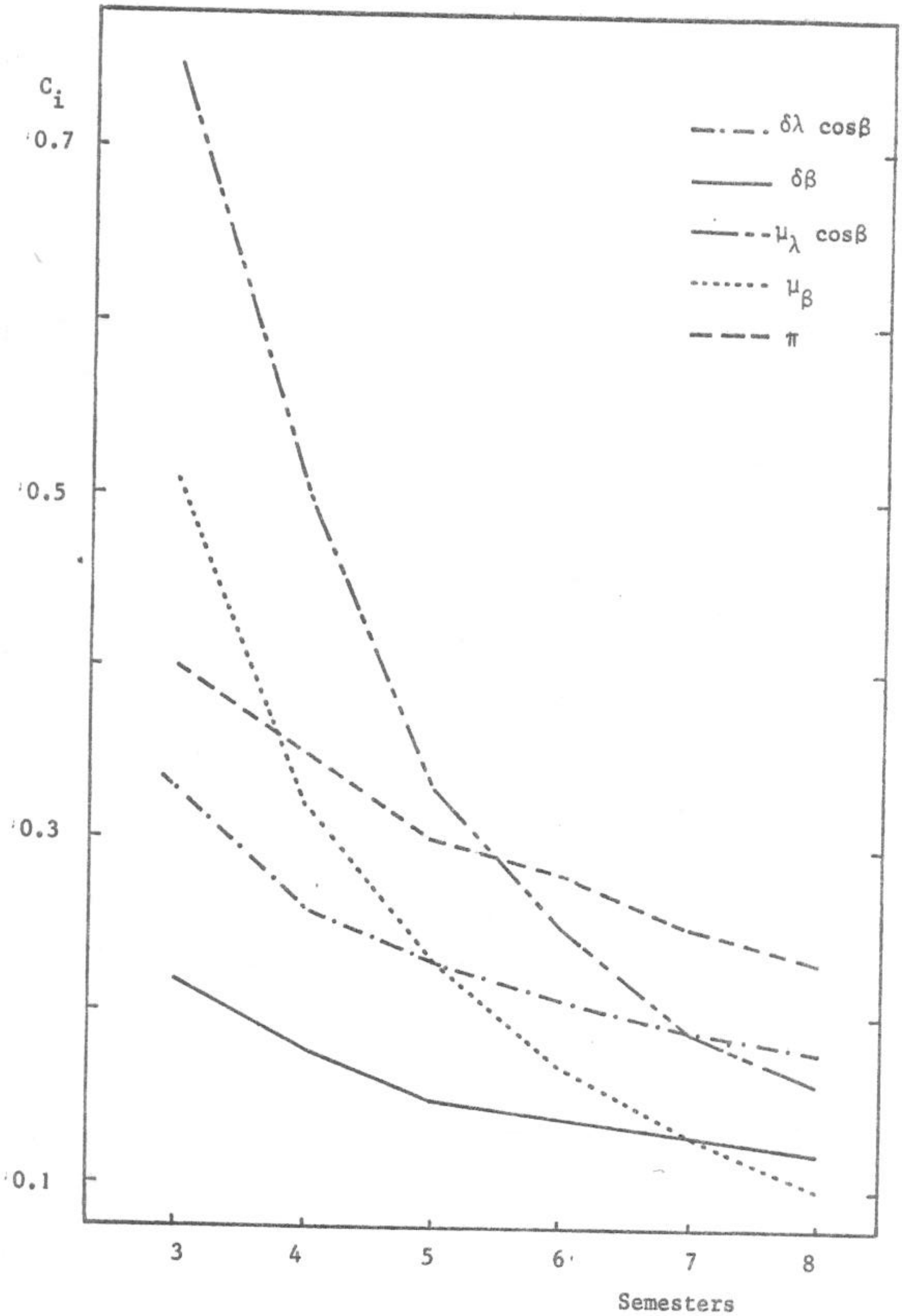

Improvement vs mission duration; scanning law (7.5, 36°)

FIGURE 5.5

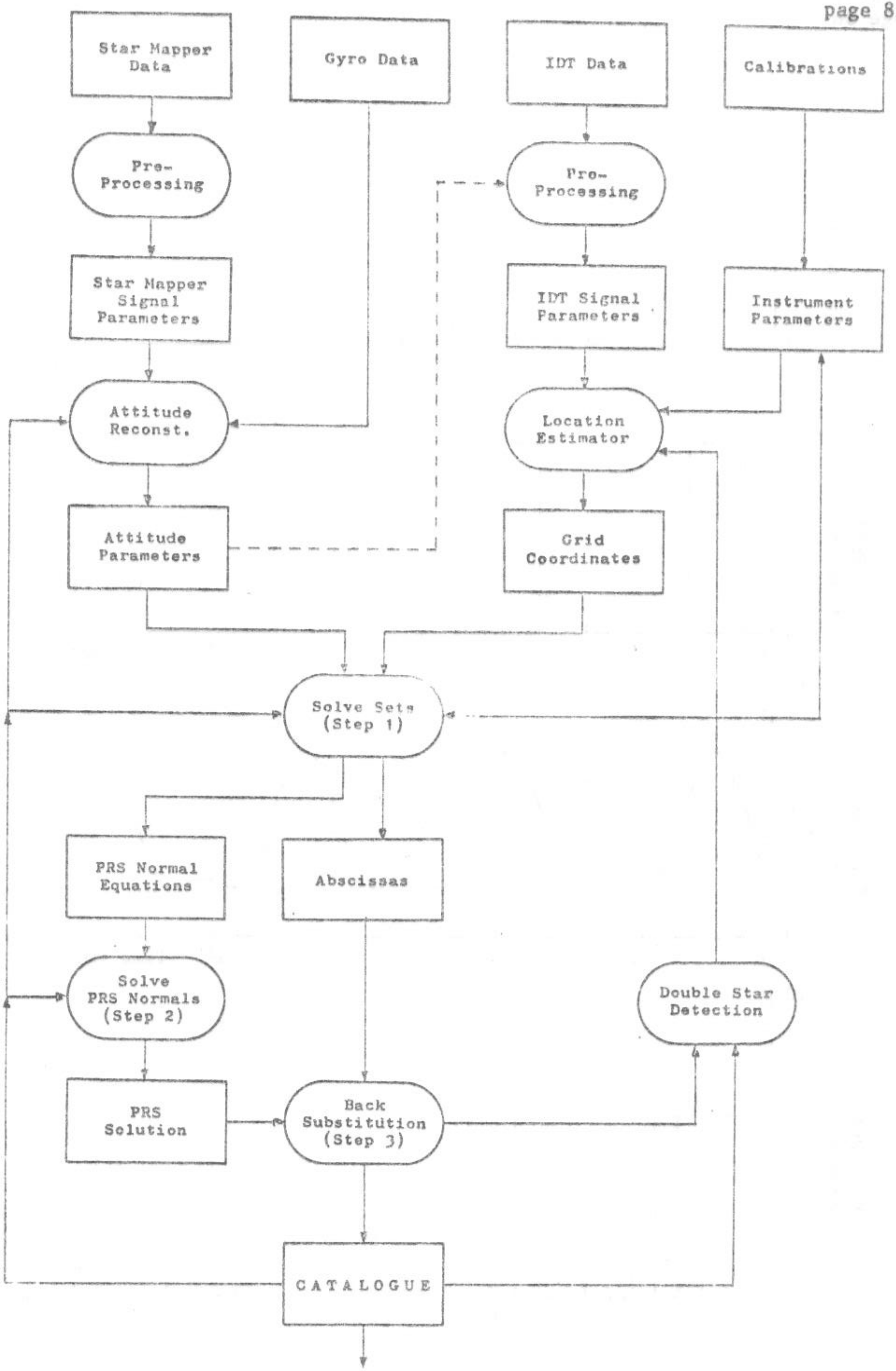

FLOW CHART OF THE SCIENTIFIC DATA PROCESSING. Rectangular boxes are data files which may be successively updated if included in a loop; oval boxes indicate procedures operating on the data. The three-step method described in the text corresponds to the lower left part of the diagram.

FIGURE 5.6

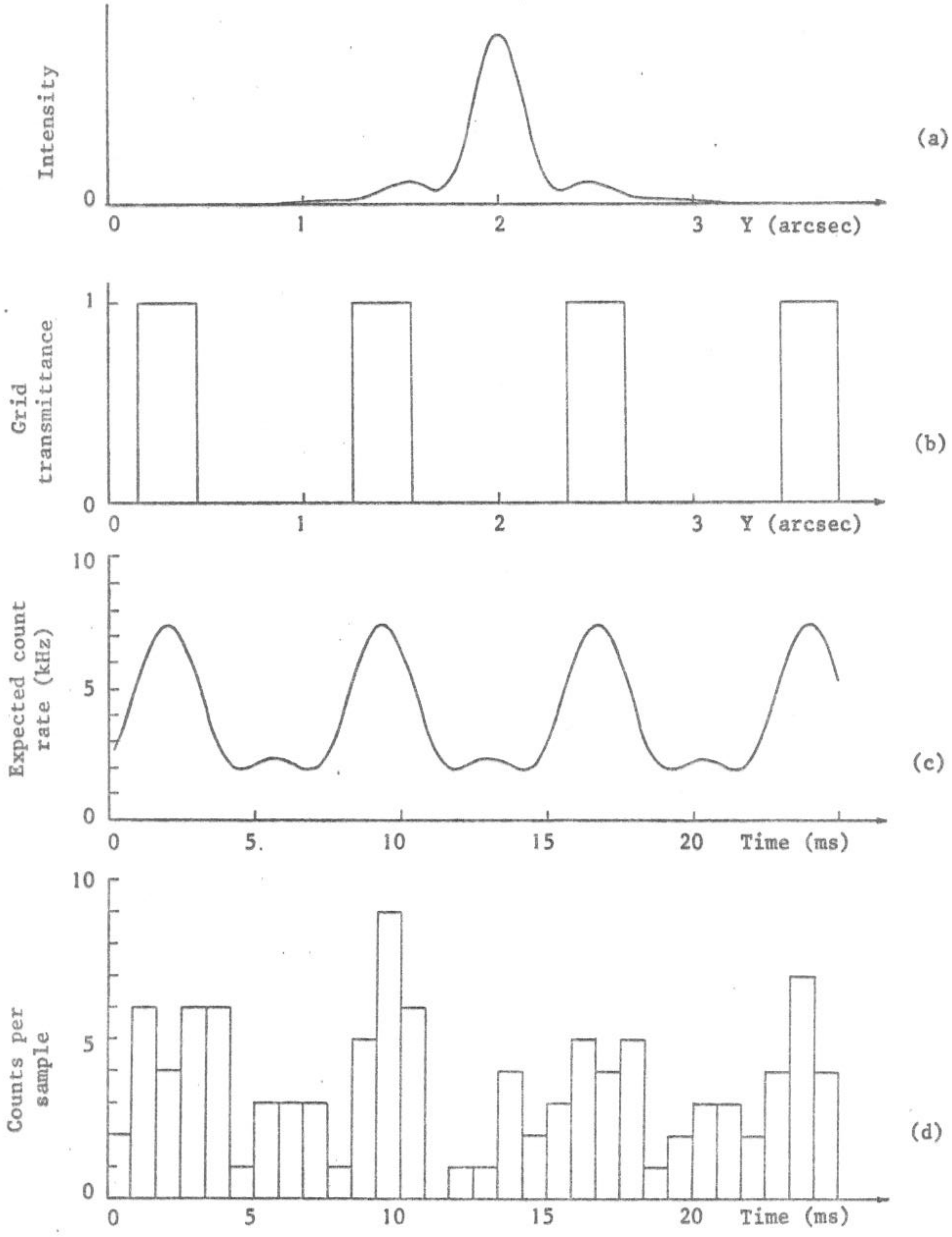

ILLUSTRATION OF THE PRINCIPLE OF LIGHT MODULATION BY THE MAIN GRID

The stellar diffraction image (a) is convolved with the grid transmittance (b) to produce a periodic intensity variation (c). The observed signal (d) is a Poisson process sampled at a fixed rate. The count rate corresponds to a star of magnitude 8.5.

FIGURE 5.7

6. MANAGEMENT AND TIME SCHEDULE

6.1 Management

6.1.1 General

As has been described in chapters 3 and 4 (see section 3.1), a satellite configuration comprising two integrated sub-assemblies with minimum interfaces is preferred:

a) spacecraft containing
- telecommunications
- data handling
- power supply
- attitude control
- apogee boost motor

b) payload containing
- optical subsystem (complex mirror, telescope, relay optics)
- modulation subsystem (grid and star mapper)
- detection subsystem (image detector tubes and photomultipliers)
- electronics

Each sub-assembly can be developed separately, integrated in its specific structure and carry its own thermal control.

With this terminology, the HIPPARCOS satellite is constituted by integration of the payload on the spacecraft.

Sections 6.1.2 and 6.1.3 outline possible management schemes for the development and procurement of the satellite and for the scientific data reduction; either of these two schemes will provide a viable and practical procurement management scheme.

In both cases, it is considered that ESA will be responsible for conducting the flight operations and providing the necessary hardware and software as described in section 4.8.2 (including the management of the observing programme and the quick-look facility); however, the scientific data handling, as described in section 5.2 is not considered as an ESA task.

6.1.2 Scheme A (national funding)

It is considered that since the payload contains a number of sufficient autonomous subsystems which can be developed separately, a management scheme analogous to that of the COS-B payload is appropriate. In this case, the responsibilities would be divided as follows:

Consortium of scientific institutes:

- design, development and procurement of the payload
- development of payload oriented software
- integration and calibration of the payload
- definition of the observing programme
- reduction of the data including the development of the required software
- publication of the final astrometric catalogue

ESA:
- design, development and procurement of the spacecraft
- integration of the payload in the spacecraft
- launch and operations
- data recording
- payload subsystem coordination

Following mission selection, the Agency will issue an A/O for payload proposals to undertake the established mission goals. The A/O will be explicit in terms of scientific requirements, technical interface, schedule, deliverable items, responsibilities of the parties, etc.

It is anticipated that the scientific community will respond with proposals for an autonomous payload from a number of collaborations or individual institutes, designating a principal investigator with a number of co-investigators.

The proposals will be expected to describe, inter alia, the management structure within the collaborations and institutes and to show how responsibilities for the scientific, technical, operations and analysis aspects will be discharged.

Payload selection will be undertaken in the time-honoured, conventional manner, through consultations with the scientific community, the advisory bodies, etc., leading to the submission of a recommendation by the Director General to the Science Programme Committee.

Fundamental to the proper conduct of the development phase and subsequent operational phase will be the establishment of the Science Working Team (SWT), comprising the PI and the Project Scientist as a nucleus and supported by co-investigators as appropriate. It is recommended that a limited number of scientific advisers be incorporated in the team, not directly associated with the instrument procurement and specifically concerned with the observing programme.

The SWT will represent the complete payload to the Agency and will be responsible for coordinating the payload development programme and preprations for the orbital operations phase.

ESA will nominate a Project Manager who will be responsible for the execution of the ESA tasks. The project management team will include a payload interfaces manager, reporting to the Project Manager.

Early in the development phase, it will be the responsibility of the Project Scientist and Project Manager to establish a Management Agreement, the Mission and Orbital Requirements and the Spacecraft/Payload Interface with the PI.

The raw data will be provided to the consortium for data reduction and subsequent publication of the catalogue. For one year after completion of the catalogue, the scientists who have contributed to the observing programme will have prime access to the use of the catalogue.

6.1.3 Scheme B (ESA funding)

This scheme assumes payload and spacecraft funding by the Agency. In order that ESA may carry out its proper management responsibilities, direct hardware procurement contracts will be placed with prime contractors. A scientific advisory team (similar to the ST/FOC) will be convened to provide ESA project management with the appropriate scientific inputs. The stars to be included in the observing programme will be selected in response to a competitive call for observing programmes. The proposals will be evaluated by a selection committee appointed by the Astronomy Working Group.

The raw data will be provided to a consortium of scientific institutes which, being selected after open competition, has committed itself to reduce the data and publish the catalogue and is funded nationally.

As in scheme A, for one year after completion of the catalogue, the scientists who have contributed to the observing programme will have prime access to the use of the catalogue.

ESA will nominate a Project Manager who will be responsible for the satellite development. The project management team will include a spacecraft manager and a payload manager, both reporting to the Project Manager.

6.2 Present Status of Definition

6.2.1 Accuracy analysis

Reliable assessment of the expected accurary with which the astrometric parameters will be yielded by HIPPARCOS is obviously an essential problem. It can be reasonably argued that, by the very nature of the physical principles involved, better results than from ground-based observations or small field space observatory are certainly predictable; however, this somewhat qualitative statement was not deemed sufficient, and quite an extensive effort has been made to quantify the achievable results. For this purpose, a sophisticated modular system of mathematical models has been developed, implemented on the ESOC computers and exploited. Description of the existing software and discussion of some numerical results are summarised in section 5.1. This existing programme constitutes a powerful tool for further optimisation of spacecraft and payload.

In addition, a number of physical analyses have been carried out regarding the effects of possible sources of errors, such as photon statistics, grid irregularities, attitude uncertainty and jitter, cathode inhomogeneities, etc. (section 5.1.5).

As a conclusion of this activity, the expected accuracy given in Table 5.1 has been established. The announced values, although being conservatively estimated, are the basis for the definition of the scientific objectives (chapter 1), thus ensuring consistency between science objectives and satellite performances.

6.2.2 Spacecraft Definition

During 1979, an internal group of ESTEC specialists in the various fields of technology has updated and further investigated the spacecraft mission, configuration, subsystems and operations. The previous Aeritalia phase A study has been thus completely reviewed and improved where necessary. As a general conclusion, the spacecraft development, although implying some complex subsystems (e.g. attitude control, data handling), is well within the well-known state of the art. The only critical area identified is related with the facilities and software necessary for the operational satellite control (i.e. management of the observation programme, section 4.8.2.2 and "quick look" facility, section 4.8.2.3), for which only preliminary data have been generated. With this exception, the spacecraft development can confidently proceeds to phase B.

6.2.3 Payload Definition

As proposed in the previous report on the phase A, (DP/PS(78)13 of 25 April 1978), it was considered by the Executive at the beginning of 1979 that, should the HIPPARCOS project be approved, the payload would be developed by a consortium of Institutes and financed directly by member states (according to scheme A, section 6.1.2). Consequently, no further ESA activities was originally planned on the payload design, except for some critical aspects (e.g. thermal control) and for the definition of interfaces with the spacecraft.

However, in its meeting on 22 and 23 May 1979, the Science Programme Committee specifically instructed the Executive to provide a full technical definition, development programme and cost evaluation of the payload. As many new design features had been generated since the end of the Aeritalia/Matra study, and as some aspects needed to be redefined and updated, a contract of about three months duration was awarded to Matra for a review of their previous study.

The main tasks carried out successfully can be summarised as follows:

- confirmation of the structure design, providing high rigidity, and definition of an isostatic attachment to the spacecraft,
- evaluation of the thermal distortions and suggestion for simplification of the thermal control subsystem,
- introduction of redundancy for the most critical items, i.e. image dissector tubes and photomultipliers,
- implementation of on-board focussing device,
- revision of the relay optics design,
- definition and design of the data handling subsystem.

As a result of all the studies conducted on the payload, it appears that its feasibility and performances are not questionable. However, some critical areas still remain, which have not yet been resolved, either because they cannot be dealt with properly by a theoretical study and need some technological tests, or because the limited amount of available time did not allow a sufficiently deep investigation. These are:

i) manufacturing methods and tolerances of the telescope mirrors and of the complex mirror; the specified tolerances, although flexible to a certain extent, (because their effect on the accuracy can be taken into account at the expense of additional computations), appear to be at the upper limit of the present state of the art. A particular problem is associated with the complex mirror, with a surface deformed according to a given law, and constituted by two parts assembled by molecular adherence;

ii) manufacturing method of the modulating grid; detailed preliminary specifications have been established on the manufacturing tolerances; they can be met within the present state of the art technology on a plane surface. However, the grid shall be traced on the best focal surface, which is a sphere of large radius (1.2 m). It has not yet been possible to conduct a full market survey and contact potential manufacturers;

iii) effect of radiations on the mirrors; particle radiations during the transfer orbit and on the geostationary orbit can deform the optical surfaces; this effect is highly dependent on the glass materials. Although this effect can be minimised by a proper selection of the glasses and compensated to some extent by the on-board refocussing device, some laboratory tests are required before choosing the best solution;

iv) calibration and optical tests of the payload; a preliminary investigation of procedures and required facilities has been carried out, showing in particular that tests would have to be made in the large ESTEC Dynamic Test Chamber. However, limited time availability has not permitted to establish a detailed calibration and test procedures and specifications, detailed facilities definition and occupancy for the various payload models.

These four points will be subject of a small technology verification programme, with the purpose of selecting the preferred manufacturing methods for the mirrors and the grids, determining the achievable fabrication accuracies and identifying the tests and calibration facilities, allowing thus a precise cost estimation of these items.

6.3 Time Schedule

The proposed time schedule for the HIPPARCOS project development is given in bar-chart form on Fig. 6.1. The payload development and the spacecraft/satellite development are shown separately, the schedule therefore can be applied in both management schemes outlined in section 6.1.

As the payload is clearly the most critical element in the schedule, it is considered that its phase B shall start slightly before that of the spacecraft, i.e. about four months in advance. For the spacecraft, the phase B will include industrial competitive periods before award of phases C/D to a prime contractor; this philosophy will also be applied for the payload procurement, at least for the management scheme described in section 6.1.3.

The precise schedule for the technology verification programme (see section 6.2.3) is still under discussion; it will be executed as early as possible, preferably in parallel with the payload phase B, starting probably before the phase B. The decomposition of the various tasks and their detailed schedule depend on a survey of the industrial capabilities and achievements in the concerned areas.

For the payload, five models are foreseen: an optical model, a structural model, a thermal model, an engineering model and a flight model (plus spares); for the spacecraft, only three models are required: a structural model, an engineering model and the flight model (plus spares).

The total duration of the programme, from start of payload phase B to satellite launch is estimated to be about 4 years and 10 months.

Table 6.1

HIPPARCOS - MASTER SCHEDULE

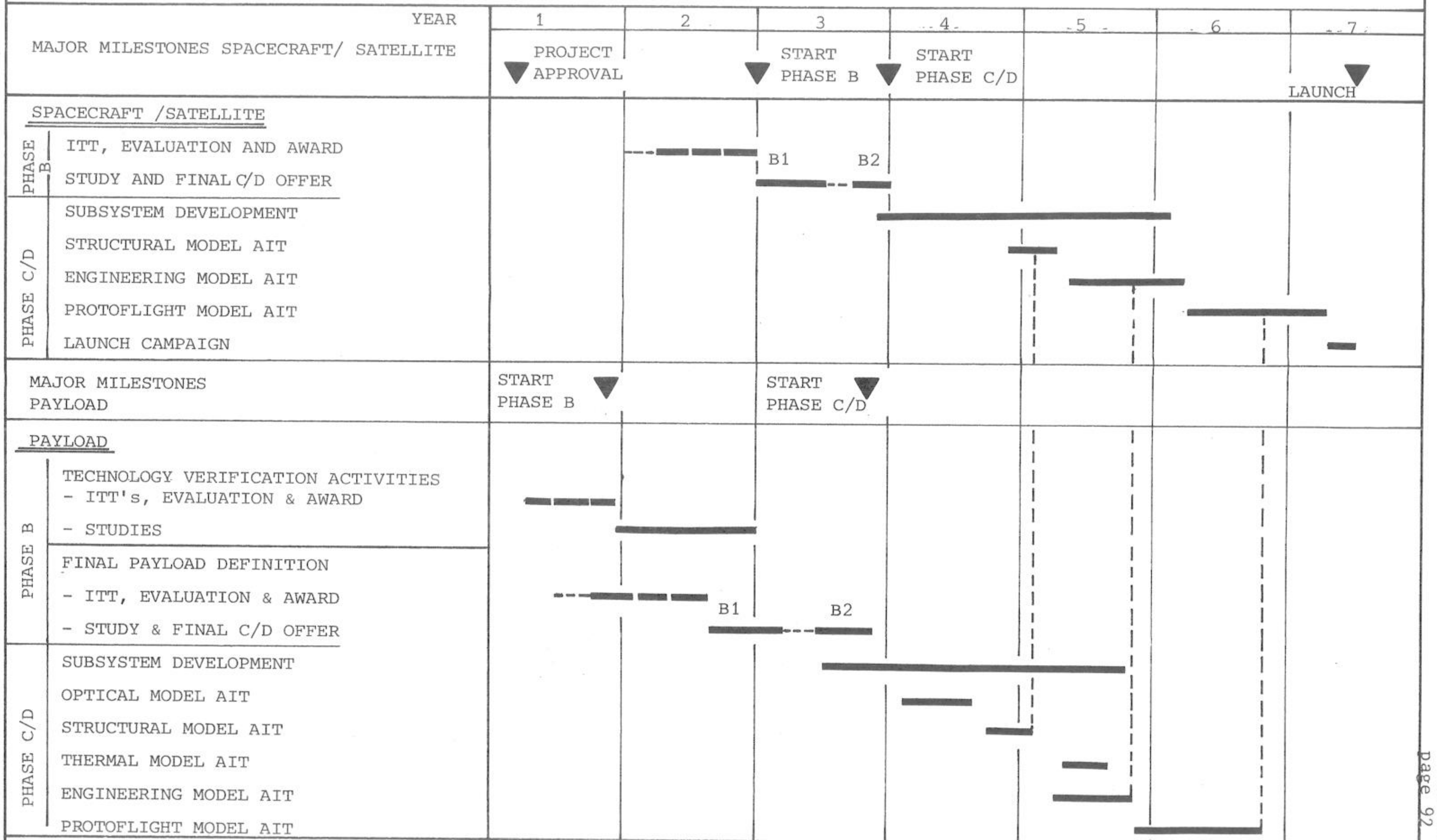

LEGEND : ITT : Invitation to tender; AIT : assembly, integration & test

APPENDIX

Background and History

The idea to realise a satellite exclusively devoted to space astrometry was raised by Professor Lacroute who submitted a detailed proposal to CNES at the end of 1967. The essential principles envisaged at that time are still the basis of the present work: measurements of large angles by means of a telescope in which two fields of view are superimposed by a complex mirror, image modulation by means of a grid and photoelectric detection. Between 1968 and 1970, CNES executed a feasibility study. As the end of 1970, CNES informed Professor Lacroute that the development could not take place within the French national programme. It was not until the end of 1973, within the long-term planning activities of the Solar System Working Group (SSWG), that Professor Kovalevsky made the Group aware of this project.

At the beginning of 1974, the LPAC (the predecessor to the Science Advisory Committee) recognised the originality of the mission, but, because of the novelty of the discipline within ESRO, requested assurance of sufficient scientific interest and an evaluation of the benefit of this mission for the scientific community.

As a consequence, the first international symposium on Space Astrometry was organised in Frascati on 22nd and 23rd October 1974. The considerable improvements to be expected in the determination of the astrometrical parameters, as well as the importance of the astrophysical consequences, were clearly evident. In fact, the two questions posed by the LPAC obtained a positive response.

In early 1975, the SSWG, seconded by the Astrometry Working Group (AWG) and followed by the LPAC, recommended that a mission definition study be carried out. This recommendation was endorsed by the Science Programme Committee (SPC). The mission definition study was then carried out between October 1975 and May 1976 and the conclusions are reported in ESA document DP/PS(76)11, rev. 1.

After a review by ESA's scientific advisory committee in mid-1976, followed by consultation of the Science Programme Committee in October 1976, the study proceeded into Phase A.

A consultation team, supported by ESA staff, was entrusted with the task of precisely defining the scientific specifications of the mission as an input to a Phase A study on the system design and a detailed numerical study to determine the expected accuracies. These studies were carried out in the period between May 1977 and March 1978 by Aeritalia (supported by Matra and CNR) and AML respectively. The results are described in document DP/PS(78)13. During the latter part of 1978 and in 1979, the technical system study was refined and updated by a team of engineers from ESA's Technical Directorate and a detailed technical study on the astrometry payload was carried out by Matra.

The software programme developed by AML was implemented at ESOC and used extensively to support the hardware studies.

The members of the Science Team were:

C. Barbieri	Istituto di Astronomia, Padova (I)
F. Beeckmans	Visiting Scientist, Space Science Dept (ESA)
E. Høg	University Observatory, Copenhagen (DK)
J. Kovalevsky	CERGA, Grasse (F)
P. Lacroute	Dijon (F)
R.S. Le Poole	Sterrewacht, Leiden (NL)
L. Lindegren	Observatory, Lund (S)
C.A. Murray	Royal Greenwich Observatory, Herstmonceux (UK)
K. Poder	Geodetic Institute, Charlottenlund (DK)
F. Scandone	Florence (I)
S. Vaghi	Visiting Scientist, ESOC

ESA staff members on the study were:

H. Olthof	AWG Secretary
R. Pacault	Future Projects Study Office
E. Roth	Mathematical Analysis Division
M. Schuyer	System Engineering Department

Requests for further information or additional copies of this report should be addressed to:

Dr. H. Olthof
Scientific Programme Directorate
European Space Agency
8-10, rue Mario-Nikis
F 75738 Paris Cedex 15.